30-7-2021

Fetal Microchimerism in the Maternal Murine Brain and Tissues

A Pioneering Study: DNA Extraction Optimization and qPCR-pilot

Soraya Smit, BSc
S3298108
MSc Biomedical Sciences – Neuroscience
Dr. M.G. Elliot
Prof. dr. J.D.A. Olivier
J.R. Smit, MSc.
University of Groningen

Deeper down in Panthalassa

A eukaryote finds her way

We return to the very first one

Greet the one we'll soon become

- Nightwish (2015), *Endless Forms Most Beautiful*

Abstract

Pregnancy is one of the many miracles of life. However, pregnancy itself appears to have some miracles of its own. During pregnancy, a bidirectional transfer of cells between mother and child was discovered. This process is called ‘microchimerism’ (Mc). When fetal cells travel into the maternal circulation and tissues we speak of ‘fetal microchimerism’ (FMc). Fetal microchimeric cells (FMCs) are known to be able to pass through the blood-brain-barrier and possibly integrate into the maternal brain. Evidence suggests that the FMCs are able to differentiate into cell types belonging to the nervous system.

It has been proposed that Mc arose approximately 93 million years ago, in the common ancestor of all eutherian mammals. In this thesis we propose a mechanism in which FMCs could integrate in the maternal brain and from there act as an extension of the placenta to improve maternal care, attachment, and resource allocation postpartum. We hypothesize that FMCs will be more abundant in areas of the maternal brain, associated with maternal behaviour, attachment and/or resource allocation. In this study we aim to assess the frequency and distribution of FMc in the maternal brain, spleen, and lung.

For this study we used a murine eGFP breeding model. By crossing a homozygous eGFP-positive male with a wildtype female, we would analyse the hemizygous eGFP-positive cells of the pups in the maternal tissues. Females were either terminated on E18/E19 or sometime after pregnancy, after which organs were collected. We analysed the maternal brain, spleen, and lungs for the presence of GFP in a qPCR-pilot. Additionally, a substantial part of this thesis will be devoted to optimizing DNA extraction from brain tissue, prior to the qPCR analysis.

After careful analysis of our qPCR dataset, we discovered there were significant issues with our GFP assay, which made it nearly impossible for us to correctly analyse the quantities of GFP in each sample. We saw non-specific amplification in the presence of very little or no GFP. However, we were able to find GFP in most of our samples. Further optimization of the qPCR and research is needed to provide more clarity on the frequency and distribution of FMCs in maternal tissues, such as the brain, spleen, and lung. Due to these issues with establishing GFP quantities, we were unable to give more insights on the evolutionary function of FMc in the maternal brain.

Acknowledgments

Eight months of hard work and a thesis of almost one-hundred pages, that is something you are not able to do on your own. During my time at the Elliot Lab at GELIFES I met some truly amazing people. First and foremost, I would like to thank Romy Smit. From the first moment I spent at the lab she made me feel so incredibly welcome. She was the basis of the amazing, warm, fun, and supportive environment we had at the Elliot Lab. I am so thankful for all the experience I gained with her help, all the responsibilities she gave me and all the courage I gained from her feedback to be independent at the lab. If I look at where I was before I started my first research project, and at where I am now, I feel I have grown and learned a lot, and Romy has played such a large role in that. However, the most precious part of our time together is all the fun and the great conversations we had.

Secondly, I would like to thank Mick Elliot for his expertise, his amazing input during brainstorming sessions, his support for all of us during the difficult times we all experienced due to the COVID-19 pandemic and the great conversations we had. I am very thankful for all the work he put into providing feedback and knowledge to finalize this thesis in a rather difficult time. Furthermore, I would like to thank Maartje de Jong. We both had completely different regions of interest for this project. Whereas she focussed on the mammary glands, I focussed on the brain. Yet, we were able to support each other with amazing brainstorming sessions and new points of view.

Last, but certainly not least, I would like to thank my partner in crime, Hedwich Meindertsma. She and I were a team, and we truly worked amazing together. We worked on the lab together, brainstormed over our results, looked for ways to improve our work, made dozens of failed schedules and were each other's moral support, but most important of all she became my friend. Despite all the new experiences, all the new knowledge and skills, a new friendship may be the best thing that I gained from my time at Elliot Lab.

Table of Contents

1. Introduction

Pregnancy is one of the many miracles of life. However, pregnancy itself appears to have some miracles of its own. Aside from a life growing in the womb of a mother, so much more happens that many people are unaware of. This thesis will be devoted to one of those phenomena. During pregnancy, a bidirectional transfer of cells between mother and child was discovered. These cells remain in the circulation and tissues of the host for a long time after pregnancy. This process is called 'microchimerism' (Mc) (*Kinder et al., 2017*). When fetal cells travel into the maternal circulation and tissues we speak of 'fetal microchimerism' (FMc) and when maternal cells travel into the fetal circulation and tissues, this is called 'maternal microchimerism' (MMc) (*Kinder et al., 2017*; Figure 1). This thesis will focus on FMc specifically. Thus, MMc being beyond the scope of this thesis.

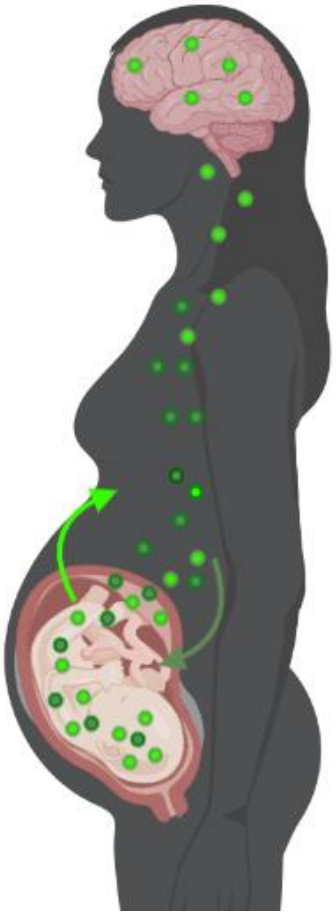

Figure 1: A visualisation of microchimerism in the human body. The light green cells represent the fetal cells migrating towards the maternal body (fetal microchimerism). The darker green cells represent the maternal cells migrating towards the fetal body (maternal microchimerism). *Figure created by S. Smit.*

So far Mc had only been found in eutherian mammals, including humans, primates, rodents, dogs, and cows (*Bianchi et al., 1996; Bakkour et al., 2014; Khosrotehrani et al., 2005; Axiak-Bechtel et al., 2013; Turin et al., 2007*). One possible explanation for the presence of microchimerism in such diverse taxa is that it is an ancestral condition that evolved approximately 93 million years ago, in the common ancestor of all living eutherian mammals (*Boddy et al., 2015*; Figure 2). However, these animals all possess different types of placentas (*Moffett & Loke, 2006; Figure 2*): haemochorial (in which maternal blood comes into direct contact with fetal tissue; humans, primates and rodents), endotheliochorial (in which maternal blood is separated from fetal tissue by the endothelium of maternal blood vessels; dogs) or epitheliochorial (in which maternal blood is separated from fetal tissue not only by the endothelium of maternal blood vessels but also by connective tissue and epithelium of the uterine lining; cow) . It seems likely that the passage of cells between fetal tissues and maternal blood must be accomplished by different mechanisms in species that differ in these forms of placental organization. Since the origin, dynamics, and function of Mc in different species is largely unknown, an alternative possibility is that the occurrence of Mc throughout the eutherian phylogenetic tree arose due to convergent evolution (*McGhee, 2011*).

This thesis will primarily focus on fetal microchimeric cells (FMCs) in the maternal brain and their possible evolutionary functions in maternal care, attachment, and resource allocation.

1.1 Fetal Microchimerism in the Brain

Several studies have attempted to uncover the secrets of FMCs in the maternal brain. FMCs are known to be able to pass through the blood-brain-barrier, as well as the blood-spinal-cord barrier (*Tan et al., 2005; Zhang et al., 2013*). Evidence suggests that the FMCs are able to differentiate into neuron-like cell types, as the cells possess surface markers characteristic of neuronal cell types, such as NeuN (*Tan et al., 2005; Zhang et al., 2013; Zeng et al., 2010*). Additionally, FMCs in the brain possess morphological structures and immunological characteristics resembling perivascular macrophage-, astrocyte-, and oligodendrocyte-like cell types (*Tan et al., 2005*) as well as stem cell markers, and immature neuronal markers, suggesting that the fetal cells could potentially go through a similar

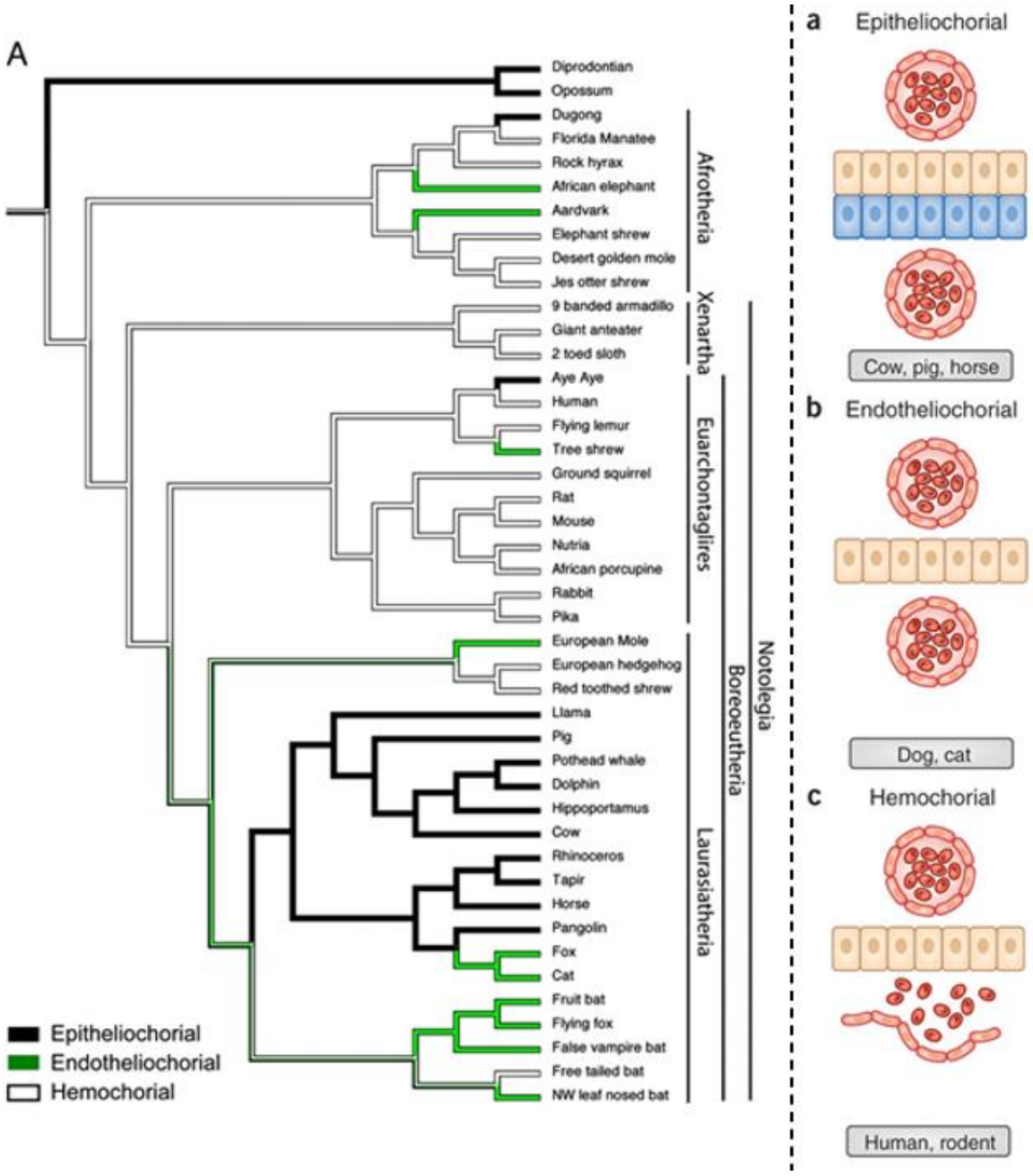

Figure 2: The phylogenetic tree of eutherian mammals and their different placental types. From the common ancestor of all eutherian mammals three different placental types have evolved: epitheliochorial, endotheliochorial, and haemochorial. In an epitheliochorial placenta the barrier between maternal blood and the chorion consists of the maternal endothelium and the uterine epithelium (a). In an endotheliochorial placenta the barrier between maternal blood and chorion consists only of maternal endothelium (b). In a haemochorial placenta the maternal blood has direct contact with the chorionic villi (c). *Left figure (phylogenetic tree) borrowed from Wildman et al., (2006); Right figure (placental types) borrowed from PrabhuDas et al., (2015).*

maturation process as adult neurogenesis (*Zeng et al., 2010*). The amount of FMc is not fixed but can increase over time by proliferation of FMCs, but it is not known whether this can occur within the brain itself, or whether the FMCs proliferate in the blood and migrate across the blood-brain-barrier, as fetal cells are reported to engraft the bone marrow as well (*Tan et al., 2005*). These interesting findings indicate the possibility that FMCs could integrate in the maternal neuronal circuitry (*Zeng et al., 2010*).

Although the exact function and dynamics of FMc are largely unknown, the frequency of FMc has been associated with both positive and negative health outcomes in several diseases including cancer, autoimmune disease, and pregnancy complications such as pre-eclampsia, miscarriage, and premature birth (*Boddy et al., 2015*). Within the brain, *Chan et al.* (*2012*) found lower numbers of FMCs in women suffering from Alzheimer's Disease (AD) than in normal controls, which they interpreted as indicating a possible health benefit for women with higher amounts of FMCs. *Zeng et al.* (*2010*) demonstrated initially higher amounts of FMc in diseased tissue from a female Parkinson's Disease (PD) murine model, but this effect did not persist long after pregnancy. *Broestl et al.* (*2018*) found FMc to be present in 80% of glioblastomas and 50% of meningiomas, but no significant correlation was found between the frequency of FMCs and the incidence of the tumours. It is important to note that these studies are epidemiological and seek correlations between the frequency of FMc and the presence or severity of disease. Causal claims regarding direct beneficial or deleterious effects of FMCs cannot be substantiated by such research. For example, as AD is a neurodegenerative disease, there could be lower frequencies of FMCs in AD patients, due to the degeneration of brain tissue altogether. As for PD, there is also a possibility that the FMCs were attracted to the diseased brain tissue, without any influence on the occurrence of the illness itself (*Zeng et al., 2010*).

The strongest evidence for a functional role of Mc cells in disease progression comes from studies of tissue healing, including in the brain. Following maternal injury, FMCs increase in frequency in the blood and migrate specifically to sites of wounding in maternal skin (*Seppanen et al., 2013*) to excitotoxic lesions and sites of ischemic shock in the maternal brain (*Tan et al., 2005*) and to the site of myocardial infarction in the maternal heart (*Kara et al., 2012*). *Ritzel et al.* (*2017*) showed that FMCs that migrate to sites of ischemic stroke in the maternal brain show signals of differentiation there into endothelium, indicative of their involvement in angiogenesis. However, even this evidence does not prove that the involvement of microchimeric cells in wound healing is a result of their microchimerism. It is perfectly possible that these migratory cells are simply MCs that randomly engrafted into bone marrow fibroblasts and are thus exhibiting the normal migratory behaviour of fibroblast-derived immune cells and are not actually behaving differently as a result of their microchimerism (*Seppanen et al., 2013*).

Though it might be an accidental feature of FMc, there is a chance that the involvement of FMCs might have evolved as an advantage for both mother and child. Maternal tissue repair comes with few costs to the fetus during pregnancy, and the fetus would benefit from supporting maternal health via this pathway. Maternal care is crucial for infant survival, especially in humans. Therefore, the fetus would benefit evolutionary from contributing to the repair of maternal tissues (*Boddy et al., 2015*). There are other possibilities for the fetus to benefit from having its cells migrate into the maternal body. Considering that FMCs seem able to migrate into the maternal brain, and possibly integrate in the maternal neurocircuitry, the fetus could benefit from influencing maternal behaviour to its own evolutionary advantage.

1.2 Maternal Behaviour

Maternal care is a collection of behaviours performed by the mother that increases the chances of her offspring's survival postpartum. Maternal behaviour is driven by specialized neural circuits that receive sensory, cortical, and hormonal input, an generate a coordinated change in behaviour (reviewed in *Smiley et al., 2019*).

It is believed that the reward circuitry is heavily involved in encouraging offspring-directed behaviour. Compared to other more overt rewards, maternal care is long-term behaviour which does not necessarily immediately generate a rewarding feeling. Therefore, it could be assumed that the brain must engage the reward circuitry in a different manner in order to promote the continuous sacrifices and enormous effort a mother needs to deliver to take care of her offspring. Mothers must prefer offspring-directed behaviour over other behaviours (reviewed in *Smiley et al., 2019*).

Olfactory, visual, auditory, and tactile stimuli all play a key role in promoting maternal behaviour. Inputs are filtered through the bed nucleus of the stria terminalis (BNST) and the medial amygdala (MeA), before being integrated in the medial preoptic area (MPOA; Figure 3). The MPOA seems to play a key role in regulating maternal behaviour (*reviewed in Smiley et al., 2019*). Additionally, the MPOA displays important roles in maternal care such as thermoregulation, sleep, and social reward (*McKinley et al., 2015; McHenry et al., 2017*). After receiving input via the MeA, the MPOA projects to the reward circuitry through activation of dopamine projections from the ventral tegmental area (VTA) to the nucleus accumbens (NA) to induce the rewarding feeling of maternal behaviour. The NA projects to the ventral pallidum (VP) which causes active maternal behaviour (*Numan et al., 2005*; *Figure 3*).

It is suggested that maternal behaviour consists of two parallel pathways: one is the promotion of offspring-directed behaviour, the other is the suppression of pup avoidance. As a result of hormonal and sensory stimulation during parturition, the MPOA and the BNST become dominant over the aversion pathway, that normally induces pup avoidance. Additionally, the MPOA and BNST maintain maternal behaviour during the lactational period (reviewed in *Smiley et al., 2019*).

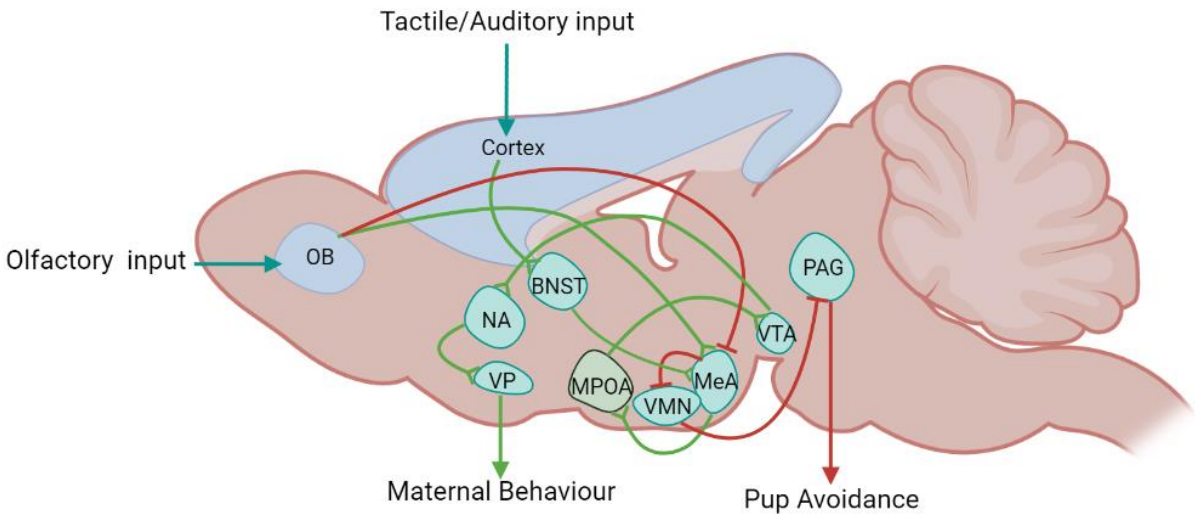

Figure 3: A schematic overview of the neurocircuitry involved in maternal behaviour and pup avoidance. Display of proper maternal behaviour requires the activation of pup-directed behaviour (green) and suppression of pup avoidance (red). Olfactory, tactile and/or auditory input is received and processed by the medial amygdala (MeA). The medial preoptic area (MPOA) functions as the nexus of maternal behaviour. (OB: olfactory bulb; BNST: bed nucleus of the stria terminalis; NA: nucleus accumbens; VP: ventral pallidum; MPOA: medial preoptic area; MeA: medial amygdala; VMN: ventromedial nucleus; PAG: periaqueductal grey; VTA: ventral tegmental area). *Figure created by S. Smit.*

1.2.1 Attachment

Evolutionary processes resulting in mammalian maternal care also result in an innate need in mothers and offspring to form close attachments with each other. This attachment increases the chances of survival, as mothers protect their offspring from predation and environmental exposure and provide resources for their offspring, for example by lactation (*Gluckman et al., 2016*).

The need for maternal attachment is especially significant for humans, who are dependent on their mother for an extended period of time in comparison with other mammals. This is partly caused by the trade-off made between bipedalism and the possession of a large brain. The human pelvis is laterally rotated, and the pelvic opening is narrow in comparison with other primates, as a consequence of the evolution of musculoskeletal adaptations to bipedalism. Even though this allows humans to walk upright and run efficiently, these features create difficulties during childbirth. If humans were to carry their offspring for sufficient time to allow full neuronal maturation, as in other primates, the fetal head would be far too large to pass through the narrow human pelvis, a so-called “obstetrical dilemma”. As

a consequence, human gestation is short relative to our body size, with the result that human offspring are born in an altricial state and, being ontogenetically delayed in comparison with our closest primate relatives such as the chimpanzee (*Coward and Grove, 2012*), are dependent on their mothers for a long period after birth (*Gluckman et al., 2016*).

There is reason to believe that the degree of attachment a mother exhibits in raising her offspring is correlated with the time that FMc remains in her body (*Dawe et al., 2007*). In humans, with lifelong attachment and high levels of maternal investment, FMc is found at least 27 years after parturition (*Bianchi et al., 1996*). In mice most of the FMc has disappeared four weeks post gestation (shortly after the weaning age of around three weeks), with exception of the brain in which FMc persists up to eight weeks (*Dawe et al., 2007*). Later studies observe the presence of FMc in the mouse body for a far longer period of time. *Zeng et al.* (*2010*) found FMCs in the maternal brain up to 210 days post gestation (P210) in mice. On the other hand, *Beksac et al*. (*2019*) found FMc up to twelve months in skin and liver tissue post gestation in mice. Moreover, they found FMCs up to twenty-four months in the tissues immunosuppressed mice (*Beksac et al., 2019*). FMCs appear to be mostly cleared out of the maternal circulation after gestation by the maternal immune system, which induces apoptosis in the fetal cells (*Kolialexi et al., 2004*). The brain, however, is an immunologically privileged site, which means there is a higher tolerance of foreign antigens and a lower chance on active immune responses of the body (*Murphy & Weaver, 2016*). This could create an opportunity for FMCs to find a relatively safe niche in the maternal body. Future studies could possibly find FMCs in the brain for a longer period of time after birth. However, up to now *Zeng et al.* (*2010*) was the only study that searched for FMCs up to P210 in the brain. Therefore, no data is available on longer periods after birth yet.

In conclusion, attachment and the affiliated maternal behaviour could be interesting mechanisms through which FMc in the brain could potentially execute any influence on the maternal behaviour, in favour of offspring survival.

1.2.2 Resource Allocation

During gestation, many adjustments are made in the maternal brain to sustain the fetus, such as changes in sleep patterns (suprachiasmatic nucleus (ScN), ventrolateral preoptic nucleus (VPN)), changes in thermoregulation (MPOA, dorsomedial hypothalamus) and the suppression of the stress response (paraventricular nucleus (PVN)). Moreover, changes in food intake are made to provide enough resources for the growing fetus (arcuate nucleus (AC), PVN) (reviewed in *Smiley et al., 2019*) (*Figure 4*). For example, reduced response to leptin causes increased appetite, resulting in the intake extra resources to accommodate the growing fetus (*Bear et al., 2015*). Additionally, fat deposition of the mother is increased during gestation, which acts as an energy reserve for late gestation and the lactation-period (*reviewed in Smiley et al., 2019*).

After gestation, the most important means of resource allocation towards the offspring is lactation. In fact, lactation is the most energetically expensive component of reproductive effort in female mammals (*Oftedal, 1984*). Important brain regions involved in regulating the lactational-period include the AC, VN and supraoptic nucleus (SoN) (reviewed in *Smiley et al., 2019*; *Figure 4*). Lactation is believed to have a rewarding effect on the maternal brain, which strengthens the bond between mother and child (*Bear et al., 2015*). A study from *Ferris et al.* (*2005*) demonstrated that the stimulus from suckling pups is more rewarding to dams than cocaine, exhibiting the importance of young-directed responses. Breastfeeding with lipid-rich milk is proven to be extremely advantageous for early brain development in infants (*Anderson et al., 1999*), and is associated with more optimal brain development and smaller ventricular volume (*Herba et al., 2012*).

For both resource allocation during and after gestation, the hypothalamus, specifically the AC, seems to play an extremely important role in the regulation of the energy balance. Any influence of the fetus via FMc in this part of the maternal brain could be beneficial for offspring survival post gestation.

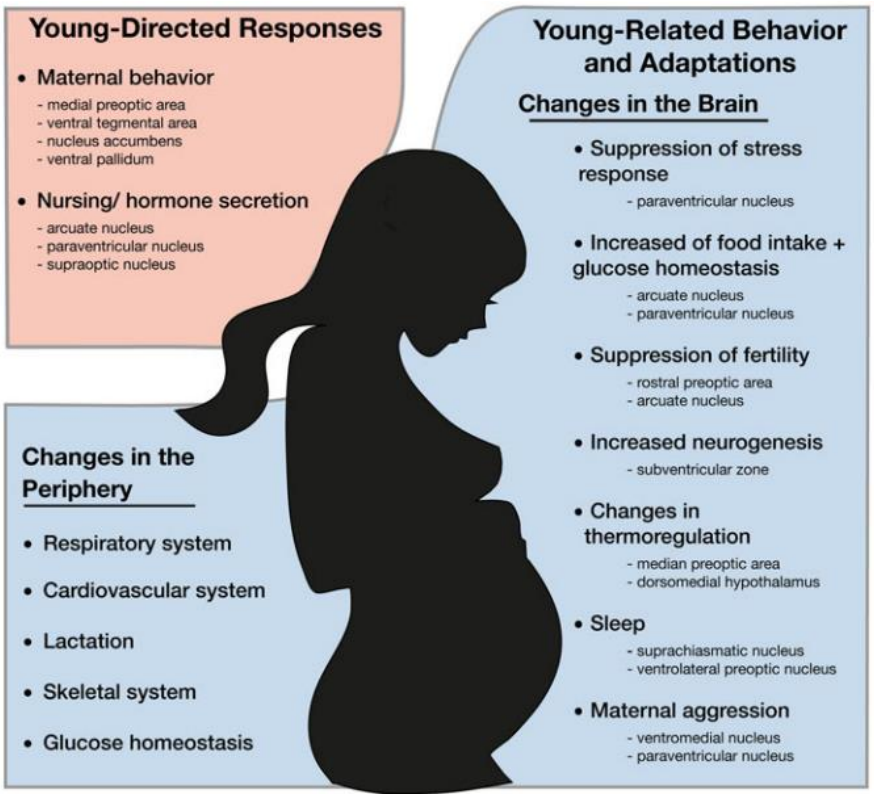

Figure 4: A summary of adaptations in the maternal body, accompanied by the major brain regions involved in orchestrating these adaptations. Neurologic changes can be divided in young-directed responses, for active response towards the offspring, and young-related behaviour and adaptations, to support the mother in displaying the adequate maternal behaviour. *Figure borrowed from Smiley et al. (2019).*

1.2.3 Fetal Microchimerism as an Extension of the Placenta Postpartum

As mentioned before, maternal behaviour, attachment and resource allocation show sides of interest for the FMCs to integrate in the maternal brain. Previous studies have shown that FMCs are possibly able to integrate in maternal neurocircuitry, to differentiate in the proper cell types to do so and could proliferate (*Tan et al., 2005; Zeng et al., 2010; Zhang et al., 2013*). As maternal care is extremely important for offspring survival and development, it would be beneficial for the offspring to have FMCs migrate to these sides of interest, associated with maternal care and resource allocation, in the maternal brain. Trophoblast cells, which are of fetal origin, are able to invade the maternal endometrium during the formation of the placenta. Therefore, it is not an off chance that FMCs, once in the maternal circulation, could be able to colonize other maternal tissues, and possibly remain there after partition. In this case, the FMc could act as an extension of the placenta post gestation. Whereas the placenta still as some influence on the mother, by secreting hormones, the FMCs could possibly take over after gestation. Via this pathway the FMCs could influence resource allocation, thermoregulation, and associated processes during gestation. Furthermore, they could influence lactation, attachment, and maternal behaviour post gestation (*Boddy et al., 2015*). This mechanism could be of evolutionary advantage to mother and offspring, possibly explaining why FMc evolved for millions of years through the eutherian phylogenetic tree.

1.3 Aim

The aim of the current pilot study was to successfully detect FMCs in the brains of murine mothers. The project is part of a larger study, but due to time and lab constraints we were not able to execute all the original plans. The data presented in this thesis will therefore focus on the first few pilots we have performed. First, our DNA extraction protocols were optimized, as FMCs are extremely rare in maternal tissues, it was of the utmost concern that our DNA extraction protocol worked properly, so

the DNA would be useful for subsequent analysis. Therefore, a large part of this thesis will be devoted to the optimization of DNA extraction from brain tissues, using the DNeasy Blood and Tissue Kit (QIAGEN, Germany). Second, a small qPCR pilot was performed where we assessed FMC by looking for extremely rare offspring-specific genes indicative of microchimerism (i.e., enhanced GFP) in brain, spleen, and lung tissues of wildtype mothers during and after gestation.

As mentioned above, maternal behaviour, attachment and resource allocation is extremely important for infant survival. Since FMCs bear the fetal genotype and natural selection is predicted to favour activities of FMCs that benefit those who share that genotype, we expect FMCs to be an extension of the placenta, to improve maternal behaviour and resource allocation, from the point of view of offspring, both pre- and post-gestation. Therefore, we expect FMc to be present in the maternal circulation at E18/E19, considering its proximity to the delivery and data from previous studies (*Fukjiki et al., 2008*). Most importantly, we expect to find FMc in the brain at this timepoint, even though *Zeng et al.* (*2010*) found no FMc on E16. Additionally, we sectioned the brain to be able to discover more about the location of the FMCs. We expected to find FMc in regions associated with maternal care, specifically the olfactory bulb (OB), Hypothalamus (specifically the MPOA), BSNT and MeA (i.e., midbrain). As *Zeng et al.* (*2010*) found that FMc could remain in the maternal brain until P210, we are hopeful we can find FMCs in the tissues of our females from later timepoints as well.

2. Methods

2.1 Animals

All experiments that were carried out for this study were in accordance with the Centrale Commissie Dierproeven (CCD) of the Netherlands (AVD1050020198884). For this study we used a specialized mouse breeding system. For analysing fetal microchimerism (FMc), which is the main scope of this thesis, we mainly used C57BL/6J-females from *Charles River Laboratories* (*USA*). Some of the samples we generated were from BALB/c-females, also from *Charles River Laboratories* (*USA*). The males for FMc were C57BL/6-Tg(CAG-EGFP)131Osb/LeySopJ (*The Jackson Laboratory, USA*). These males are homozygous for enhanced green fluorescent protein (eGFP), which is under the control of a chicken beta-actin promoter and cytomegalovirus enhancer. The eGFP-positive animals are fully green fluorescent under a dual fluorescent protein flashlight, (*Model DFP-1, Nightsea, USA*), with an exception for erythrocytes and hair (*The Jackson Laboratory, n.d.-a*).

Furthermore, we also collected tissues from surplus females that we received from the animal caretakes. These females had just weaned their pups. Details about all the females used in this study can be found in *Table 1*. Additional information about the animals used in this study can be found in *Appendix 7.1: Datasheet – Animal ID and Tissues*.

Table 1: Overview and details about the animals used in this study.

Animal ID	Age	Litter			Termination		Genetic background	Purpose
	(days)	Size	Date of birth	Date of weaning	Date	Days since weaning	Animal	
D	106	4	17/11/20	7/12/20	8/12/20	1	KO TNF-R1(C57BL/6J)	Optimization
E	141	5	17/11/20	7/12/20	8/12/20	1	C57BL/6J (Backcross)	Optimization
F	204	10	11/11/20	7/12/20	8/12/20	1	tg Camk2a-tTA(C57NL/6J)	Optimization
G	141	8	16/11/20	7/12/20	8/12/20	1	C57BL/6J (Backcross)	Optimization
H	103	9	17/11/20	7/12/20	8/12/20	1	KO TNF-R2(C57BL/6J)	Optimization
I	188	X	X	X	10/12/20	X	Pcdh9 KO(C57BL/6J)	Optimization
J	188	X	X	X	10/12/20	X	Pcdh9 KO(C57BL/6J)	Optimization
K	136	X	X	X	10/12/20	X	Pcdh9 KO(C57BL/6J)	Optimization
L	136	X	X	X	10/12/20	X	Pcdh9 KO(C57BL/6J)	Optimization
M	192	X	X	X	26/1/21	X	tg J20 B(C57BL/6J)	Optimization
1	253	8	11/11/20	10/12/20	25/3/21	105	C57BL/6J	qPCR-pilot
2	253	7	25/12/20	21/1/21	25/3/21	63	C57BL/6J	qPCR-pilot
9	138	10	X	X	30/11/20	X	C57BL/6J	qPCR-pilot
11	253	X	X	X	25/3/21	X	C57BL/6J	Optimization

12	138	8	X	X	30/11/20	X	C57BL/6J	qPCR-pilot
13	132	11	X	X	26/1/21	X	BALB/c	qPCR-pilot
14	132	9	X	X	26/1/21	X	BALB/c	qPCR-pilot
15	175	8	28/1/21	18/2/21	25/3/21	35	BALB/c	qPCR-pilot
30	175	8	28/1/21	25/2/21	25/3/21	28	C57BL/6J	qPCR-pilot
33 (M)	79	X	X	X	28/1/21	X	C5BL/6J-eGFP(+,-)	Optimization
39 (M)	84	X	X	X	17/3/21	X	C5BL/6J-eGFP(+,-)	Optimization
40 (M)	84	X	X	X	17/3/21	X	C5BL/6J-eGFP(+,-)	Optimization
41 (M)	84	X	X	X	17/3/21	X	C5BL/6J-eGFP(+,-)	Optimization
46 (M)	84	X	X	X	21/4/21	X	C5BL/6J-eGFP(+,-)	Optimization
49 (M)	84	X	X	X	21/4/21	X	C5BL/6J-eGFP(+,-)	Optimization

2.1.1 Housing

Our animals were kept on a 12h/12h dark-light cycle (13:00 light off) in a 20°C room. Food and water were provided ad libitum (*Altromin, Germany*). Animals were weighed weekly. Some females, relevant for our breeding system, were handled daily for estrus checks (see 2.1.3). The animals were otherwise not disturbed. Cages were cleaned on the same day as the weighing. All our females were group-housed, with a maximum of four animals per cage. Pregnant dams were separated a few days before parturition. Our homozygous eGFP males were single housed. Brothers generated for our breeding line were group-housed, with a maximum of three animals per cage. In case of excessive fighting, they were separated and housed individually. Every cage contained enrichment, e.g., a toilet roll, a shelter and nesting material. Pregnant dams were also provided with cotton rolls to support nestbuilding in their separate cages. Litters remained with their mother for three to four weeks until weaning.

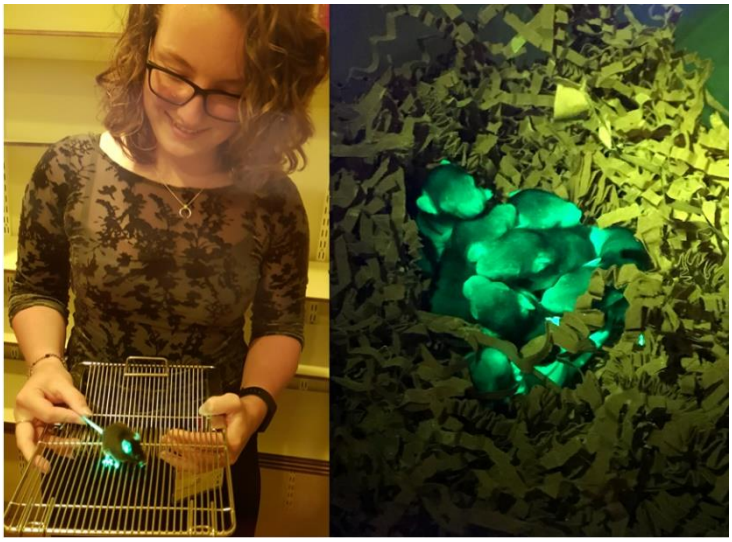

Figure 5: Images of hemizygous eGFP-positive mice from our breeding line. On the left you see me holding an adult hemizygous eGFP-positive female. On the right you see a litter of hemizygous eGFP-positive pups. Both images were taken using the Royal Blue-light of the dual fluorescent protein flashlight from Nightsea (Model DFP-1). *Photos were taken by H.J. Meindertsma and S. Smit.*

2.1.2 Breeding for experiment

For our breeding system we crossed a homozygous eGFP male with a wildtype female (C57BL/6J or BALB/c). This resulted in offspring that is hemizygous for eGFP (*Figure 5-6*). Both the homozygous eGFP males and the hemizygous eGFP offspring is fully green fluorescent under a special fluorescent lamp, with an exception for erythrocytes and hair (*The Jackson Laboratory, n.d.-a*). This breeding system allows us to track the fetal fluorescent cells of the offspring in the maternal circulation and tissues, as the mother is wildtype and thus shows no fluorescence of her own. Additionally, this model

allows us to analyse the influence of an immunologic challenge on the frequency of FMc. The homozygous eGFP males have a C57BL/6J background. When crossed with a C57BL/6J-female we expect no or a minimal immunologic challenge (*Model A-1 & A-2; Figure 6*). When crossed with a BALB/c-female we expect a slight immunologic challenge (*Model B-1 & B-2: Figure 6*) (*Appendix 7.1: Datasheet – Animal ID and Tissues*). BALB/c mice have a different genetic background and HLA haplotype compared to C57BL/6J mice (*ThermoFisher Scientific, n.d.-b*). The offspring will be a mix of two different HLA haplotypes and be genetically different from the mother. We want to analyse whether this has any effect on the frequency of the FMc in the maternal body.

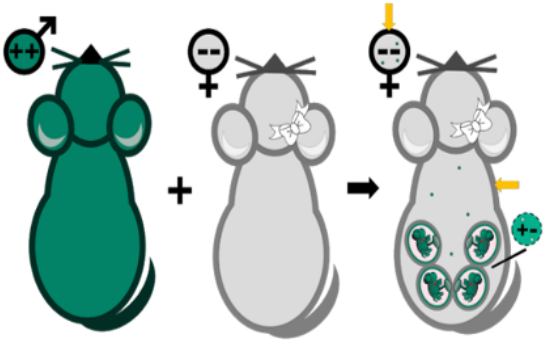

Model	Genotype	Timepoint
A-1	C57BL/6J	E18/E19
A-2	C57BL/6J	Later
B-1	BALB/c	E19/E19
B-2	BALB/c	Later
C	Surplus animals	

Figure 6: An overview of our breeding model. Homozygous eGFP-positive males were crossed with wildtype females, this resulted in hemizygous eGFP-positive offspring. Both the homozygous male and the offspring are fully green. Different maternal genotypes and timepoints were analysed. Surplus animals (Model C) were used for optimization. (E18/E19: gestational day 18/19). *Figure (left) borrowed from J.R. Smit; Table (right) created by S. Smit.*

As mentioned before, surplus animals were also used for this study. We received these females from the animal caretakers and were from non-specific breeding systems. Mostly, these contained females with a C57BL/6J-background who had weaned their pups some time before (*Table 1*). Tissues from the surplus females were mostly used in the optimization of DNA Extraction (*Chapter 3*) and for exploratory research regarding later timepoints after gestation.

2.1.3 Estrus Checking

Female estrus cycle was checked for females to be used in our experiment. Checking occurred only when we had an experiment planned, for which we had to know the exact day of gestation. Estrus checks were performed with two different methods. First, estrus checks were performed with vaginal lavage. For this we used autoclaved demi water, 300µl filter pipette tips and a latex bulb. The lavage was performed by pipetting one droplet up and down at the surface of the vagina. The droplet from the vaginal lavage was placed on a microscope slide. We waited till the droplet dried before proceeding with the staining (*McLean et al., 2012*). Later, we switched to using inoculating loops for estrus checks in mice. The loop was dipped in autoclaved demi water, inserted superficially, and turned a little inside the vagina. The sample was smeared out on a microscope slide and left to dry.

A Giemsa-staining was used for the staining of the estrus checks. We used a 50mM Tris-HCl buffer (*Tris Base, Roche Diagnostics GmbH, Germany*) + 0,9% NaCl (pH: 7,0-7,4) and filtered Giemsa (*Giemsa azure eosin methylene blue solution, Merck KGaA, Germany*). One staining basin contained 8,75 mL filtered Giemsa and 119mL 50mM Tris-HCl. The slides with the estrus checks were placed in the Giemsa-staining for ten minutes. The back of the slides was rinsed first with tap water, and then with demi water. Thereafter, the slides were dried before assessing the estrus stage under the microscope.

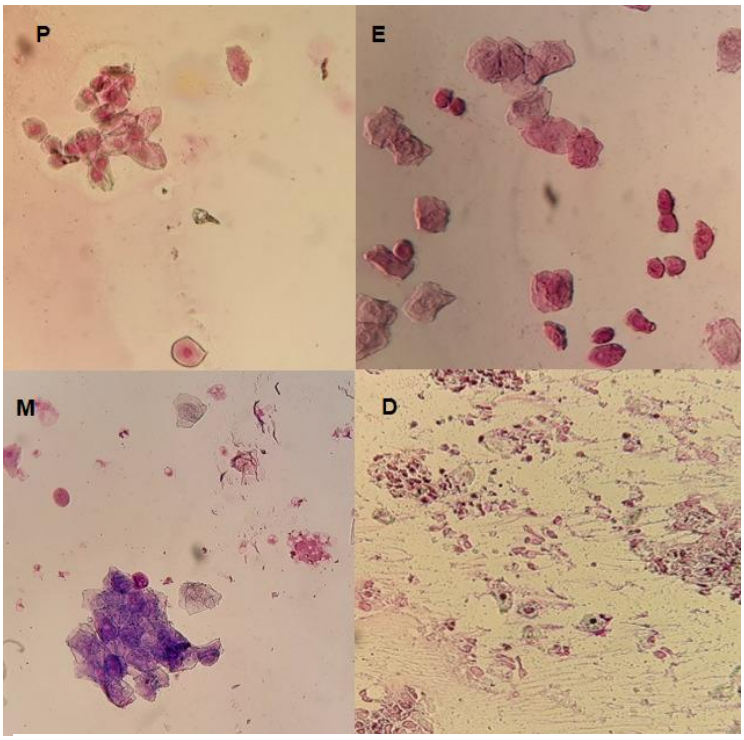

Figure 7: Characteristic cells for each of the four phases in the murine estrus cycle. In the proestrus phase mostly nucleated epithelial cells are found (P). In the estrus phase the females are receptive. This phase is characterized by cornified epithelial cells (E). In the metestrus a combination of cornified epithelial cells and leukocytes is found (M). In the diestrus phase primarily leukocytes are found (D). *Figure made by M.E. de Jong.*

With microscopy we looked for cornified epithelial cells, which indicate that the female is in the estrus-phase of estrus-cycle (*McLean et al., 2012*) (*Figure 7*). If the female was found to be in estrus, she was placed with a male during the dark phase of that same day. If the mating was successful, the day after the female was placed with the male would be gestational day 1. Pregnancy was identified by weight-gain approximately ten days after mating (*Appendix 7.2: Protocol – Estrus Checks*).

2.1.4 Termination

Pregnant females were terminated on gestational day 18 or 19 (E18/E19). First, the females were anesthetized. Anaesthesia was induced with 5,0% isoflurane and was maintained with 2,0% isoflurane via inhalation. Subsequently, a cardiac puncture through the skin was performed and blood was collected. The uterus, containing the foetuses, was removed prior to saline perfusion (0,9% NaCl + Heparin 500U/ml). Females were cut open, a needle was inserted in the left ventricle, and the right atrium was cut. The females were decapitated as secondary measure of termination. Animals from model A-2/B-2 and surplus animals (Model C) were sacrificed using a full CO_2 procedure and decapitated as secondary measure of termination (*Appendix 7.3: Protocol – Termination*).

After decapitation the brains of the females were first collected. Thereafter, other organs were collected. All tissues were washed with washing solution (0,01M PB) and dried before processing. For most animals half of the tissues were frozen for qPCR analysis, whereas some would be fixed in PFA for immunohistochemistry (*Table 2*). The immunohistochemistry part of the project will not be discussed in this thesis. Most brain samples used in this thesis are from one hemisphere, which was determined randomly. In some cases, we did collect the whole brain for qPCR analysis. Additionally, the tails of the foetuses were taken and frozen to determine embryo sex.

Table 2: Overview of the tissues collected from each animal used in this study. The underlined organs are of interest in the current study.

Tissues collected from each animal used in this study		
Tissue	**Frozen**	**PFA**
Brain	X	X
Mammary Gland 4	X	X
Mammary Gland 5	X	X
Pancreas	X	
Spleen	X	
Liver	X	X
Lungs	X	X
Heart	X	
Thymus	X	
Thyroid	X	
Adrenal Gland	X	X
Kidney	X	X
Ovary	X	X
Uterus (if not pregnant)	X	
Stomach	X	
Muscle (Hindleg)	X	
Mesenteric white adipose tissue	X	
Perirenal white adipose tissue	X	
Retroperitoneal white adipose tissue	X	
Subcutaneous brown adipose tissue	X	

2.2 Tissue Processing

The blood collected from the cardiac bleed was centrifuged at 5°C for 10 minutes. The blood plasma was collected and stored in -80°C until further notice. All the organs collected for qPCR were snap frozen with liquid nitrogen and stored in -80°C until further use. Before DNA extraction the organs were cut into smaller sections in the cryostat at -20°C (*Slee MNT, Slee Medical GmbH, Germany*). For the brains we used a brain matrix for accurate cutting. Other organs were cut in a glass petri-dish. For cutting we used razor blades (*single edged razor blades, GEM Scientific, USA*). All sections were weighed and cut according to the optimal DNA extraction weight, as reported by the kit we used and by our own optimization (details per organ in *Table 3*). Between cutting and transportation the sections were stored in dry ice. Eventually, these sections were stored in -80°C until further use (*Appendix 7.4: Protocol – Tissue cutting in the Cryostat*).

Table 3: Overview of the target weights for each organ while sectioning. All sections were weighed and cut according to the optimal DNA extraction weight, as reported by the kit we used and by our own optimization.

Organ	Target Weight
Brain	20 – 40 mg
Spleen	10± mg
Lung	15 – 25 mg

2.3 qPCR

2.3.1 DNA Extraction

DNA from the sectioned tissues was extracted using the *DNeasy Blood and Tissue Kit* from *QIAGEN* (*Germany*) (*QIAGEN, n.d.*). After an initial pilot extraction according to the protocol in the handbook of the DNeasy Kit, we decided that the protocol needed optimization. As FMc is known to be extremely rare, it was of the utmost concern to make our DNA extraction as efficient as possible. The

process of optimization can be found in *Chapter 3* of this thesis. The original DNeasy Blood and Tissue protocol and our optimized protocol can be found in Appendix 7.8 and Appendix 7.9, respectively. The beads used for the *TissueLyser II* (*QIAGEN, Germany*) were cleaned according to protocol (*Appendix 7.5: Protocol – Bead Cleaning*).

2.3.2 qPCR Procedure

To detect FMc in the maternal tissues we performed a qPCR analysis on the StepOnePlus (Applied Biosystems, USA). For the qPCR pilot we used the assay the Jackson Laboratory recommended for genotyping the eGFP mice. IDT manufactured the assays and the gBlock. Assay details are shown in *Table 4* The assay contained double quenched probes. Double quenched probes increase qPCR sensitivity and precision, which would improve our chances of detecting eGFP in the maternal tissues (*Packer, 2013*). The assays were resuspended in IDTE (pH=8,0, 0,2µm filtered, IDT, USA) to reach a x20 concentration. The sensitivity and quality of the assay was tested in a gBlock dilution series, which would be used as our standard in further experiments. Later we tested the assay on ear notches taken from mice from our own breeding line to distinguish homozygous and hemizygous individuals.

Table 4: Details about the GFP assay, Apob assay and gBlock used for the qPCR-pilot.

	Primers/Probe	Reporter dye	5' ----------> 3'	Quencher	Wavelength (nm)	Size (bp)
GFP	fwd-GFP		AGTGCTTCAGCCGCTACC			96
	rev-GFP		GAAGATGGTGCGCTCCTG		*Ab: 494*	
	probe-GFP	*FAM*	TTCAAGTCCGCCATGCCCGAA	*ZEN / Iowa Black FQ*	*Em: 518*	
Apob	fwd-Apob		CACGTGGGCTCCAGCATT			78
	rev-Apob		TCACCAGTCATTTCTGCCTTTG		*Ab: 538*	
	probe-Apob	*VIC/SUN*	CCAATGGTCGGGCACTGCTCAA	*TAO / Iowa Black RQ*	*Em: 554*	
gBlock	x	x	GCATCTTGGTTCCCGCACGTGGG AGGCCCATCCCGGCCTTGAGCA CAATGACCCGCGCTCCTCGTTGC CCCGCGGTGCGCTCTCTGCTGC GCAGCCGATACCGGGAGGTGTG GCCGCTGGCAATTTTTGGAAGGA GCAGGACCTTTTTCATGACAGGA GAAAAGTCAGTATCTAAACCAACT AGGAATCTCAGACTTAAAAATCAT AGCAAGGGGGAGTGTTGGCATA GGTAGGAGAAAAGGCCAGTGTCA	x	x	251

The original plan was to assess FMc frequency in our own animals (Models A+B) with GFP and with SRY for surplus animals we received from the animal caretakers (C). Unfortunately, due to time constraints and problems with the qPCR machine, we were only able to assess FMc frequency in our own animals. Where the GFP signal was compared to Apob (endogenous control) and standardized to the gB-dilution. The settings for the qPCR cycling can be found in *Figure 8*. The full qPCR protocol can be found in *Appendix 7.6: Protocol – qPCR*. Furthermore, the plate set-ups can be found in *Appendix 7.16: qPCR Plate Set-ups*.

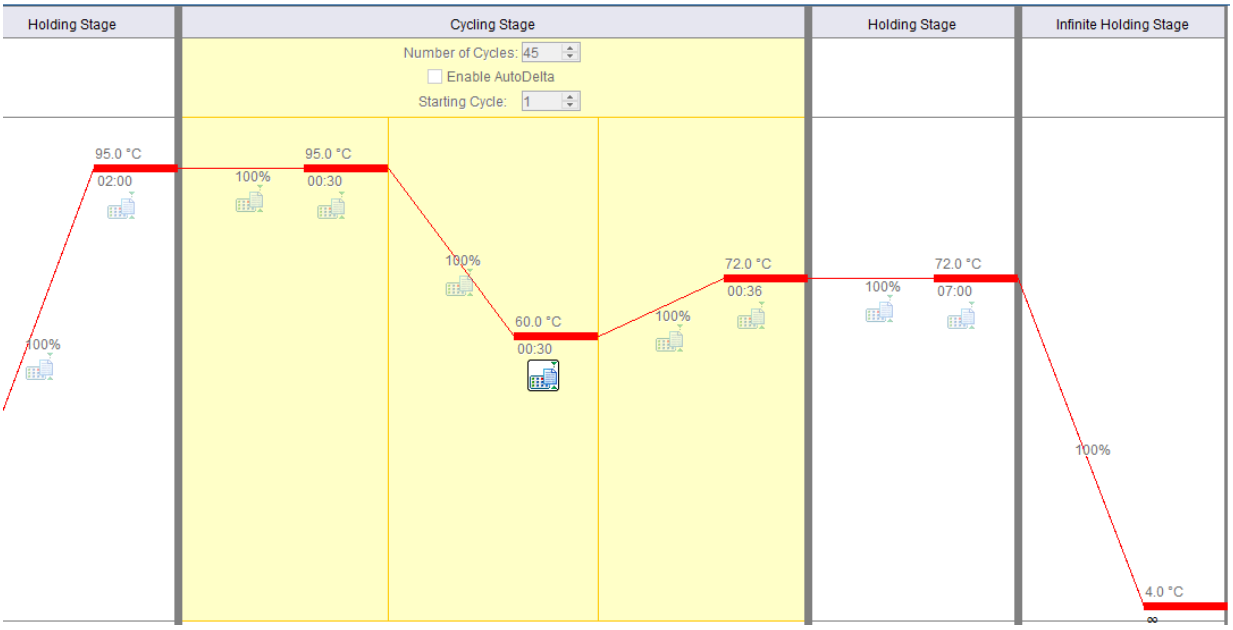

Figure 8: An overview of the settings for our qPCR-cycling during the pilot. We used 45 cycles with a denaturation phase at 95°C for 30 seconds, followed by an annealing phase at 60°C for 30 seconds. Lastly, we had an extension phase for each cycle at 72°C for 36 seconds. *Figure was taken from the StepOnePlus-software (run method).*

2.3.4 Statistical Analysis

All statistical analyses were performed in Prism (*Version 6.01, GraphPad, USA*). First, our datasets were checked for normal distribution with the D'Agostino & Pearson omnibus normality test. If the data had a normal distribution, comparison between two columns was performed using the unpaired t-test. Comparison between multiple groups was performed with a one-way ANOVA, including multiple comparisons. If the dataset had no normal distribution, comparison between two columns was performed using the Mann-Whitney U test. Comparison between multiple groups was then performed using a Kruskal-Wallis test, including multiple comparisons. Non-Gaussian data, and therefore a non-parametric test will be indicated with brackets enclosing the data, with an exclamation mark. When analysing for the effects of pregnancy in combination with organ-type, a two-way ANOVA, with multiple comparisons was performed. Additionally, the mean, SD and SEM were calculated for all datasets. This procedure was used for both the results of DNA Extraction Optimization and the qPCR-pilot.

2.3.4.1 qPCR-pilot

The data from the qPCR-pilot was generated by the software of the StepOnePlus (*Applied Biosystems, USA*). Here we used the quantities of both Apob and GFP in further calculations (that were based on the standard curve generated by the gBlock dilution series). Additionally, we analysed the amplification data from the StepOnePlus in LinRegPCR (*version 2018.0*). LinRegPCR generated the Cq-values and Individual Efficiency of each well. The same statistical procedure as described above was used to analyse this data. However, for the quantities and frequencies of GFP/Apob (which were calculated by dividing the quantity of Apob by the quantity of GFP, as calculated by the StepOnePlus) we used the ROUT-method with a false discovery rate (FDR) of Q=0,1%, to identify definite outliers

3. DNA Extraction Optimization

3.1 Introduction

Extracting DNA from the cells is necessary before we could perform a qPCR or other subsequent analysis. To isolate DNA from the cells, different methods have been developed by researchers. The DNeasy Blood and Tissue Kit from QIAGEN uses a silica-based extraction, based on column with a silica membrane. In this method the DNA binds to the silica membrane, with the assistance of chaotropic salts. With following washings steps proteins and other contaminants are washed away. Finally, the DNA is eluted from the membrane (*New England Biolabs, n.d.*).

3.1.1 Reagents of the DNeasy Blood and Tissue Kit

The DNeasy Blood and Tissue Kit from QIAGEN contains several reagents. Though the exact content of each buffer is classified, some information about the function of each buffer is available. Known information of the included reagents will be elaborated below.

Buffer ATL

The Buffer ATL is a tissue lysis buffer. This buffer contains Sodium Dodecyl Sulfate (SDS). SDS is an anionic surfactant which acts as a detergent in cell lysis. It disrupts non-covalent bonds in proteins to denature and unfold the proteins of the cell membrane (*VanDerBilt University, 2019*)

Proteinase K

Proteinase K is a catalysing enzyme that aids in the breakdown of cellular proteins by splitting them into smaller peptides and/or amino acids. Additionally, it degrades nucleases, which in turn protects the DNA (*VanDerBilt University, 2019*). The SDS in the ATL buffer increases the Proteinase K activity (*AG Scientific, 2021*). Furthermore, during this protocol the lysis will be incubated at 56 °C. A temperature above 50 will unfold some proteins, making it easier for Proteinase K to reach them (*AG Scientific, 2021*). Additionally, this is improved by placing the samples in a water bath or vortexing them regularly.

Buffer AL

The Buffer AL is also classified as a lysis buffer. This buffer promotes cell membrane lysis, denaturation of proteins and other macromolecules. Furthermore, it inactivates nucleases. This protects the DNA. Lastly, this buffer promotes binding of the DNA to the pure silica material of the spin column. The chaotropic agent in this buffer is called Guanidine Hydrochloride. It interferes with the hydrogen bonds, hydrophobic effects, and Van Der Waals forces. This leads to accumulation of the chaotropic salts in the cell lipid bilayer, compromising its integrity, which leads to membrane collapse. Also, chaotropic salts interrupt the hydrogen bonds between the DNA stands. This facilitates the binding of DNA to the pure silica material of the spin column, by making the strands hydrophobic (*VanDerBilt University, 2019*)

Buffer AW1 and AW2

Less information could be found about both Buffer AW1 and Buffer AW2. Both buffers are washing buffers, designed to wash away everything in the column, except for the DNA. Buffer AW1 is said to be a more stringent wash to remove proteins and contains guanidine hydrochloride. Therefore, this wash buffer still promotes DNA binding to the silica membrane. The Buffer AW2 is said to be a Tris-based ethanol solution. This removes the chaotropic salts, so only the DNA should remain (*Protocol Online, 2013*).

Buffer AE

Buffer AE is the Elution Buffer, which elutes the DNA from the membrane. This buffer contains 10 mM Tris-Cl, 0,5 mM EDTA and has a pH of 9,0. AE elutes the DNA by rehydrating it, so it will come

loose from the membrane. Additionally, this buffer allows stable storage of DNA for years in either the refrigerator or freezer (*QIAGEN, 2020; VanDerBilt University, 2019*)

3.2 Progress

The handbook of the DNeasy Blood and Tissue Kit provided us with a protocol for the use of the mini-spin columns. Additionally, QIAGEN provided us with a user-protocol, which implemented the use of the TissueLyser II (*QIAGEN, Germany*). Before we started the optimization, we tried both protocols, with and without TissueLyser. The original protocol provided by QIAGEN can be found in Appendix 7.8: Protocol – QIAGEN DNeasy Blood and Tissue Kit.

3.2.1 Extraction 1 - Practice

The first time we used the DNeasy Blood and Tissue Kit we tried the user protocol, including the TissueLyser II, on two practice samples. The practice samples were from brain J, a C57BL/6J-female acquired from the animal facility (*Table 1*). Two sections were cut in a petri dish at room temperature before being disrupted with the TissueLyser II at 15Hz for 20 seconds. We quantified the extracted DNA using a Nanodrop One (*ThermoFisher Scientific, USA*). We saw an extremely low concentration, as well as high impurity of the extracted DNA. However, the initial aim of this practice extraction was to familiarize ourselves with the protocol. Eventually, we decided to proceed without the TissueLyser II at first, as it required additional steps to be added to the protocol and thus a higher workload, with the risk of shearing the DNA. Data from this extraction was lost.

3.2.2 Extraction 2 – Setting a baseline

For this extraction we used Brain G, which was a surplus brain of a C57BL/6J-female from the breeding line of the animal facility (*Table 1*). We performed the extraction according to the protocol provided by QIAGEN in the handbook of the kit, this time without the TissueLyser II (*Table 5*). We had a total of twelve samples with a mean weight of 14,9mg. After the extraction we immediately quantified our DNA with the Nanodrop One. We found that our samples had a mean concentration of 80,17ng/µl, which equals a mean yield of 16,03µg (dissolved in 200µl AE buffer) (*Figure 9*). The handbook states that the expected yield when using 25mg brain tissue was 15-30µg. We normalized the data with the weight of the samples, resulting in a mean yield/weight of 124,441 µg/mg (*Figure 9*). Therefore, we concluded that even though our mean starting weight was lower, we expected that we could significantly improve our DNA concentrations after some optimization.

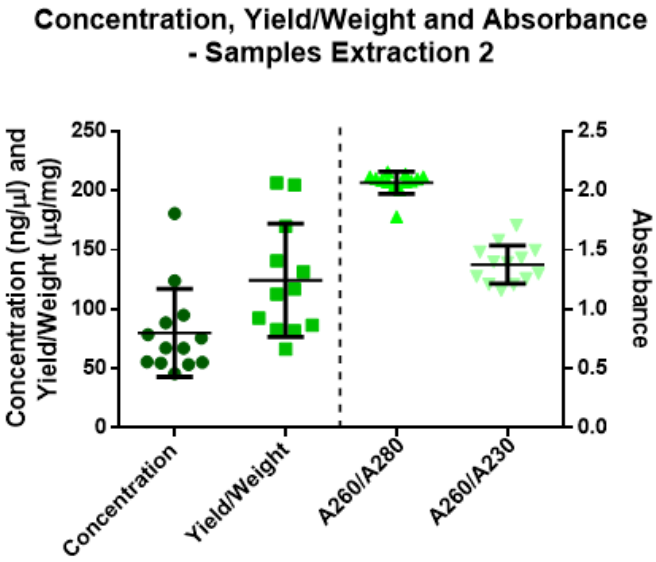

Figure 9: Concentration, yield/weight, and Absorbance-ratios from extraction 2. Yield/weight was calculated by dividing the yield (µg) (concentration*200µl*0,001) by the sample weight (mg).

We also wanted to assess the purity of our DNA sample. The Nanodrop provides two ratios to assess the purity of a sample. The first ratio is A260/A280 and is indicative of RNA contamination. The A260/A280 for dsDNA should be approximately ~1,8, this indicates "pure" DNA. Higher values, of approximately ~2,0 indicate the presence of RNA in the sample (*ThermoFisher Scientific, n.d.-c*). Our mean A260/A280 for this extraction was 2,066, which clearly indicates that there was RNA in our sample (*Figure 9*). For our subsequent analysis with the qPCR this would not be a problem. However, at the time it seemed best for us to strive for as pure DNA as possible. The second ratio the Nanodrop

provides is the A260/A230 ratio, which gives an indication about the general purity of your nucleic acid. This ratio should between 1,8-2,2. Lower ratios could indicate contamination with proteins, ethanol, guanidine HCl, EDTA or even silica from the column membrane (*Koetsier & Cantor, n.d.*). Late, we discovered that the A260/A230 ratio is correlated with the DNA concentration, with a lower DNA concentration yielding a lower ratio (*Koetsier & Cantor, n.d.*). Our mean A260/A230 for Extraction 2 was 1,377 (*Figure 9*), too low to even determine what exactly was contaminating our sample.

With this data we set up an optimization plan, which we hoped to optimize within two weeks. However, this turned out to be a process that would take up a lot more of our time. We knew we had to use RNase to remove RNA contamination from our DNA samples. This reagent had a longer delivery time than expected, so we started optimizing the A260/A230 first. We decided on an extra wash with the AW2 buffer, which is an extra step done by several other users of the DNeasy Blood and Tissue Kit.

3.2.3 Extraction 3 – Adding extra wash step with AW2

For this extraction we used brains D and L, both from females with a C57BL/6J background acquired from the animal facility (*Table 1*). We followed the original protocol from QIAGEN, without the TissueLyser II. We added a washing step for all the samples from brain L (*Table 5*). As mentioned before, AW2 is a Tris-based ethanol wash, which removes chaotropic salts from the membrane. With our low A260/A230 from the previous extraction, we hypothesized that we had contamination in our sample following the extraction. This could either be proteins, ethanol, guanidine HCl, EDTA or even silica material from the membrane (*Koetsier & Cantor, n.d.*). As AW1 still contains guanidine HCl, we decided to wash twice with AW2. The first time we would centrifuge only one minute at 14,000rpm, as the full three minutes accompanying the wash was functioning as a dry spin, to eliminate ethanol contamination. The second wash we would centrifuge for three minutes at 14,000rpm (*Table 5*).

Samples from brain D had a mean weight of 24,625 mg. Brain D had a mean concentration of 70,141ng/µl, which equals a mean yield of 14,028 µg (dissolved in 200µl AE buffer) (*Figure 10*). Samples from brain D had a mean yield/weight of 74,923 µg/mg (*Figure 10*). Compared to Extraction 2, this is a great deal lower. Furthermore, brain D had A260/A280- and A260/A230-ratios of 2,057 and 1,292, respectively (*Figure 10*). Samples from brain L had a mean weight of 23,155 mg. Brain L yielded a mean concentration of 59,146 ng/µl, which equals a mean yield of 11,829 µg (dissolved in 200µl AE buffer) (*Figure 10*). Samples from brain L had a mean yield/weight of 61,868 µg/mg (*Figure 10*). Lastly, brain L had A260/A280- and A260/A230-ratios of 2,054 and 1,147, respectively (*Figure 10*). Despite lower values seen in brain L, we saw no significant difference between brain D (1x AW2) and brain L (2x AW2) for any of the parameters (Concentration, Yield/Weight, A260/A280 and A260/A230) (*Figure 10*). Therefore, there was no significant effect of the second AW2-wash. However, we hypothesized that it could possibly be due to the shorter spinning time for the first AW2 wash of brain L. This could have resulted in additional ethanol contamination, and we later realised that concentrations under 200 ng/µl measured by the NanoDrop never reach an A260/A230-ratio of 2.0, as that result is DNA concentration dependent.

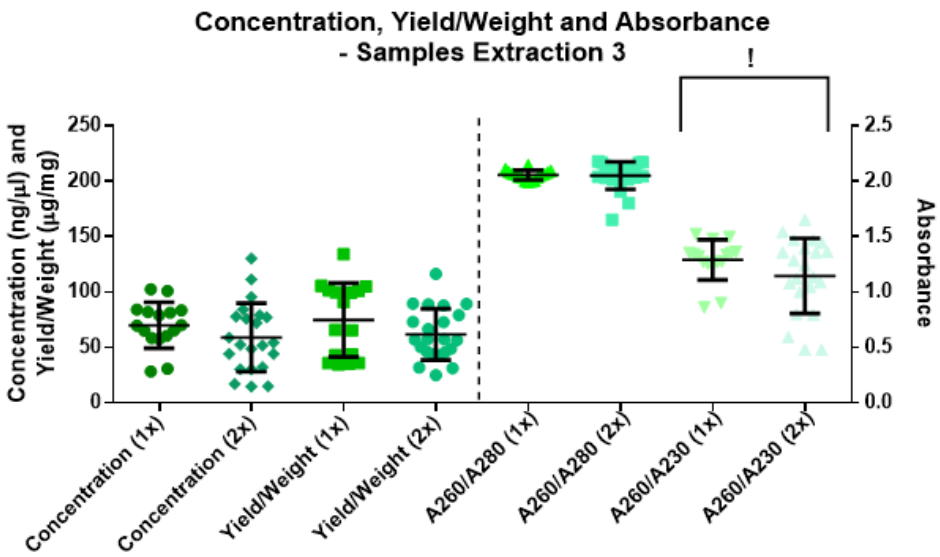

Figure 10: Concentration, yield/weight, and Absorbance-ratios from extraction 3 – 1x AW2 vs. 2x AW2. No significant differences were found between one wash with AW2 and two washes with AW2 for any of the parameters. Statistical analysis of the A260/A230 was performed using the Mann Whitney U test (!). Yield/weight was calculated by dividing the yield (µg) (concentration*200µl*0,001) by the sample weight (mg).

3.2.4 Extraction 4 – Premixing and dry spinning

For this extraction we used samples from brains E, H and J. All samples were from females with a C57BL/6J background acquired from the animal facility (*Table 1*). We adjusted the original protocol from QIAGEN, without the TissueLyser II, and created four different protocols. All protocols had the two washing steps with AW2, both times followed by centrifuging for three minutes at 14,000rpm. For protocol A this was the only adjustment. Protocol B and D both contained an additional dry spin after the second AW2 wash of three minutes at 14,000rpm (*Table 5*). Furthermore, we decided to look at the effects of premixing AL and ethanol. Therefore, we included a premixing step in protocols C and D (*Table 5*).

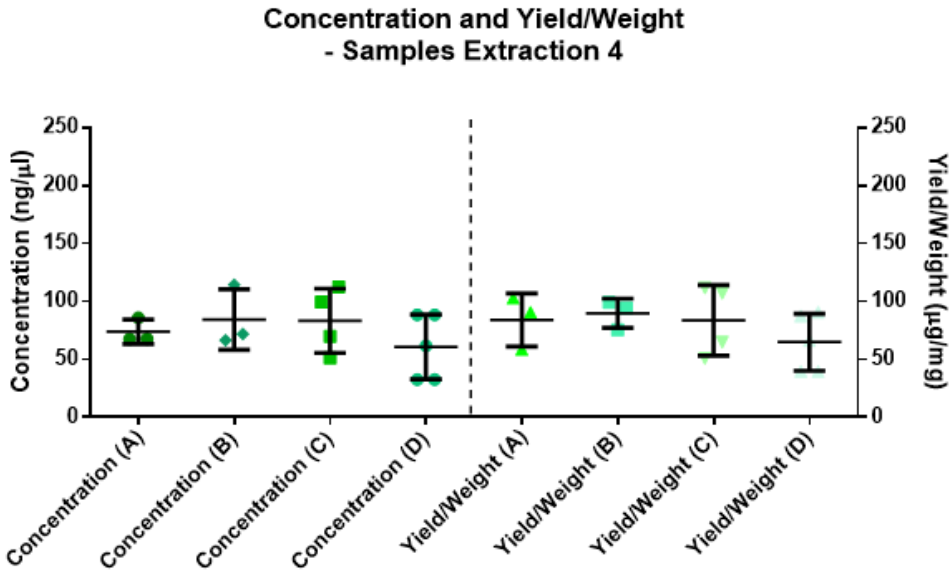

Figure 11: Concentration and yield/weight from extraction 4 – Protocols A-D. No significant differences were found between the four protocols for any of the parameters. Yield/weight was calculated by dividing the yield (µg) (concentration*200µl*0,001) by the sample weight (mg).

Samples from protocol A had a mean weight of 18,4 mg. Protocol A yielded a mean concentration of 73,771 ng/µl, which equals a mean yield of 14,754 µg (dissolved in 200µl AE buffer) (*Figure 11*). Samples from protocol A had a mean yield/weight of 84,100 µg/mg (*Figure 11*). Furthermore, protocol A had A260/A280- and A260/A230-ratios of 2,081 and 1,428, respectively. Samples from protocol B had a mean weight of 18,9 mg. Protocol B yielded a mean concentration of 84,352 ng/µl, which equals a mean yield of 16,870 µg (dissolved in 200µl AE buffer) (*Figure 11*). Samples from protocol B had a mean yield/weight of 89,791 µg/mg (*Figure 11*). Furthermore, protocol B had A260/A280- and A260/A230-ratios of 2,073 and 1,491, respectively. Samples from protocol C had a mean weight of 20,125 mg. Protocol C yielded a mean concentration of 83,333 ng/µl, which equals a mean yield of 16,667 µg (dissolved in 200µl AE buffer) (*Figure 11*). Samples from protocol C had a mean yield/weight of 83,721 µg/mg (*Figure 11*). Furthermore, protocol C had A260/A280- and A260/A230-ratios of 2,057 and 1,435, respectively. Samples from protocol D had a mean weight of 18,620 mg. Protocol D yielded a mean concentration of 60,758 ng/µl, which equals a mean yield of 12,152 µg (dissolved in 200µl AE buffer) (*Figure 11*). Samples from protocol D had a mean yield/weight of 64,798 µg/mg (*Figure 11*). Furthermore, protocol D had A260/A280- and A260/A230-ratios of 2,111 and 1,269, respectively.

We found no significant difference between the four protocols for any of the parameters (concentration, yield/weight, A260/A280 and A260/A230) (*Figure 11*). However, after adding the second AW2-wash, with both times centrifuging for 3 minutes at 14,000rpm, we did see a slight improvement in the A260/A230 compared to Extraction 3. Therefore, we decided to include the extra wash in our protocol from hereon.

3.2.5 Extraction 5 – TissueLyser II

After ruling out guanidine HCl and ethanol contamination by adding a washing step and centrifuging thoroughly, respectively, only proteins, EDTA and silica material remained as possible contaminants. After consulting troubleshooting section of the handbook of the DNeasy Blood and Tissue Kit, we decided to go ahead and try the use of the TissueLyser II. Additionally, in accordance with the trouble shooting of the handbook, we decided to pipette the mixture onto the column in two steps, to prevent obstruction of the membrane (*Table 5*). For this extraction we used samples from brains E, H, J and M. All samples were from females with a C57BL/6J background, acquired from the animal facility (*Table 1*). We used a total of five different settings for the TissueLyser II (15Hz, 20s; 15Hz, 1m; 30Hz, 20s; 30Hz, 1m; 30Hz, 2x1m) (*Table 5*).

The samples had a mean weight of 26,16 mg. Extraction 5 yielded a mean concentration of 174,479 ng/µl, which equals a mean yield of 34,895 µg (dissolved in 200µl AE buffer) (*Figure 12*). Samples had a mean yield/weight of 132,921 µg/mg (*Figure 12*). Furthermore, extraction 5 had A260/A280- and A260/A230-ratios of 2,042 and 1,892, respectively (*Figure 12*). This is notably improved, compared to previous extractions. Additionally, pipetting the mixture onto the column in two steps also improved the parameters slightly. Therefore, we decided to proceed with the TissueLyser II and pipetting in two steps from hereon.

3.2.6 Extraction 6 – RNase

A while after we started optimizing the DNA Extraction the RNase finally arrived. We had been waiting with anticipation, because we were very hopeful that the RNase would significantly improve the A260/A280. For this extraction we used samples from brains 40 and 41. These were acquired from hemizygous eGFP-positive males from our own breeding line (*Table 1*). Aside from adding 4µl RNase after the lysis, we also included a second elution, to acquire as much DNA as possible (*Table 5*).

The samples had a mean weight of 32,28 mg. Extraction 6 yielded a mean concentration of 120,21 ng/µl, which equals a mean yield of 24,041 µg for the first elution (dissolved in 200µl AE buffer) (*Figure 12*). Samples had a mean yield/weight of 102,72 µg/mg (*Figure 12*). Furthermore, the first elution of extraction 6 had A260/A280- and A260/A230-ratios of 1,863 and 1,449, respectively

(*Figure 12*). For the second elution, the concentration and yield were a lot lower. This was expected, as the second elution elutes any leftover DNA from the membrane. The second elution had a mean concentration of 21,25 ng/µl, which equals a mean yield of 2,125 µg (dissolved in 100µl AE buffer). The second elution had a mean yield/weight of 8,681 µg/mg. Lastly, the second elution of extraction 6 had A260/A280- and A260/A230-ratios of 1,877 and 0,708, respectively. In *Figure 12*, the result from extraction 5 and the first elutions of extraction 6 are compared. The concentration of samples from extraction 5 is significantly higher, compared to the samples of extraction 6 (*p=0,0238*) (*Figure 12*). Furthermore, the yield/weight of extraction 5 is significantly higher, compared to the samples of extraction 6 (*p=0,0052*) (*Figure 12*). In hindsight, we should have performed statistical tests, while working through this optimization. This would have saved us from a lot of issues and will be discussed later on. For extraction 6 we were primarily focussed on lowering the A260/A280-ratio by using RNase, in which we succeeded. The A260/A280-ratio of samples of extraction 6 are significantly lower, compared to extraction 5 (*p<0.0001*) (*Figure 12*). Finally, the A260/A230-ratio of the samples of extraction 6 dropped significantly, compared to extraction 5 (*p=0,0082*) (*Figure 12*). However, we also discovered that this probably was affected by the lower concentration, as we removed all the possible contaminants from our protocol.

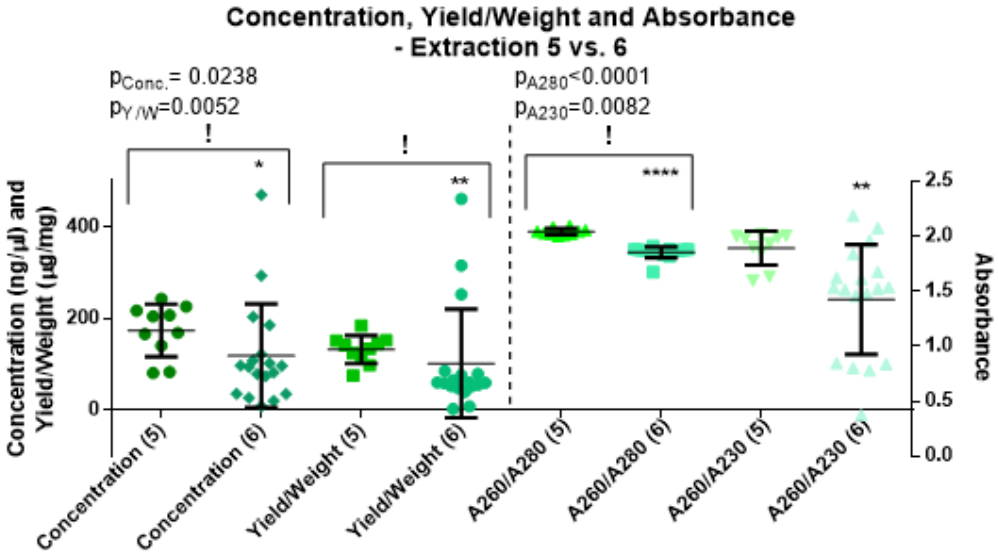

Figure 12: Concentration, yield/weight, and Absorbance-ratios from extraction 5 and 6. The concentration of extraction 5 was significantly higher, compared to extraction 6 (*p=0.0238*). Additionally, the yield/weight of extraction 5 was significantly higher, compared to extraction 6 (*p=0.0052*). The A260/A280 of extraction 6 was significantly lower, compared to extraction 5 (*p<0.0001*). Lastly, the A260/A230 of extraction 5 was significantly higher, compared to extraction 6 (*p=0.0082*). Statistical analysis of the concentration, yield/weight and the A260/A280 was performed using the Mann Whitney U test (!). Yield/weight was calculated by dividing the yield (µg) (concentration*200µl*0,001) by the sample weight (mg). Significance: * = *p<0.05*, ** = *p<0.01*, **** = *p<0.0001*.

3.2.7 Extractions 7 - 11 – Issues

We continued to use the RNase for the next four extractions. However, we ran into some issues. For extraction 7 we used samples from brain 39, acquired from a hemizygous eGFP-positive male from our own breeding line (*Table 1*). The aim of this extraction to see whether it was better to leave the lysis for approximately three hours (extraction 6) or to leave it overnight (extraction 7) (*Table 5*).

The samples had a mean weight of 23,12 mg. Extraction 7 yielded a mean concentration of 56,638 ng/µl, which equals a mean yield of 11,327 µg (dissolved in 200µl AE buffer) (*Figure 13*). Samples had a mean yield/weight of 44,664 µg/mg (*Figure 13*). Furthermore, extraction 7 had A260/A280- and A260/A230-ratios of 1,846 and 1,257, respectively (*Figure 13*). We found no significant differences in concentration, yield/weight or A260/A230-ratio between extraction 6 and extraction 7 (*Figure 13*). However, the A260/A280-ratio of extraction 6 was slightly higher compared to extraction 7 (*p=0,0360*) (*Figure 13*). Our main issue after this extraction was the low concentrations, yield/weight and the subsequent A260/A230-ratio. We were right back at the start of the optimization, which worried us greatly.

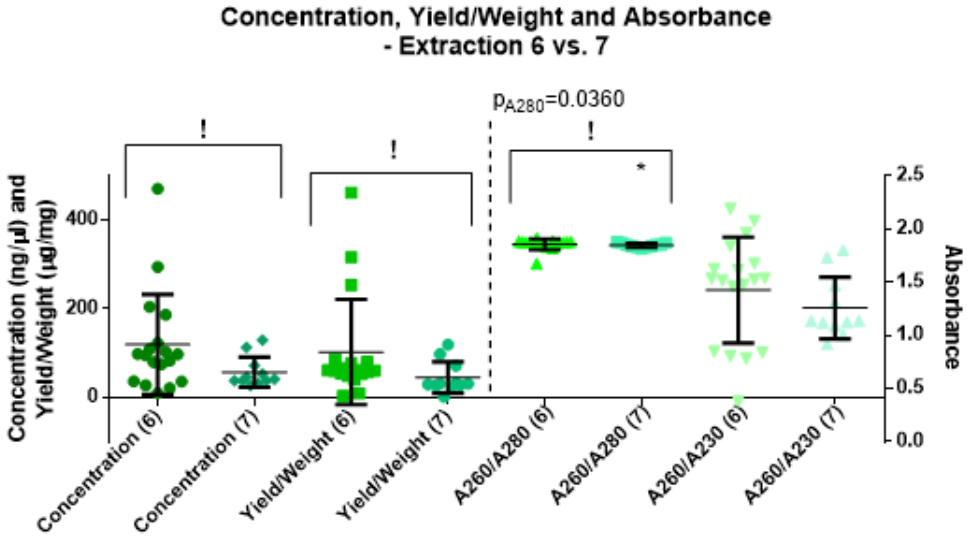

Figure 13: Concentration, yield/weight, and Absorbance-ratios from extraction 6 and 7. No significant differences between extraction 6 and 7 were found for concentration, yield/weight and A260/A230. The A260/A280-ratio of extraction 6 was significantly higher, compared to extraction 7 (p=0.0360). Statistical analysis of the concentration, yield/weight and the A260/A280 was performed using the Mann Whitney U test (!). Yield/weight was calculated by dividing the yield (µg) (concentration*200µl*0,001) by the sample weight (mg). Significance: * = *p<0.05*.

After extraction 7, we performed four other extractions with similar protocols (*Table 5*). However, all of these extractions yielded unsatisfactory results, despite our best efforts. We included the possibilities of a too long lysis, where Proteinase K could possibly affect our DNA, and even DNase contamination on our beads for the TissueLyser II. Yet, all the extractions yielded similar, disappointing results. For the full dataset and accompanying graphs consult *Appendix 7.11 and 7.12*, respectively.

3.2.8 Extractions 12 & 13 – The NucleoSpin Kit

For Extraction 12 we used samples from brains 46 and 49. Both brains were acquired from hemizygous eGFP-positive males from our own breeding line (*Table 1*). As we continuously encountered issues with the kit, and seemed unable to make the optimization work, we considered using another kit. Therefore, we tested both the NucleoSpin Kit (C) and NucleoSpin XS (D) Kit in Extraction 12 (*Macherey-Nagel, Germany*). The protocols for both kits can be found in *Appendix 7.10: Protocol – NucleoSpin Kit and NucleoSpin XS*. Additionally, we tested the DNeasy Blood and Tissue Kit again, both with (A) a without RNase (B). Lastly, we performed the elution at 70°C instead of room temperature (*Table 5*).

The samples had a mean weight of 17,75 mg. Samples from DNeasy+RNase (A) yielded a mean concentration of 63,95 ng/µl, which equals a mean yield of 12,79 µg (dissolved in 200µl AE buffer) (*Figure 14a*). Samples had a mean yield/weight of 71,85 µg/mg (*Figure 14a*). Furthermore, samples from DNeasy+RNase had A260/A280- and A260/A230-ratios of 1,880 and 1,420, respectively

(*Figure 14b*). Samples from DNeasy-RNase (B) yielded a mean concentration of 264,0 ng/µl, which equals a mean yield of 52,80 µg (dissolved in 200µl AE buffer) (*Figure 14a*). Samples had a mean yield/weight of 302,709 µg/mg (*Figure 14a*). Furthermore, samples from DNeasy+RNase had A260/A280- and A260/A230-ratios of 1,988 and 1,980, respectively (*Figure 14b*). Samples from NucleoSpin (C) yielded a mean concentration of 435,6 ng/µl, which equals a mean yield of 43,56 µg (dissolved in 100µl AE buffer) (*Figure 14a*). Samples had a mean yield/weight of 262,093 µg/mg (*Figure 14a*). Furthermore, samples from NucleoSpin had A260/A280- and A260/A230-ratios of 1,978 and 2,305, respectively (*Figure 14b*). Samples from NucleoSpin XS (D) yielded a mean concentration of 443,8 ng/µl, which equals a mean yield of 8,88 µg (dissolved in 50µl AE buffer) (*Figure 14a*). Samples had a mean yield/weight of 46,584 µg/mg (*Figure 14a*). Furthermore, samples from NucleoSpin XS had A260/A280- and A260/A230-ratios of 2,053 and 2,160, respectively (*Figure 14b*).

There was a significant overall effect of four different protocols on the yielded concentration (*p=0.0329*) (*Figure 14a*). Furthermore, the concentration of DNeasy+RNase (A) was significantly lower compared to the concentration yielded by NucleoSpin XS (D) (*p<0.05*) (*Figure 14a*). Additionally, there was a significant overall effect of the four different protocols on the yield/weight (*p=0.0005*) (*Figure 14a*). The yield/weight of both DNeasy-RNase (B) and NucleoSpin (C) was significantly higher, compared to DNeasy+RNase (A) (*p<0.05*) (*Figure 14a*). Furthermore, the yield/weight of DNeasy-RNase (B) was significantly

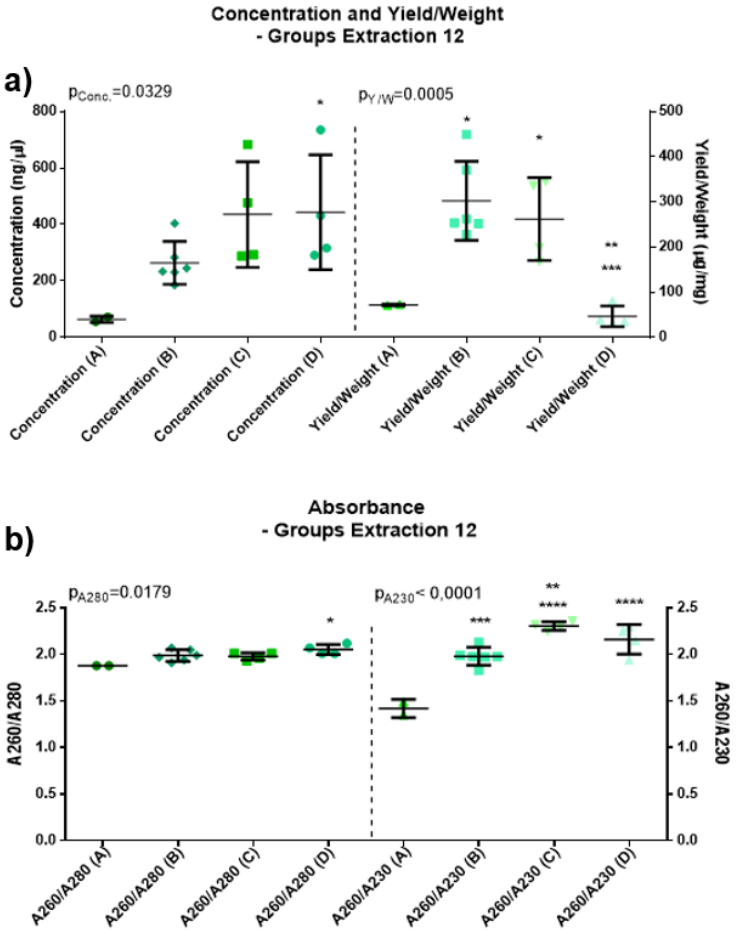

Figure 14: Concentration (a), yield/weight (a) and Absorbance-ratios (b) from extraction 12. A significant overall effect of four different protocols on the yielded concentration was found (*p=0.0329*) (a). Furthermore, the concentration of DNeasy+RNase (A) was significantly lower compared to the concentration yielded by NucleoSpin XS (D) (*p<0.05*) (a). There was a significant overall effect of the four different protocols on the yield/weight (*p=0.0005*) (a). The yield/weight of both DNeasy-RNase (B) and NucleoSpin (C) was significantly higher, compared to DNeasy+RNase (A) (*p<0.05*) (a). The yield/weight of DNeasy-RNase (B) was significantly higher, compared to NucleoSpin XS (D) (*p<0.001*) (a). The yield/weight of NucleoSpin (C) was also significantly higher, compared to NucleoSpin XS (D) (*p<0.01*) (a). An overall significant effect of the protocol on the A260/A280 was found (*p=0.0179*) (b). The A260/A280 of the DNeasy+RNase (A) was significantly lower, compared to NucleoSpin XS (*p<0.05*) (b). Furthermore, there was an overall significant effect of protocol on the A260/A230 (*p<0.0001*) (b). The A260/A230 of DNeasy+RNase (A) was significantly lower compared to DNeasy-RNase (B) (*p<0.001*) (b). Furthermore, the A260/A230 of both NucleoSpin (C) and NucleoSpin XS (D) were significantly higher, compared to DNeasy+RNase (A) (*p<0.0001*) (b). Lastly, the A260/A230 of DNeasy-RNase (B) was significantly lower, compared to NucleoSpin (C) (*p<0.01*) (b). Yield/weight was calculated by dividing the yield (µg) (concentration*200µl*0,001) by the sample weight (mg). Significance: * = *p<0.05*, ** = *p<0.01*, *** = *p<0.001*, **** = *p<0.0001*.

higher, compared to NucleoSpin XS (D) (*p<0.001*) (*Figure 14a*). The yield/weight of NucleoSpin (C) was also significantly higher, compared to NucleoSpin XS (D) (*p<0.01*) (*Figure 14a*).

There was an overall significant effect of the protocol on the A260/A280-ratio (*p=0.0179*) (*Figure 14b*). The A260/A280-ratio of the DNeasy+RNase (A) was significantly lower, compared to NucleoSpin XS (*p<0.05*) (*Figure 14b*). Furthermore, there was an overall significant effect of protocol on the A260/A230-ratio (*p<0.0001*) (*Figure 14b*). The A260/A230-ratio of DNeasy+RNase (A) was significantly lower compared to DNeasy-RNase (B) (*p<0.001*) (*Figure 14b*). Furthermore, the A260/A230-ratio of both NucleoSpin (C) and NucleoSpin XS (D) were significantly higher, compared to DNeasy+RNase (A) (*p<0.0001*) (*Figure 14b*). Lastly, the A260/A230-ratio of DNeasy-RNase (B) was significantly lower, compared to NucleoSpin (C) (*p<0.01*) (*Figure 14b*).

Here we finally saw the detrimental effect of RNase on our DNA-samples. We decided to leave the RNase out of our protocol from hereon, because the costs of RNA-free DNA were too high, given the consequent reduction in our DNA yield. Additionally, it was not strictly necessary for our subsequent analysis to have RNA-free DNA. Additionally, this extraction restored our faith in the DNeasy Blood and Tissue Kit. We ruled the NucleoSpin XS out of our options entirely, as it did not give us satisfactory results. However, we wanted to do one last test on the NucleoSpin Kit, before deciding how to proceed with either the DNeasy Blood and Tissue Kit or the NucleoSpin Kit.

For extraction 13 we used samples from brains 46 and 49. Both brains were acquired from hemizygous eGFP-positive males from our own breeding line (*Table 1*). For this extraction we combined the protocols of the DNeasy Blood and Tissue Kit and the NucleoSpin Kit. Protocol A was the full DNeasy protocol, whereas protocol D consisted of the full NucleoSpin protocol. Protocol C consisted of the DNeasy lysis (including incubation), with the NucleoSpin column extraction. Protocol D was the other way around, with the NucleoSpin lysis (including incubation), with the DNeasy column extraction (*Table 5*). This plan was designed to make a final call about the functionality of the DNeasy Blood and Tissue Kit versus the NucleoSpin Kit.

Samples had a mean weight of 22,07 mg. Samples from protocol A yielded a mean concentration of 318,6 ng/µl, which equals a mean yield of 63,72 µg (dissolved in 200µl AE buffer). Samples had a mean yield/weight of 309,561 µg/mg. Furthermore, samples from protocol A had A260/A280- and A260/A230-ratios of 2,020 and 2,058, respectively. Samples from protocol B yielded a mean concentration of 587,2 ng/µl, which equals a mean yield of 58,72 µg (dissolved in 100µl AE buffer). Samples had a mean yield/weight of 249,297 µg/mg. Furthermore, samples from protocol B had A260/A280- and A260/A230-ratios of 2,028 and 2,275, respectively. Samples from protocol C yielded a mean concentration of 264,8 ng/µl, which equals a mean yield of 52,96 µg (dissolved in 200µl AE buffer). Samples had a mean yield/weight of 238,290 µg/mg. Furthermore, samples from protocol C had A260/A280- and A260/A230-ratios of 1,998 and 2,008, respectively. Samples from protocol D yielded a mean concentration of 330,0 ng/µl, which equals a mean yield of 33,0 µg (dissolved in 100µl AE buffer). Samples had a mean yield/weight of 152,091 µg/mg. Furthermore, samples from protocol D had A260/A280- and A260/A230-ratios of 2,003 and 2,278, respectively.

We made the final decision after this extraction to proceed with the full DNeasy Blood and Tissue Kit, as this generated the highest yield/weight. For both extraction 12 and 13 the DNeasy Blood and Tissue Kit showed the highest yield/weight. Moreover, we confirmed the issues we had encountered with the kit were caused by the use of RNase.

3.2.9 Extraction 15 – Overnight or One Day?

Before we would start with the real extractions, we wanted to run one more test before complying to the final protocol. We needed to decide about the length of the lysis. So far, we had switched between overnight lysis and a lysis of approximately six hours, which would allow us to perform an extraction within one day. Therefore, in Extraction 15 we would look at the effects of overnight lysis, or an

extraction in one day (*Table 5*). For this extraction we used samples from brain 33, which was from a hemizygous eGFP-positive male from our own breeding line (*Table 1*).

The samples had a mean weight of 27,9 mg. Samples from Overnight yielded a mean concentration of 344,025 ng/µl, which equals a mean yield of 68,805 µg (dissolved in 200µl AE buffer) (*Figure 15*). Samples had a mean yield/weight of 331,2 µg/mg (*Figure 15*). Furthermore, samples from Overnight had A260/A280- and A260/A230-ratios of 2,030 and 2,008, respectively (*Figure 15*). Samples from One Day yielded a mean concentration of 360,90 ng/µl, which equals a mean yield of 72,18 µg (dissolved in 200µl AE buffer) (*Figure 15*). Samples had a mean yield/weight of 239,1 µg/mg (*Figure 15*). Furthermore, samples from One Day had A260/A280- and A260/A230-ratios of 2,035 and 2,065, respectively (*Figure 15*).

We found no significant effect of the length of the lysis on any of the parameters (concentration, yield/weight, A260/A280 and A260/A230) (*Figure 15*). However, we did see a slightly higher mean yield/weight for the Overnight samples. By reason of this, in addition to the practical benefits, we decided to extract brain samples overnight from hereon. With this last extraction, were able to finalize our optimization of the DNA Extraction, using the DNeasy Blood and Tissue Kit.

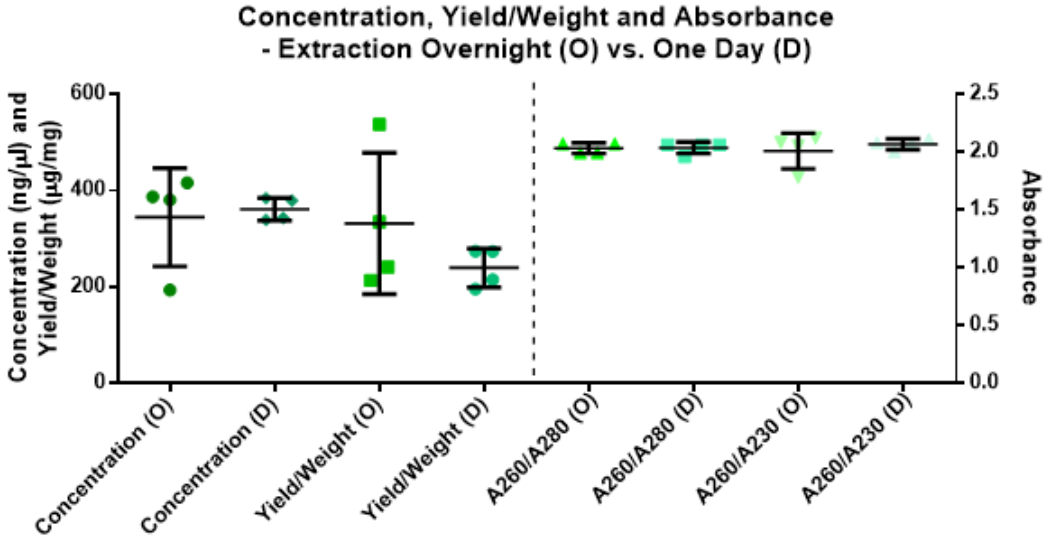

Figure 15: Concentration, yield/weight, and Absorbance-ratios from extraction 15 – Overnight vs. One Day. No significant differences between overnight and one day were found for any of the parameters of extraction 15. Yield/weight was calculated by dividing the yield (µg) (concentration*200µl*0,001) by the sample weight (mg).

After optimizing our DNA extraction for brain samples, we performed a few trial runs for other organs. We used our fully optimized protocol on *lung*, *spleen*, and *mammary* gland samples. The only factor that we actively changed were the sample weights (*Table 3*) and whether the lysis should be performed overnight. Lung samples were lysed overnight, whereas extractions for spleen and mammary gland were performed in one day (lysis of ~6 hours).

3.2.10 RNase

Over the course of our optimization, we encountered a range of technical problems, but the most apparent one was the use of RNase, which significantly slowed down our optimization process. We eventually discovered that it is possible for RNase to be co-purified with DNase, which could seriously damage the DNA (*Stervander, 2013; Donà & Houseley, 2014*). We immediately saw an improvement from leaving RNase out of our protocol. In the graph below data from Extraction 6 (+RNase) and Extraction 12 and 13 (-RNase) are presented (*Figure 16*).

There was a significant effect on the concentration of the samples, where the samples without RNase have a significantly higher concentration than the samples with RNase (*p=0.0004*) (*Figure 16*). Furthermore, the yield/weight was significantly higher in samples without RNase (*p=0.0003*) (*Figure 16*), and the A260/A280-ratio of the samples was significantly lower for the samples with RNase, as expected (*p<0.0001*) (*Figure 16*). Finally, the A260/A230-ratio of the samples without RNase was significantly higher (*p=0.0012*) (*Figure 16*).

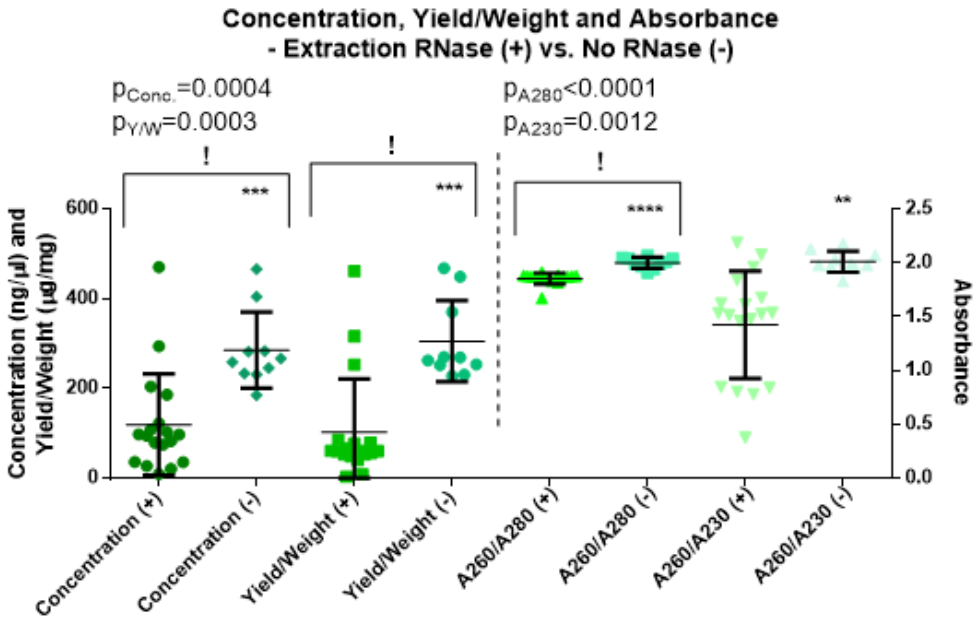

Figure 16: Concentration, yield/weight, and Absorbance-ratios from extraction 6, 12 and 13 – Rnase (+) vs. No RNase (-). The concentration without RNase was significantly higher, compared to extractions with the use of RNase (*p=0.0004*). Furthermore, the yield/weight of extractions without the use of RNase is significantly higher, compared to extractions with the use of RNase (*p=0.0003*). The A260/A280 of extractions with RNase is lower, compared to extractions without RNase (*p<0.0001*). Lastly, the A260/A230 of extractions with RNase is significantly lower, compared to extractions without the use of RNase (*p=0.0012*). Statistical analysis of the concentration, yield/weight and the A260/A280 was performed using the Mann Whitney U test (!). Yield/weight was calculated by dividing the yield (µg) (concentration*200µl*0,001) by the sample weight (mg). Significance: ** = *p<0.01*, *** = *p<0.001*, **** = *p<0.0001*.

3.2.11 Gels – DNA Shearing

Beside the use of the Nanodrop to analyse our extracted DNA, we also ran several agarose gels. We used the protocol from *Appendix 7.7: Protocol – Gel Electrophoresis*. For gels from the DNA extraction, we used 0,8% agarose gels. Here we clearly saw the effects of DNA shearing, due to the use of the TissueLyser II. The original protocol of the DNeasy Blood and Tissue Kit warned us for the use of the TissueLyser II at higher frequencies than 15Hz. As can be seen in the gel-image in *Figure 17*, there is no DNA shearing when using only 15Hz. Those samples have clear single small bands. This in contrary to the samples that were lysed with 30Hz. There you see a smear of the DNA, with smaller fractions of DNA. Yet, in our final protocol we chose to use 30Hz anyway. In *Figure 17* you can see that the 30Hz, 20 seconds-samples do have some shearing, but not an excessive amount. Therefore, we eventually chose to use the TissueLyser II at 30Hz for twice fifteen seconds. We decided that the costs of using the TissueLyser II at this frequency outweighs the benefits of the higher DNA yield obtained.

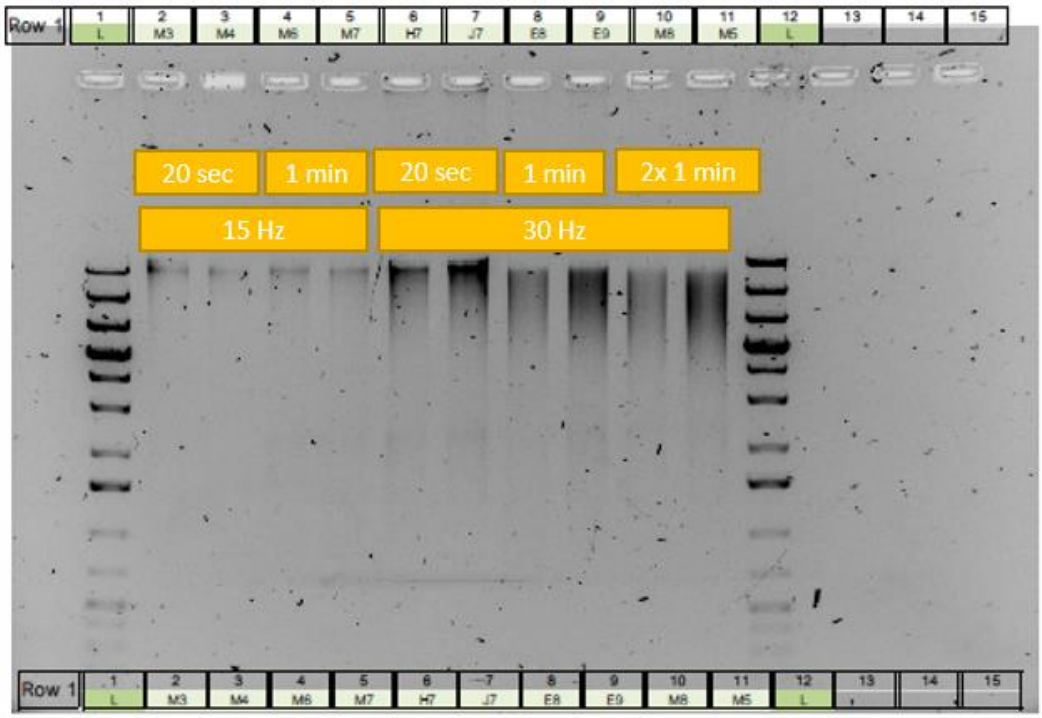

Figure 17: A 0,8% agarose gel displaying the effects of the TissueLyser II on DNA shearing. The gel contains samples from extraction 5. In the gel it can be seen that at 15Hz there is no DNA shearing. However, at 30Hz the DNA is smeared out over the gel, indicating DNA shearing. This increases with longer durations of the TissueLyser II-program. *Gel was made by J.R. Smit and S. Smit.*

The complete datasheet with results from the various DNA extractions and additional graphs can be found in *Appendix 7.11* and *Appendix 7.12*, respectively. Additionally, all the gels we ran for the optimization can be found in *Appendix 7.13*.

3.3 Optimization Overview

Table 5: An overview of the protocols used for the different extractions along the process of optimization. (rpm=rounds per minute).

Extraction	ATL	TissueLyser	Prot. K	Incubation	AL+Ethanol	Column	AW1	AW2	Elution
1	180µl	15Hz, 20sec	20µl	56°C - ~3hours	200µl+200µl	1x - 1min, 8000rpm	1x - 1min, 8000rpm	1x - 3min, 14000rpm	200µl - 1min RT -1min, 8000rpm
2	180µl	**X**	20µl	56°C - Overnight	200µl+200µl	1x - 1min, 8000rpm	1x - 1min, 8000rpm	1x - 3min, 14000rpm	200µl - 1min RT -1min, 8000rpm
3	180µl	X	20µl	56°C - Overnight	200µl+200µl	1x - 1min, 8000rpm	1x - 1min, 8000rpm	**D: 1x - 3min, 14000rpm L: 2x – 1min, 14000rpm – 3min, 14000rpm**	200µl - 1min RT -1min, 8000rpm
4	180µl	X	20µl	56°C - Overnight	**All: 200µl+200µl C & D: Premixed AL+Ethanol**	1x - 1min, 8000rpm	1x - 1min, 8000rpm	**All: 2x – 3min, 14000rpm B & D: Dryspin – 3min, 14000rpm**	200µl - 1min RT -1min, 8000rpm
5	180µl + Bead	**15Hz, 20sec – 15Hz, 1min – 30Hz, 20sec - 30Hz, 1min – 30Hz, 2x1min**	Remove Bead - 20µl	56°C - Overnight	200µl+200µl	**A: 1x - 1min, 8000rpm B: 2x~350µl – 1 min, 8000rpm**	1x - 1min, 8000rpm	2x – 3min, 14000rpm	200µl - 1min RT -1min, 8000rpm
6	180µl + Bead	**30Hz, 30sec**	Remove Bead - 20µl	**56°C - ~6hours - 4µl RNase**	200µl+200µl	2x~350µl – 1 min, 8000rpm	1x - 1min, 8000rpm	2x – 3min, 14000rpm	200µl - 1min RT -1min, 8000rpm + **Second elution (100µl)**
7	180µl + Bead	**15Hz, 2x15sec**	Remove Bead - 20µl	56°C - **Overnight** - 4µl RNase	200µl+200µl	2x~350µl – 1 min, 8000rpm	1x - 1min, 8000rpm	2x – 3min, 14000rpm	200µl - 1min RT -1min, 8000rpm

8	180µl + Bead	15Hz, 2x15sec	Remove Bead - 20µl	56°C - Overnight - 4µl RNase	200µl+200µl	2x~350µl – 1 min, 8000rpm	1x - 1min, 8000rpm	2x – 3min, 14000rpm	200µl - 1min RT -1min, 8000rpm + **Second elution (100µl)**
9	180µl + Bead	15Hz, 2x15sec	Remove Bead - 20µl	56°C - Overnight - 4µl RNase	200µl+200µl	2x~350µl – 1 min, 8000rpm	1x - 1min, 8000rpm	2x – 3min, 14000rpm	200µl - 1min RT -1min, 8000rpm + **Second elution (200µl) + Third elution (50µl)**
11	180µl + Bead	15Hz, 2x15sec	Remove Bead - 20µl	56°C - Overnight - 4µl RNase	200µl+200µl	2x~350µl – 1 min, 8000rpm	1x - 1min, 8000rpm	2x – 3min, 14000rpm	200µl - 1min RT -1min, 8000rpm + **Second elution (100µl)**
12	180µl + Bead	15Hz, 2x15sec	Remove Bead - 20µl	56°C - **~6hours** A: 4µl RNase **B: No RNase**	200µl+200µl	2x~350µl – 1 min, 8000rpm	1x - 1min, 8000rpm	2x – 3min, 14000rpm	200µl - 1min RT -1min, 8000rpm **B: 200µl - 1min 70°C - 1min, 8000rpm**
13	180µl + Bead	15Hz, 2x15sec	Remove Bead - 20µl	56°C - ~6hours - **No RNase**	200µl+200µl	2x~350µl – 1 min, 8000rpm	1x - 1min, 8000rpm	2x – 3min, 14000rpm	**200µl - 1min 70°C -1min, 8000rpm**
14	180µl + Bead	**20Hz, 20sec – 25Hz, 20sec – 30Hz, 15 sec**	Remove Bead - 20µl	56°C - ~6hours - No RNase	200µl+200µl	2x~350µl – 1 min, 8000rpm	1x - 1min, 8000rpm	2x – 3min, 14000rpm	200µl - 1min 70°C -1min, 8000rpm
15	180µl + Bead	**30Hz, 2x15sec**	Remove Bead - 20µl	56°C – **A: ~6hours B: Overnight** - No RNase	200µl+200µl	2x~350µl – 1 min, 8000rpm	1x - 1min, 8000rpm	2x – 3min, 14000rpm	200µl - 1min 70°C -1min, 8000rpm

3.4 Discussion

The optimization of our DNA extraction protocol took us several weeks, during which we learned several valuable lessons regarding optimizing a protocol. In contrary to our initial expectations, a well-developed kit, like the DNeasy Blood and Tissue Kit, does not necessarily work perfectly for any project. As we have shown, there are always was to improve the results. Early steps within an experimental design have the capacity to influence the effectiveness of the final analysis. Therefore, it is important to always optimize the protocol for each step of a project.

To properly optimize a protocol like DNA extraction it is important to learn the protocol by heart, including its subtle details. One must spend time to understand the constituents of each reagent and their function within the kit. It is important to question each step of the protocol and wonder why this step is performed and to what purpose. This detailed knowledge is essential to thinking about the possible steps one could take when optimizing a protocol. Additionally, it is wise to consult other researchers with experience in the problem domain. New insights and knowledge shared between researchers could significantly improve and ease the process of optimization.

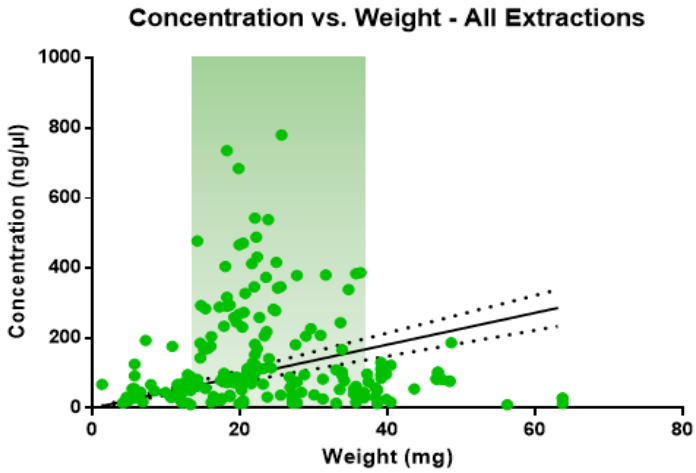

Figure 18: A correlative graph of concentration (ng/µl) and weight (mg) of all samples from the DNA extraction optimization process. The optimal sample weight, for the highest concentration, ideally lies around 20 mg, with a maximum of 40 mg.

Furthermore, it can be interesting to push the limits of a kit. In this way a dataset of outcomes can be generated under different experimental scenarios allowing analysis of the optimal conditions for the protocol. One of the parameters analysed in this study was the optimal sample weight for the highest concentration. In *Figure 18*, it can be seen that for our brain samples this is a sample weight of approximately 20 mg, as this yields the highest concentrations when considering all the data we have gathered during this optimization process. This information allows simultaneous maximalization of DNA obtained and the minimalization of wasted material.

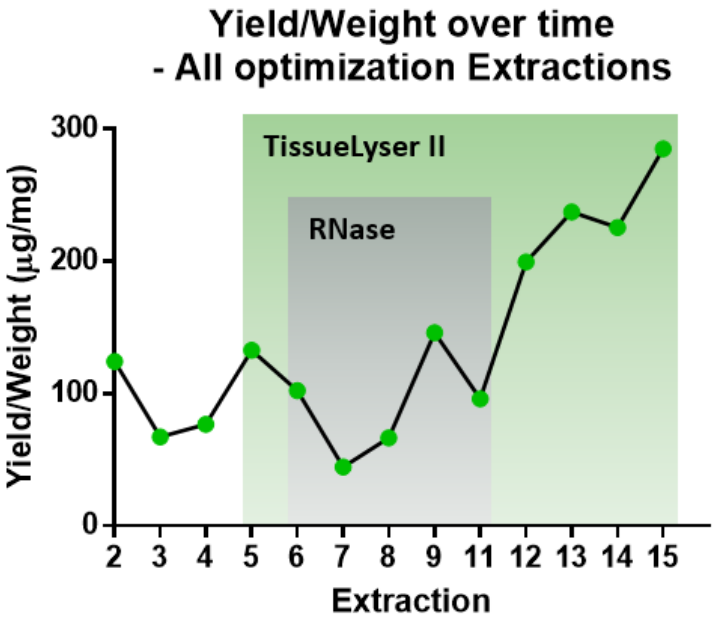

Figure 19: The mean yield/weight (µg/mg) of each extraction from the DNA extraction optimization process. At the end of the optimization our yield/weight had more than doubled. Also, a significant drop in yield/weight can be seen after adding RNase to the protocol (extraction 6-11). Yield/weight was calculated by dividing the yield (µg) (concentration*200µl*0,001) by the sample weight (mg).

When changing steps in a protocol during optimization, it is important to carefully analyse the effects of this step, before drawing any conclusions. For example, we were very glad that the TissueLyser II significantly improved our DNA quality (Extraction 5) with the data from the NanoDrop.

However, after running a gel, we soon discovered that is caused DNA shearing (*Figure 17*). In the end we decided that the gains of higher DNA yield outweighed the costs of the DNA shearing. Yet, it was important to be aware of this effect of the TissueLyser II, both for the further optimization, but also for later analysis of the DNA. If any problems occur later in analysis, the shearing of the DNA during tissue disruption could be a cause, and it is important to be aware of this.

In our use of RNase we were unaware of this issue, for example. This was mainly because during our optimization we changed multiple factors at the same time (new reagents, new beads for the TissueLyser II). Furthermore, we were convinced that our DNA quality would significantly benefit from adding RNase, but as can be seen in *Figure 19*, there was a significant decline in yield/weight in the extractions where RNase was added (Extraction 6-11). Contrary to our expectations, removal of RNase from the protocol resulted in a clear improvement (Extraction 12), but it took considerable effort to figure this out. Furthermore, it would have been wise to research the effect of RNase some more, by consulting other more-experienced researchers. In this way we eventually found out that indeed RNase could create unforeseen problems and should not be used if not necessary for subsequent analyses. As mentioned before, it is possible that RNase is purified together with DNase, which will have detrimental effects on your DNA (*Stervander, 2013; Donà & Houseley, 2014*).

In conclusion, optimization of protocols is an important aspect of research. By carefully learning to understand a kit, its constituents, the chemical reactions it depends upon, by consulting other researchers and pushing the limits of a kit, it is possible to develop a protocol that works best for your particular application. This time and effort can yield benefits in subsequent analyses.

4. Results

In this chapter the results from the qPCR-pilot and from the DNA extraction of our experimental samples will be discussed. For the qPCR-pilot analysed the individual efficiency and Cq-value of each well from the two pilot plates (*Appendix 7.16: qPCR Plate Set-ups*). Furthermore, we will discuss the found quantities of GFP and the GFP/Apob ratios for each organ. Here we will distinguish between pregnant and non-pregnant females (*Model A-1/B-1 vs. Model A-2/B-2*), as well as C57BL/6J- and BALB/c-females (*Model A-1/A-2 vs. Model B-1/B-2*). For the DNA extraction of our experimental samples, we will shortly discuss the weight and yield/weight of the samples.

4.1 DNA Extraction – Samples

4.1.1 Sample Weight

Table 6 describes target weights for each organ, according to the QIAGEN DNeasy Blood and Tissue Kit Handbook and our own optimization, along with the mean, SD, and SEM of the sample weights in practice for each organ. As expected, there was a significant difference between the weights of the organs (*p=<0.0001*). The samples from both the *brain* (*p=<0.0001*) and *lungs* (*p=<0.0001*) were significantly heavier, compared to the *spleen* (*Figure 20*). Sections from the *brain* had the highest mean weight, whereas the sections from the *spleen* had the lowest mean weight (*Figure 20*) (*Table 6*).

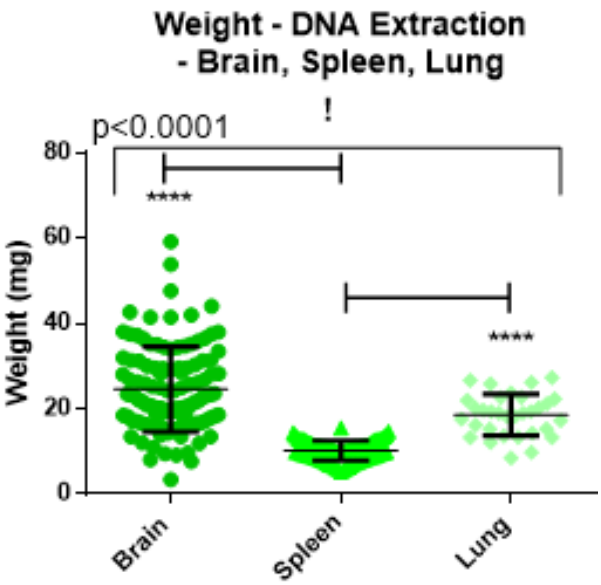

Figure 20: The sample weight of the brain, spleen and lung tissues. There was a significant effect of organ-type on the sample weight (*p<0.0001*). Furthermore, both brain and lung samples had a higher sample weight compared to spleen samples (*p<0.0001* and *p<0.0001*, respectively). Statistical analysis of the sample weight was performed using the Kruskal-Wallis test (!). Significance: **** = *p<0.0001*.

Table 6: Mean, SD and SEM for sample weights of the brain, spleen, and lung tissues. Significance: **** = *p<0.0001*

Organ	Brain (n=114)	Spleen (n=77)	Lung (n=32)
Target Weight	20 – 40 mg	10± mg	15 – 25 mg
Mean	24,6 (****)	10,21	18,58 (****)
SD	9,997	2,333	4,866
SEM	0,9363	0,2658	0,8601

4.1.2 Yield/Weight

The yield/weight was established for each organ used in the qPCR-pilot, to establish the efficiency of the DNA extractions for each organ.

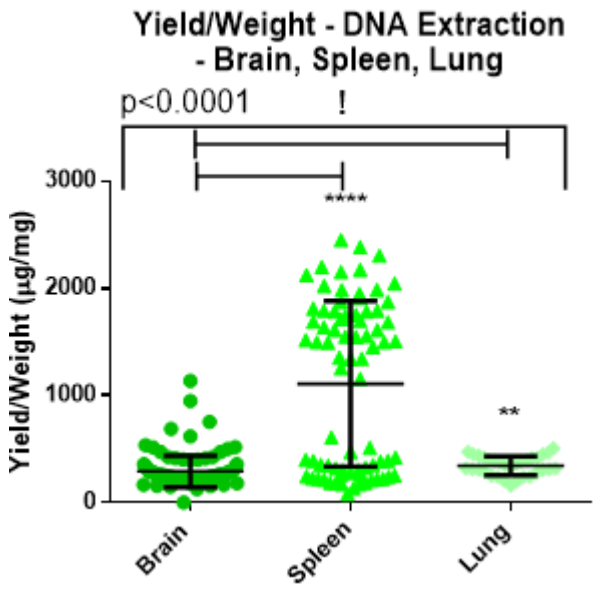

Figure 21: The yield/weight of the brain, spleen and lung samples. There was a significant effect of organ-type on yield/weight (*p<0.0001*). Both spleen and lung samples had a significantly higher yield/weight, compared to brain samples (*p<0.0001* and *p<0.01*, respectively). Statistical analysis of the yield/weight was performed using the Kruskal-Wallis test (!). Yield/weight was calculated by dividing the yield (µg) (concentration*300µl*0,001) by the sample weight (mg). Significance: ** = *p<0.01*, **** = *p<0.0001*.

4.1.2.1 Organ differences

We were interested in the difference in DNA yield between organs. We found that there was a significant effect of organ-type on the yield/weight (*p<0.0001*) (*Figure 21*). The samples from the *spleen* and the *lung* had a significantly higher yield/weight than to the samples from the *brain* (*p<0.0001* and *p<0.01*, respectively) (*Figure 21*). There was no significant difference in yield/weight between samples from the *spleen* and *lung (Figure 21*). The *spleen* had the highest mean yield/weight (*Figure 21*; *Table 7*). However, as can also be seen in *Figure 21*, there appear to be two separate clusters among the samples from the *spleen*. One cluster appears to have a lower yield/weight, similar to that of samples from *brain* or *lung*. The other cluster appears to have a far higher yield. The higher cluster belonged to the samples from formerly pregnant but currently non-pregnant females. Therefore, below we distinguish the effects of pregnancy status on the yield/weight of an organ.

Table 7: Mean, SD and SEM for yield/weight of the brain, spleen, and lung samples. Significance: ** = *p<0.01*, **** = *p<0.0001*

Organ	Brain (n=114)	Spleen (n=77)	Lung (n=32)
Mean	291,2	1109 (****)	344,2 (**)
SD	148,3	772,2	89,18
SEM	13,89	88	15,77

4.1.2.2 Combined effect of pregnancy and organ-type

We performed a two-way ANOVA with multiple comparison on our samples to test for the effect of pregnancy and organ-type on the yield/weight (*Figure 22*). There was a significant effect of pregnancy (*p<0.0001*) and organ-type (*p<0.0001*) on the yield/weight (*Figure 22*). There was a significant effect of pregnancy on the yield/weight for the samples of the *spleen* (*p<0.0001*). Additionally, there was a significant effect of organ-type for the non-pregnant samples. Both the samples from the *brain* (*p<0.0001*) and *lung* (*p<0.0001*) had a significantly lower yield/weight compared to the non-pregnant samples from the *spleen* (*Figure 22*; *Table 8*).

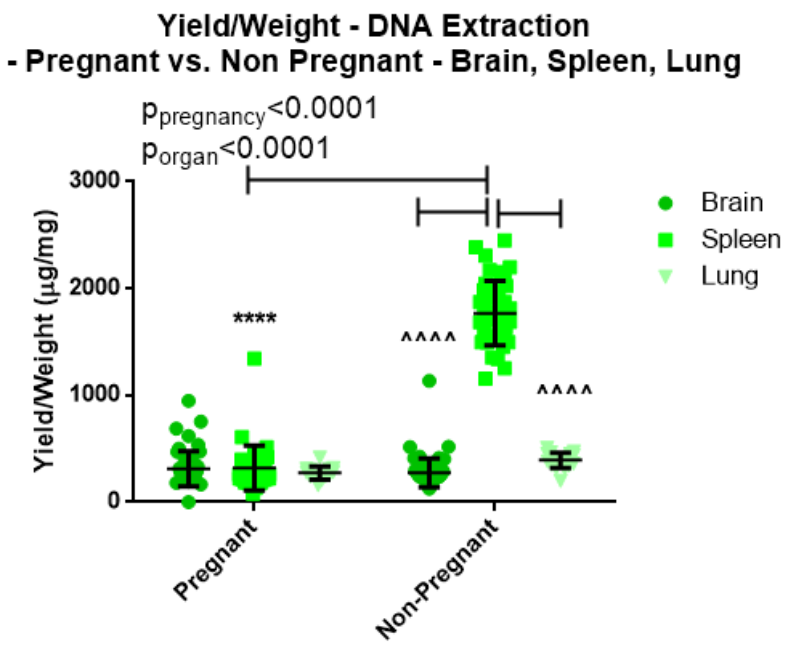

Figure 22: Yield/weight for brain, spleen and lung samples – pregnant vs. non-pregnant. A significant overall effect of pregnancy and organ-type on yield/weight was found (*p<0.0001* and *p<0.0001*, respectively). Non-pregnant females had a significantly higher yield/weight in spleen samples, compared to pregnant females (*p<0.0001*). Furthermore, non-pregnant females had significantly higher yield/weight in spleen samples, compared to brain and lung samples (*p<0.0001* and *p<0.0001*, respectively). Yield/weight was calculated by dividing the yield (µg) (concentration*300µl*0,001) by the sample weight (mg). Significance for pregnancy: **** = *p<0.0001*. Significance for organ-type: ^^^^ = *p<0.0001*.

Table 8: Mean, SD and SEM for yield/weight of the brain, spleen, and lung samples – pregnant vs. non-pregnant. Significance for pregnancy: **** = *p<0.0001*. Significance for organ-type: ^^^^ = *p<0.0001*.

Organ	Brain		Spleen		Lung	
Group	Pregnant (n=48)	Non-Pregnant (n=66)	Pregnant (n=35)	Non-Pregnant (n=42)	Pregnant (n=13)	Non-Pregnant (n=19)
Mean	313,9	274,8 (^^^^)	319,3 (****)	1768	273,5 (****)	392,6 (^^^^)
SD	165,3	133,6	210,5	302,7	62,88	70,61
SEM	23,85	16,44	35,58	46,7	17,44	16,2

The full datasheet of the DNA extractions of the experimental samples and additional graphs can be found in *Appendix 7.14* and *Appendix 7.15*, respectively.

4.2 qPCR

For the qPCR-pilot we ran two separate plates (*Appendix 7.16: qPCR Plate Set-ups*). We used the data generated by the StepOnePlus-software for calculation of the quantity of GFP in each sample. The frequency of GFP/Apob was calculated by dividing the quantity of GFP by the quantity of Apob, as calculated by the StepOnePlus. Additionally, we used the amplification data from the StepOnePlus-software to calculate the Individual Efficiency (IE) and Cq-values in LinRegPCR. All outliers were excluded for the GFP Quantities and GFP/Apob-ratios using the ROUT-method with a false discovery rate (FDR) of Q=0,1%, to identify definite outliers.

4.2.1 Cq-value

The Cq-value is the number of cycles needed for the sample to intersect the threshold-line for fluorescence. In the event that GFP is found, we would expect a higher Cq-value compared to the Cq-value of Apob, as the microchimeric GFP sequence will be present in far lower quantities and Apob being our reference gene. The values for *Figure 23* and *Table 9* exclude the data from the gBlock-dilutions and the NTCs. Data provided in the graphs and table only include data from tissue samples and the positive controls. Whereas the mean Cq-value of Apob was around 20, so was that of GFP (*Figure 23*; *Table 9*). When looking at *Figure 23*, a few outliers can be seen for Apob, which are between Cq-values of 0-10. For GFP a lot of outliers between 0-10 can be seen. Such low values, especially for GFP, will be considered as artefacts in the remainder of this chapter. These values are too low to be considered valid and are therefore not included in the graphs and tables below. A ROUT-outlier test was performed, with a FDR of Q=0,1%, to exclude definite outliers. The accompanying graph can be found in *Appendix 7.18*. An overview of the Cq-values for each well of both pilot plates can be found in *Appendix 7.16: qPCR Plate Set-ups*.

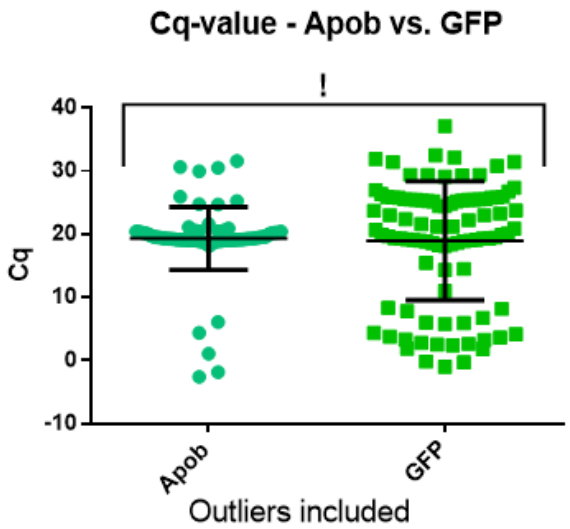

Figure 23: Cq-values of Apob and GFP as calculated by LinReg. No significant difference was found between the Cq-values of Apob and GFP. Statistical analysis was performed using the Mann Whitney U test (!).

Table 9: Mean, SD and SEM for Cq-values of Apob and GFP as calculated by LinReg.

Gene	Apob (n=96)	GFP (n=96)
Mean	19,34	18,99
SD	4,979	9,414
SEM	0,5081	0,9608

4.2.2 Individual Efficiency

Individual Efficiency (IE) identifies how effective the qPCR-reactions were for each well. Ideally, this value is around 1.8 or higher, which equals an efficiency of ~80% or higher. The values are shown in *Figure 24* and *Table 10* and exclude the data from the gBlock-dilutions and the NTCs. Data provided in the graphs and table only include data from tissue samples and positive controls. The mean IE of Apob is approximately 1,7(±0,02317). When looking at *Figure 24* it can be seen that the Apob assay contains some wells with a rather low IE. The average IE of the GFP (1,3±0,029) assay is significantly lower than the Apob assay ($p<0.0001$) (*Figure 24*). Furthermore, there appears to be a high degree of variance in IE among the GFP assay samples (*Figure 24*; *Table 10*). When analysing the outliers of the Apob assay with a lower IE, the samples correspond to the outliers of the GFP assay with a higher IE (*Appendix 7.17*). An overview of the IE for each well of both pilot plates can be found in *Appendix 7.16: qPCR Plate Set-ups*.

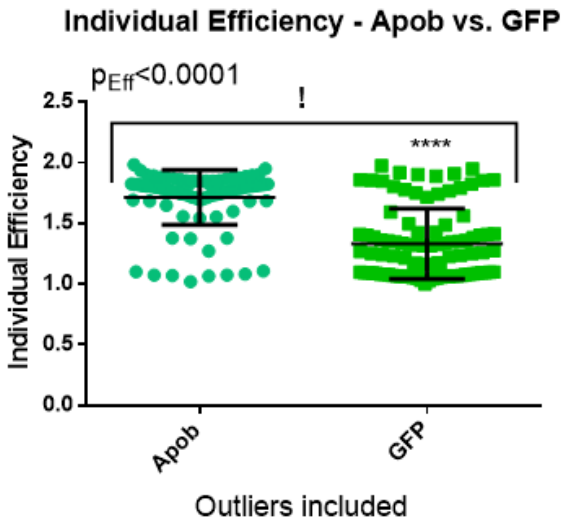

Figure 24: Individual Efficiency (IE) of Apob and GFP as calculated by LinReg. Apob had a significantly higher IE, compared to GFP (*p<0.0001*). Statistical analysis was performed using the Mann Whitney U test (!). Significance: **** = *p<0.0001*.

Table 10: Mean, SD and SEM for Individual Efficiency of Apob and GFP as calculated by LinReg. Significance: **** = *p<0.0001*.

Gene	Apob (n=96)	GFP (n=96)
Mean	1,713	1,333 (****)
SD	0,227	0,2894
SEM	0,02317	0,02954

4.2.3 Quantity of GFP

We analysed the quantity (ng) of GFP for each sample, based on the gBlock dilution series. Here we looked at pregnant vs. non-pregnant. As we found no significant difference between C57BL/6J and BALB/c in frequency (*Figure 30*; See 4.2.4.3), we left this analysis for quantity of GFP out of the thesis.

4.2.3.1 Individual organs

No significant difference was found in GFP-quantity between pregnant and non-pregnant females for *brain*, *spleen*, or *lung* samples (*Figure 25a-c*; *Table 11*). However, we saw two clusters in non-pregnant females for *spleen* (*Figure 25b*) and *lung* samples (*Figure 25c*). After analysing the complete datasheet, we discovered the samples belonged to females 1 and 2 (Model A-2). These mice were sacrificed months after weaning, compared to weeks after weaning in females 15 and 30. Therefore, we decided to leave these out of further analysis of the GFP-quantity, as they can be considered a separate group within our models, and re-analyse the effect of pregnancy for each of the organs (*Figure 25d-f*; *Table 11*).

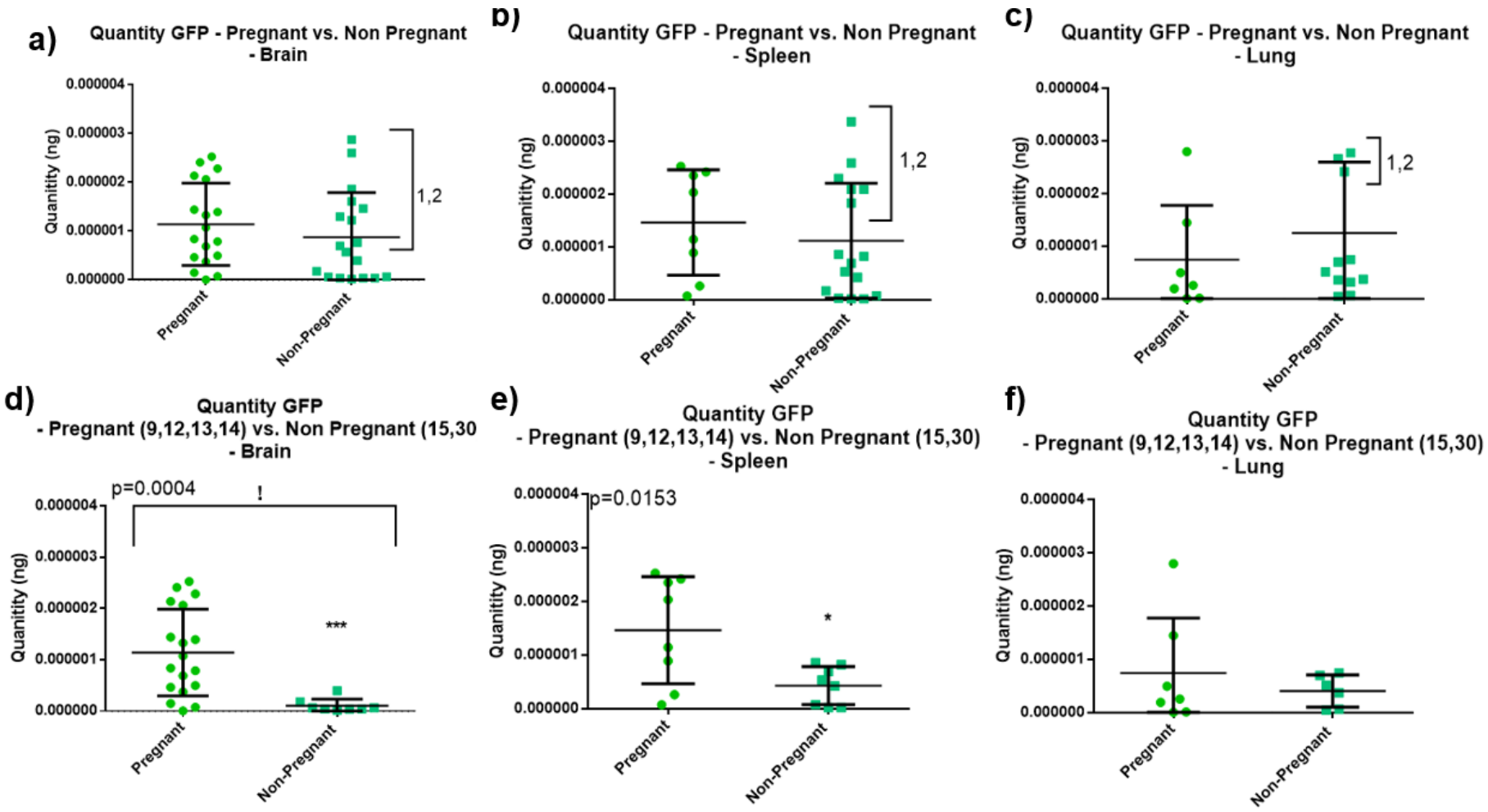

Figure 25: The quantity of GFP (ng) in brain (a,d), spleen (b,e), and lung (c,f) samples as calculated by StepOnePlus – pregnant vs. non-pregnant – females 1 and 2 included (a-c) vs. females 1 and 2 excluded (d-f). There was no significant difference between pregnant and non-pregnant females for brain, spleen, and lung samples with females 1 and 2 included (a-c). After excluding females 1 and 2 from the data, there was a significant difference for both brain and spleen samples. Pregnant females had a significantly higher quantity of GFP in brain and spleen samples, compared to non-pregnant females (*p=0.0004* and *p=0.0153*, respectively) (d,e). No significant differences between pregnant and non-pregnant females were found in lung samples after excluding females 1 and 2 (f). Statistical analysis for graph (d) was performed using the Mann Whitney U test (!). Significance: * = *p<0.05*, *** = *p<0.001*.

Table 11: Mean, SD and SEM for the Quantity of GFP for brain, spleen, and lung samples as calculated by StepOnePlus – pregnant vs. non-pregnant. Datasets were divided including and excluding females 1 and 2. Significance: * = *p<0.05*, *** = *p<0.001*.

Organ	Brain		Spleen		Lung	
Females 1 and 2 included						
Group	**Pregnant (n=18)**	**Non-Pregnant (n=18)**	**Pregnant (n=8)**	**Non-Pregnant (n=16)**	**Pregnant (n=7)**	**Non-Pregnant (n=12)**
Mean	1,14E-06	8,79E-07	1,46E-06	1,12E-06	7,43E-07	1,25E-06
SD	8,46E-07	9,14E-07	9,98E-07	1,09E-06	1,03E-06	1,35E-06
SEM	2E-07	2,15E-07	3,53E-07	2,73E-07	3,9E-07	3,9E-07
Females 1 and 2 excluded						
Group	**Pregnant (n=18)**	**Non-Pregnant (n=8)**	**Pregnant (n=8)**	**Non-Pregnant (n=8)**	**Pregnant (n=7)**	**Non-Pregnant (n=6)**
Mean	1,14E-06	1,04E-07 (*)	1,46E-06	4,3E-07 (***)	7,43E-07	4,06E-07
SD	8,46E-07	1,28E-07	9,98E-07	3,55E-07	1,03E-06	3,04E-07
SEM	2E-07	4,54E-08	3,53E-07	1,26E-07	3,9E-07	1,24E-07

After eliminating elderly females 1 and 2 from our data, pregnant females had a significantly higher quantity of GFP in the *brain*, (*p=0.0004*) and the *spleen* (*p=0.0153*) than non-pregnant females (*Figure 25d,e*). There was no significant difference between pregnant and non-pregnant females in *lung* samples (*Figure 25f*; *Table 11*). For comparisons of the pregnant mice (9, 12, 13 and 14) with the mice that had been pregnant weeks (15 and 30) and months (1 and 2) prior, please visit the master thesis by Maartje de Jong that distinguished the non-pregnant groups.

4.2.3.2. Combined effect of pregnancy and organ-type

We performed a two-way ANOVA to test for the effects of pregnancy and organ-type on the quantity of GFP. The ANOVA excludes samples from the eldery females 1 and 2. There was an overal effect of pregnancy on the quantity of GFP (*Figure 26*). Pregnant females had a significantly higher amount of GFP, than non-pregnant females (*p=0.0004*) (*Figure 26*). There was no significant effect of organ-type on for the quantity of GFP (*Figure 26*). Additionally, there was a significantly higher quantity of GFP in *brain* samples from pregnant females, than non-pregnant females (*p<0.05*) (*Figure 26*). No significant difference was found between the quantity of GFP in the *spleen* and *lung* of pregnant versus non-pregnant females (*Figure 26*; *Table 11*).

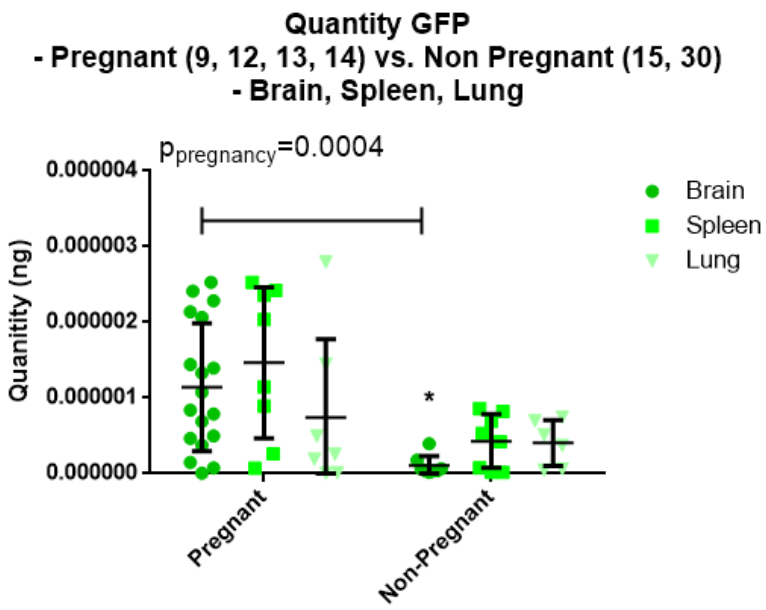

Figure 26: Quantity of GFP (ng) in brain, spleen, and lung samples for pregnant and non-pregnant females. An overall effect of pregnancy was found, where pregnant females had higher quantities of GFP compared to non-pregnant females (*p=0.0004*). Additionally, a significantly higher quantity of GFP was found in brain samples of pregnant females, compared to non-pregnant females (*p<0.05*). Significance for pregnancy: * = *p<0.05*.

4.2.3.3 Scaled quantity of GFP

After re-evaluation of the previous results for quantity we performed a further analysis. We included all data, except for definite outliers (FDR Q=0,1%) and the samples with divergent Apob Cq-values and IE. We standardized our Apob quantities to 0,0001 ng, and according to this we scaled our GFP quantities, by multiplying the original GFP quantity from the StepOnePlus with the multiplier needed to transform the accompanying Apob quantity to 0,0001 ng. After a two-way ANOVA analysis, we found no significant effects of either pregnancy or organ-type (*Figure 27*; *Table 12*).

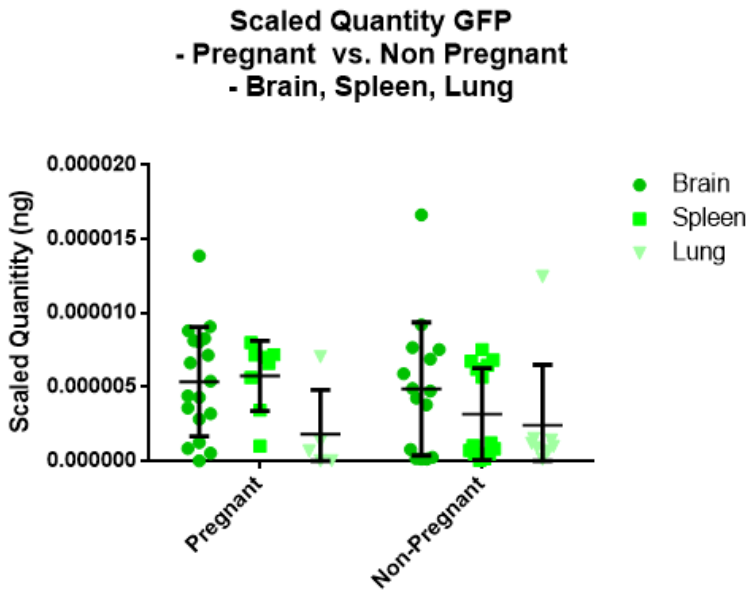

Figure 27: Scaled Quantity of GFP (ng) in brain, spleen, and lung samples for pregnant and non-pregnant females. No significant effect of pregnancy or organ-type was found between pregnant females and non-pregnant females for any of the organs. The scaled quantity of GFP was calculated by standardizing all Apob to a value of 0,0001 ng. The GFP quantity was scaled according to this, by multiplying the quantity with the multiplier needed to transform the accompanying Apob quantity to 0,0001 ng.

Table 12: Mean, SD and SEM for the scaled quantity of GFP for brain, spleen, and lung samples as calculated by StepOnePlus – pregnant vs. non-pregnant. Females 1 and 2 were excluded in this data.

Organ	Brain		Spleen		Lung	
Group	**Pregnant (n=18)**	**Non-Pregnant (n=15)**	**Pregnant (n=8)**	**Non-Pregnant (n=14)**	**Pregnant (n=5)**	**Non-Pregnant (n=8)**
Mean	5,36178E-06	4,8722E-06	5,75985E-06	2,37118E-06	1,82795E-06	2,42025E-06
SD	3,69214E-06	4,50197E-06	3,18287E-06	3,104E-06	2,97483E-06	4,08533E-06
SEM	8,70245E-07	1,1624E-06	8,38337E-07	8,29579E-07	1,33039E-06	1,44438E-06

4.2.4 Frequency – Quantity Ratio (GFP/Apob)

To illustrate the frequency of GFP-positive cells in the maternal tissues, and thus the frequency of FMCs, we calculated the ratio of the quantities of GFP and Apob. Here the quantity of Apob would be proportionate to the total number of cells that was present in the sample, whereas the quantity of GFP would represent the number of FMCs. By dividing the quantity of GFP through the quantity of Apob a ratio is calculated, which we could use to estimate the ratio of GFP-positive cells in the sample.

4.2.4.1 Individual organs

We did find a significant difference between pregnant and non-pregnant females for *spleen* samples. The GFP/Apob-ratio was significantly higher in pregnant females (*p=0.0230*) (*Figure 28b*). Additionally, we did not find a significant difference between pregnant and non-pregnant females for *brain* and *lung* samples (*Figure 28a,c*; *Table 13*). However, when looking at the graphs in *Figure 28a-c*, there are clearly two clusters for *brain* and *spleen* samples of the non-pregnant females. When analysing the complete datasheet, we discovered that the samples from clusters with a higher GFP/Apob-ratio belonged, again, to females 1 and 2 (Model A-2). Therefore, we decided to re-analyse the results without the data of females 1 and 2 (*Figure 28d-f*; *Table 13*).

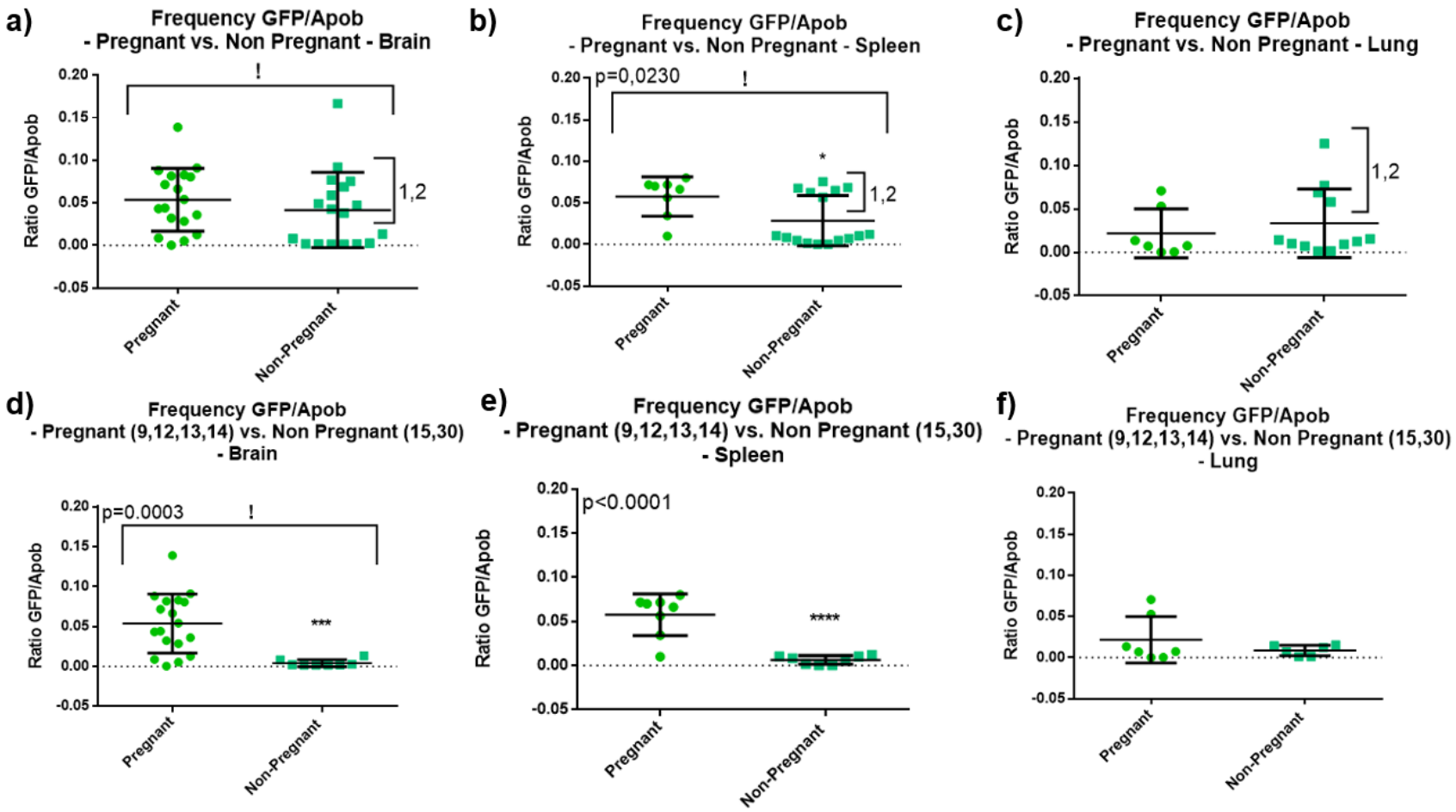

Figure 28: **The frequency of GFP/Apob in brain (a,d), spleen (b,e), and lung (c,f) samples as calculated by StepOnePlus – pregnant vs. non-pregnant – females 1 and 2 included (a-c) vs. females 1 and 2 excluded (d-f).** There was no significant difference between pregnant and non-pregnant females for brain and lung samples with females 1 and 2 included (a,c). There was a significant difference between pregnant and non-pregnant females for spleen samples with females 1 and 2 included (*p=0.0230*) (b). After excluding females 1 and 2 from the data, there was a significant difference for both brain and spleen samples. Pregnant females had a significantly higher quantity of GFP in brain and spleen samples, compared to non-pregnant females (*p=0.0003* and *p<0.0001*, respectively) (d,e). No significant differences between pregnant and non-pregnant females were found in lung samples after excluding females 1 and 2 (f). The frequency of GFP/Apob was calculated by dividing the quantity of GFP as calculated by StepOnePlus by the quantity of Apob. Statistical analysis for graphs (a,b,d) were performed using the Mann Whitney U test (!). Significance: * = *p<0.05*, *** = *p<0.001*.

Table 13: Mean, SD and SEM for the frequency of GFP/Apob for brain, spleen, and lung samples as calculated by StepOnePlus – pregnant vs. non-pregnant. Datasets were divided including and excluding females 1 and 2. Significance: * = *p<0.05*, *** = *p<0.001*, **** = *p<0.0001*

Organ	Brain		Spleen		Lung	
Females 1 and 2 included						
Group	Pregnant (n=18)	Non-Pregnant (n=18)	Pregnant (n=8)	Non-Pregnant (n=16)	Pregnant (n=7)	Non-Pregnant (n=12)
Mean	0,05362	0,04152	0,0576	0,02852 (*)	0,02166	0,03319
SD	0,03692	0,04415	0,02371	0,03033	0,0282	0,03944
SEM	0,008702	0,01041	0,008383	0,007583	0,01066	0,01138
Females 1 and 2 excluded						
Group	Pregnant (n=18)	Non-Pregnant (n=8)	Pregnant (n=8)	Non-Pregnant (n=8)	Pregnant (n=7)	Non-Pregnant (n=6)
Mean	0,05362	0,003947 (***)	0,0576	0,006381 (****)	0,02166	0,008548
SD	0,03692	0,004335	0,02371	0,004914	0,0282	0,006282
SEM	0,008702	0,001533	0,008383	0,001737	0,01066	0,002565

After excluding the data from females 1 and 2, the frequency of GFP in the *brain* and *spleen* is significantly higher in pregnant females than in non-pregnant females (*p=0.0003* and *p<0.0001*, respectively) (*Figure 28d,e*). This difference was significantly larger due to exclusion of females 1 and 2 (*Figure 28b-28e*). Again, there was no significant difference between pregnant and non-pregnant females in the *lung* (*Figure 28f*; *Table 13*).

4.2.4.2 Combined effect of pregnancy and organ-type

We performed a two-way ANOVA to analyse for the effects of pregnancy and organ-type on the ratio of GFP/Apob (*Figure 29*). There was an overall significant effect of pregnancy, with pregnant females having higher frequencies of GFP (*p<0.0001*) (*Figure 29*). Furthermore, we did not find a significant effect of organ-type on the GFP/Apob-ratio (*Figure 29*). We found that non-pregnant females had a significantly lower frequency of GFP in *brain* and *spleen* samples, compared to pregnant females (*p<0.001* and *p<0.01*, respectively)(*Figure 29*). We found no significant difference between pregnant and non-pregnant females in the *lung* (*Figure 29; Table 13*).

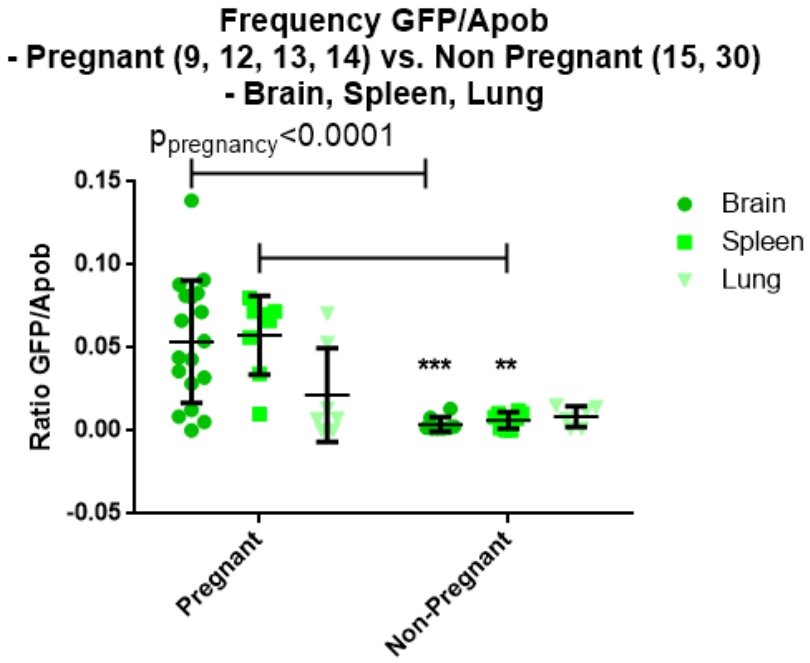

Figure 29: The frequency of GFP/Apob in brain, spleen and lung samples for pregnant and non-pregnant females. Pregnant females had a higher overal GFP/Apob-ratio, compared to the non-pregnant females (*p<0.0001*). Furthermore, the brain and spleen samples of pregnant females had a higher frequency of GFP/Apob, compared to the non-pregnant females (*p<0.001* and *p<0.01*, respectively). The frequency of GFP/Apob was calculated by dividing the quantity of GFP as calculated by StepOnePlus by the quantity of Apob. Significance: ** = *p<0.01*, *** = *p<0.001*.

4.2.4.3 Effects of genotype

We analysed the difference in GFP-frequency between the C57BL/6J- and BALB/c-females, to see whether an immunologic challenge had any effect on the quantity of FMCs in the maternal tissues. This data includes all the pregnant females, as well as all the non-pregnant females (*Table 1*). Females 1 and 2 that were excluded previously, are included in this data. However, there was no significant difference between C57BL/6J and BALB/c for any of the organs (*Figure 30*; *Table 14*).

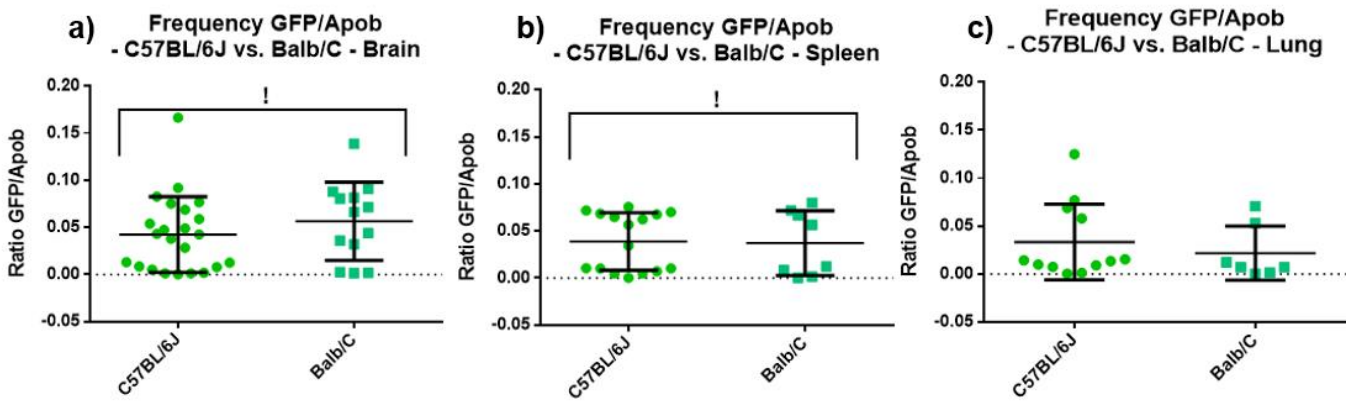

Figure 30: The frequency of GFP/Apob for brain, spleen, and lung samples – C57BL/6J vs. BALB/c. No significant difference between the two maternal genotypes was found. The frequency of GFP/Apob was calculated by dividing the quantity of GFP as calculated by StepOnePlus by the quantity of Apob. Statistical analysis for graphs (a,b) were performed using the Mann Whitney U test (!).

Table 14: The frequency of GFP/Apob for brain, spleen, and lung samples – C57BL/6J vs. BALB/c. Females 1 and 2 were included in this data.

Organ	Brain		Spleen		Lung	
Group	C57BL/6J (n=23)	BALB/c (n=13)	C57BL/6J (n=16)	BALB/c (n=8)	C57BL/6J (n=12)	BALB/c (n=7)
Mean	0,04247	0,05658	0,03875	0,03714	0,03324	0,02159
SD	0,0401	0,04143	0,03044	0,0345	0,03944	0,02817
SEM	0,008362	0,01149	0,007611	0,0122	0,01138	0,01065

4.2.5 Brain Regions

4.2.5.1 Quantity of GFP

We analysed the original quantity of GFP (not scaled to 0,0001 ng Apob) in separate *brain* regions in our animals, regardless of pregnancy, to see whether the FMCs were localized to specific regions of the *brain*. As said in the introduction, I hypothesize that the FMCs will be more frequent in structures associated with maternal behaviour, attachment, and resource allocation. However, there was no significant difference in quantity of GFP between any of the *brain* regions we analysed (*Figure 31*; *Table 15*).

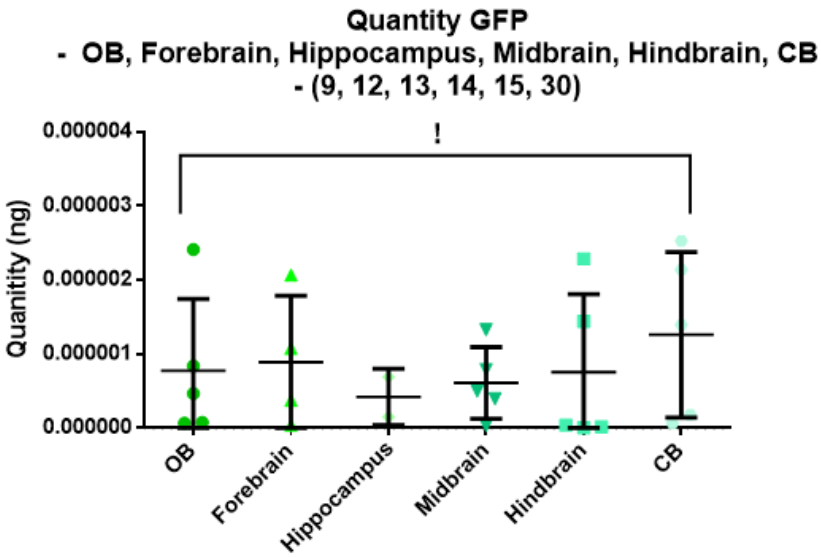

Figure 31: The quantity of GFP (ng) in the olfactory bulb (OB), forebrain, hippocampus, midbrain, hindbrain, and cerebellum (CB) as calculated by StepOnePlus. No significant differences between any of the brain regions we analysed was found. Statistical analysis of the quantity was performed using the Kruskal-Wallis test (!).

Table 15: The quantity of GFP in the olfactory bulb (OB), forebrain, hippocampus, midbrain, hindbrain, and cerebellum (CB) as calculated by StepOnePlus. Females 1 and 2 were excluded from this data.

Region	OB (n=5)	Forebrain (n=4)	Hippocampus (n=2)	Midbrain (n=5)	Hindbrain (n=5)	CB (n=5)
Mean	7,71E-07	0,001363	4,18E-07	6,09E-07	7,56E-07	1,26E-06
SD	9,7E-07	0,003046	3,81E-07	4,84E-07	1,05E-06	1,12E-06
SEM	4,34E-07	0,001362	2,69E-07	2,16E-07	4,71E-07	5E-07

4.2.5.2 Frequency – Quantity Ratio (GFP/Apob)

We analysed the ratio of GFP/Apob in separate *brain* regions in our animals as well, regardless of pregnancy, to see whether the FMCs were localized to specific regions of the *brain*. However, there was no significant difference in ratio of GFP/Apob between any of the *brain* regions we analysed (*Figure 32*; *Table 16*).

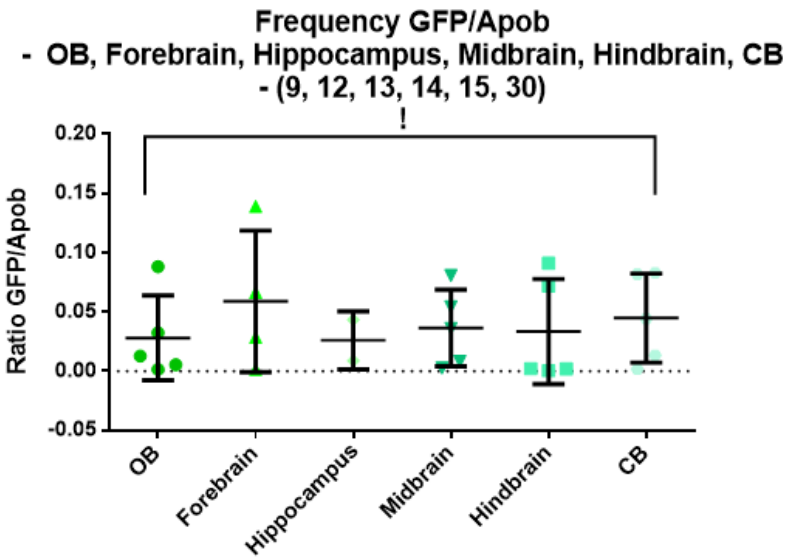

Figure 32: The frequency of GFP/Apob in olfactory bulb (OB), forebrain, hippocampus, midbrain, hindbrain and cerebellum (CB). No significant differences between the different brain regions was found. The frequency of GFP/Apob was calculated by dividing the quantity of GFP as calculated by StepOnePlus by the quantity of Apob. Statistical analysis of the frequency of GFP/Apob was performed using the Kruskal-Wallis test (!).

Table 16: The frequency of GFP/Apob in olfactory bulb (OB), forebrain, hippocampus, midbrain, hindbrain, and cerebellum (CB). Females 1 and 2 were excluded from this data.

Region	OB (n=5)	Forebrain (n=4)	Hippocampus (n=2)	Midbrain (n=5)	Hindbrain (n=5)	CB (n=5)
Mean	0,02792	0,05875	0,02586	0,03621	0,03326	0,04461
SD	0,03565	0,05965	0,02445	0,03244	0,04434	0,03766
SEM	0,01594	0,02982	0,01729	0,01451	0,01983	0,01684

The complete datasheet for the qPCR-pilot data from both the StepOnePlus-software and LinReg, as well as additional graphs can be found in *Appendix 7.17* and *Appendix 7.18*, respectively.

4.2.6 Gel Electrophoresis

Since we found several odd outliers in our data, for Cq-value, IE, quantity of GFP, and GFP/Apob-ratio, we decided to run a gel on several wells of our qPCR-plates. To our disappointment, we found multiple bands in a lot of the samples (*Figure 33*). In accordance with our assay, we would expect bands at 78bp and 96bp, for Apob and GFP, respectively. The lowest band of our ladder, which is the GeneRuler 1 kb Plus DNA Ladder (*Thermo Fisher Scientific, USA*), is at 75bp (*See Appendix 7.7: Protocol – Gel Electrophoresis*). We do see two bands for nearly all wells at the molecular weight of Apob (78bp) and GFP (96bp), as hoped, meaning that both Apob and GFP were amplified. However, we see a lot of bands with higher molecular weight ranging from 200 to 700 bp (*Figure 33*). Interestingly, we see no additional bands in well A6, which contained *brain* sample from our positive control, a hemizygous eGFP-positive male from our own breeding line. This sample did contain GFP for certain, and it can be seen that no other products were amplified. Therefore, there is a very high possibility that the assay amplifies in a non-specific manner when there is no or little GFP present. We

do not expect primer-dimers, self-dimers, or primer-probe binding to be the cause of this, considering the large size of the products. It is more likely that the assay is binding somewhere else on the genome entirely, amplifying larger products ranging from 200bp to 700bp (*Figure 33*).

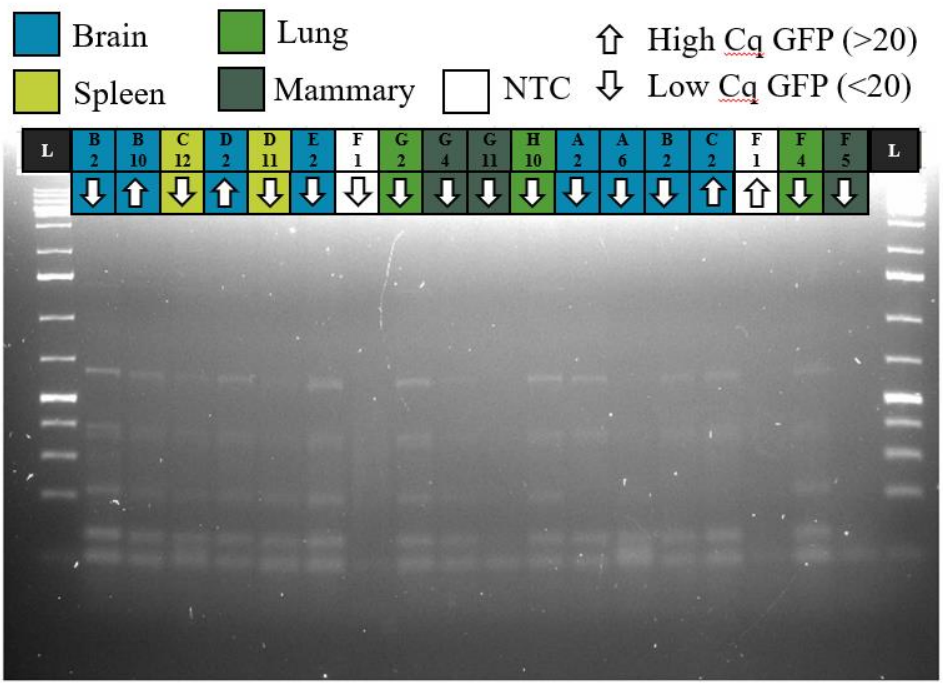

Plate 1	
B2	B9-4
B10	B2-4
C12	S35-2
D2	B9-10
D11	S2-7
E2	B9-12
F1	NTC
G2	L9-3
G4	M12-3
G11	M2-3
H10	L2-3
Plate 2	
A2	B15-14
A6	B33-3
B2	B15-10
C2	B15-7
F1	NTC
F4	L30-1
F5	M30-1

Figure 33: A 2.0% agarose gel with a selection of samples from our qPCR-pilot plates. We only expected bands for GFP (96bp) and Apob (78bp). However, we see a lot of additional bands ranging from 200bp to 700bp. We expect that we are suffering from aspecific amplification in the absence of sufficient target for GFP. The positive control for the brain (A6) does not show additional bands. Furthermore, we do see that we found GFP in most of our samples. *Gel was made by M.E. de Jong; Figure created by S. Smit*.

5. Discussion

During this project we focussed on DNA extraction optimization, as well as a qPCR-pilot for detecting FMc in the maternal brain, spleen, and lung. While the process of DNA extraction optimization has been extensively discussed in Chapter 3, this chapter will be devoted to a thorough analysis of the results of the qPCR-pilot.

Sadly, we found some discomforting results in our qPCR-pilot. Apob had some outliers in Cq-value and IE. For the Apob issues, there is a correlation between the samples with divergent Cq-values and low IE. Therefore, we believe that something went wrong during the qPCR-procedure for these specific reactions. Furthermore, the Cq-values of GFP in many samples appear to be incorrect. Whereas the Cq-values for Apob were around 20, the Cq-values for GFP should be a lot higher, as we expect relatively low amounts of GFP to be present. However, at least forty of our ninety-six samples had Cq-values below 20 for GFP, of which approximately half had a Cq-value below 10. This was an indication for us that there is something wrong with our GFP assay. The issues became clearer after running the gel shown in *Figure 33*. Besides the bands for GFP and Apob we saw a lot of bands for larger products (200-700bp). This indicates non-specific binding of our GFP-assay. We hypothesize that this was mostly the case when no, or little GFP was present in the sample. The brain sample from our positive control, a hemizygous eGFP-positive male, showed no additional bands besides Apob and GFP, suggesting that there is no non-specific amplification when GFP is present in large quantities. On the bright side, the gel does show that GFP was amplified in most samples, meaning there was GFP present in these samples.

Unfortunately, as other products were also amplified, our qPCR results cannot be fully trusted. Therefore, it is difficult to analyse the quantities of GFP and the frequencies of GFP/Apob. With the presence of other products, there is no certainty that the calculated quantity of GFP is correct specifically for GFP. As seen, samples from females 1 and 2 gave rather high values for both the quantity of GFP and the frequency of GFP/Apob. There is a high chance, because the females were terminated months after they gave birth, that there was less or no GFP present, compared to the other females from model A-2. However, *Zeng et al.* (*2010*) found FMc on day P210 in the maternal brain. Therefore, it is not inconceivable that there would be some GFP present. In fact, one of the brain samples that was run on the gel (*Figure 33*) originated from female 2 and shows a positive band for GFP. However, a qPCR run with a dysfunctional GFP assay is not sensitive enough to detect realistic and reliable quantities of GFP in this case. We are slightly more confident that there is GFP present in the samples from females 15 and 30, as they were terminated only a few weeks after weaning. However, we cannot give a clear answer on the quantity and frequency of FMc, due to the issues with the GFP assay. Finally, GFP was identified in females from E18/E19, according to the gel in some of the samples from these females. Even though there was no record of FMc at any timepoint before birth in previous studies, our lab managed to find GFP-positive cells in the maternal tissues on E18 with a FACS experiment (*Meindertsma et al., 2021*). Therefore, we are quite confident that there were low levels of GFP in the samples from E18/19, but again we cannot confidently quantify FMc with these current samples. Optimization of our qPCR protocol and GFP assay is required to provide reliable quantities in further research.

Furthermore, we found no difference in the distribution of GFP throughout the different brain regions we analysed. Again, the problems with our GFP assay make it impossible to give trustworthy statements about the distribution of GFP throughout the maternal brain. However, this does not rule out the hypothesis that FMCs would populate regions associated with maternal behaviour and resource allocation, as an extension of the placenta. We need more data and an improved GFP assay to provide more clarity on this matter. Of course, the possibility remains that FMc distribution is completely random and therefore an epiphenomenon of pregnancy. It is still possible that the mother still benefits from the presence of FMc, considering the possibility of its involvement in tissue repair and its ability to replenish stem cell niches, in which case the fetus would benefit from improved maternal health

indirectly (*Boddy et al., 2015*). However, this still creates an opening for an evolutionary function for the FMCs.

There is another element that should be considered in our results. All the E18/E19 females were perfused during termination, whereas the females from later timepoints were not. This was due to the agreements made in our CCD, which states that we could only perfuse the E18/E19 females, whereas other females were considered surplus animals. This could clearly be seen in *Figure 22*, where the yield/weight of some organs showed difference between pregnant (perfused) and non-pregnant (not perfused). The yield/weight of non-pregnant, and thus not perfused, females was a lot higher. Even though *Tan et al.* (*2005*) perfused the mice that were used for the experiment, it was interesting that FMCs seemed to populate areas close to blood vessels. Additionally, *Tan et al.* (*2005*) found that FMCs also had various morphological and immunological characteristics that were closely associated to blood vessels. Furthermore, *Ritzel et al.* (*2017*) found that the FMCs also contributed to the angiogenesis after ischemic stroke in the maternal brain and displayed epithelial-like surface markers. Therefore, it is important to consider the possibility that FMCs might be more closely related to the blood, and not necessarily to nervous tissue (*Zeng et al., 2010; Zhang et al., 2013*). However, further research is needed to give more clarification on the exact cell types of FMCs.

5.1 Limitations

The biggest limitation of our qPCR-pilot was time. Due to time constraints partially cause by COVID-19, partially by long shipping times, we were not able to optimize our qPCR assay. Normally we would have spent time and effort into optimizing the appropriate primer, probe, and DNA concentrations, while also adjusting the qPCR program on the StepOnePlus to determine the optimal settings regarding the temperature and duration of all steps.

We used an assay suggested by the Jackson Laboratory, which was suggested to be functional for genotyping mice (*The Jackson Laboratory, n.d.-b*). As we have seen in the gel *of Figure 33*, it indeed works for hemizygous eGFP-positive males, where there is a lot of GFP present. However, when having significantly smaller amounts of GFP, there appears to be non-specific amplification, which caused our values for quantity to be incorrect. Therefore, the issue could be the amount of GFP, which makes the assay designed by the Jackson Laboratory not appropriate for this experimental design. However, other factors could have negatively impacted our results.

In the protocol of the Jackson Laboratory they used faster settings for the change of temperature during the qPCR run, with the use of high speed Taq polymerase (~1000bp/sec) (*The Jackson Laboratory, n.d.-b*). We programmed the StepOnePlus to run a standard procedure, which has normal temperature changes during the qPCR run, resulting in a longer runtime. Additionally, we added an extension phase during the cycling, which would give the assay the time to amplify products as large as 700bp (*Figure 33*). The Jackson Laboratory only used a denaturation phase and an annealing phase. Finally, the annealing phase of our settings could be too long, allowing non-specific binding.

Other limitations are the limited number of samples we used. We only used 200ng of each sample, and we only analysed the samples in mono. This again was mostly due to time constraint. However, it would be useful to analyse more samples in the future, as well as analysing them in duplo or triplo on one qPCR plate. Furthermore, because the StepOnePlus can only analyse a limited amount of reference dyes for the probes, we were unable to multiplex. We wanted to multiplex GFP with SRY originally, with Apob as a reference gene. This would have provided us with information on the contribution of male versus female FMc. However, this could not be done on the StepOnePlus with the assay we originally obtained from IDT. The original plan was to perform all PCR analyses on a dPCR, however, due to delivery issues, we did not receive the dPCR in time. On the dPCR we would have been able to multiplex, which is something we definitely want to try in the near future.

Finally, the biggest constraint we, and possibly any researcher, has experienced was the ongoing COVID-19 pandemic. This put a lot of constraints on our lab space, created issues with delivery, and caused us to work more from home. We can only hope that the pandemic will pass quickly, so we can improve our efficiency on the lab once more.

5.2 Future Directions

As a consequence of this qPCR-pilot a lot of new questions about FMc arose. To answer these questions in the future, there are several other study designs that would be interesting to look in to.

For this study we looked at E18/E19, and several time points after weaning. In the future it would be interesting to look at more timepoints, including timepoints before weaning. Most importantly, it would be useful to increase the number of animals, and thus the number of samples, to have a broader dataset. This would, to some extent, compensate for small errors and random noise in the qPCR or dPCR results. This would result in a broader picture of the dynamics of FMc in the maternal brain, and other organs. To further establish the location of the FMc in the maternal brain, it would be interesting to do an immunohistochemistry study, as well as to micro punch the frozen brain sections for a more location-specific analysis of FMc with qPCR or dPCR. Finally, our lab performed a FACS-pilot as well. It was found that FACS works successfully for our specific experimental design, which is why it is relevant to further optimize a FACS analysis for FMc and MMc. FACS also creates the opportunity for subsequent RNA sequencing. This could give insights in the function and dynamics of the FMCs and allow us to detect whether FMCs have a distinct biological function from neighbouring host cells as indicated by the transcriptome.

The above-mentioned future directions are mostly dedicated to uncovering the location, morphology, dynamics, and function of FMCs in the maternal body, and more specifically, the maternal brain. However, we hypothesize that FMc could be involved in promoting maternal care, several other experiments would be interesting to uncover the evolutionary function of FMc. For example, a famine study, to see whether the FMc frequency differs in mothers exposed to famine during pregnancy. If FMc is indeed related to maternal behaviour and resource allocation, the FMCs would increase in frequency in famished females. Higher amounts of FMc could then improve and promote the resource allocation towards the fetus/offspring. The fetus could via this mechanism prepare itself for an environment with limited amounts of food availability. Additionally, it would be interesting to look for FMc in marsupials, considering these are mammals without the prolonged placentation that is found in eutherian mammal, such as mice (*Guernsey et al., 2017*). If FMCs are found in these species, a lot of new questions would arise about how the FMCs migrate from the fetus towards the mother. The same recommends seeking FMc in placental fish or reptiles. These species do not actively care for their offspring, like mammals do. If FMc indeed has an evolutionary purpose, I would predict a lack of FMCs in these taxa. However, here FMc could also be an epiphenomenon of the close association between maternal and fetal tissues during placentation. Finally, it would be interesting to look in to monogamous and promiscuous species. This could be interesting because there is lower level of intra-litter relatedness among offspring of promiscuous species, resulting in increased sibling competition and – if microchimerism is a means of maternal manipulation on the part of the fetus - increased FMc in the maternal tissues. This would reflect increased levels of conflict between mother and offspring, in which each offspring seeks to improve its own position, compared to its siblings, while the mother seeks to divide her resources equally over her current and future offspring.

We hope to be able to conduct several of these studies in the future to get a clearer picture of the FMCs and their dynamics and function in the maternal body. Sadly, in this study we were unable to provide clarity concerning the quantity of FMc in the maternal tissues, due to issues with our GFP assay. We were, however, able to detect GFP, and thus FMc, in the maternal tissues at several timepoints.

6. References

AG Scientific. (2021, February 9). *Frequently Asked Questions About Proteinase K*. https://agscientific.com/blog/2019/04/proteinase-k-faqs/

Anderson, J. W., Johnstone, B. M., & Remley, D. T. (1999). Breast-feeding and cognitive development: a meta-analysis. *The American Journal of Clinical Nutrition*, *70*(4), 525–535. https://doi.org/10.1093/ajcn/70.4.525

Axiak-Bechtel, S. M., Kumar, S. R., Hansen, S. A., & Bryan, J. N. (2013). Y-chromosome DNA Is Present in the Blood of Female Dogs Suggesting the Presence of Fetal Microchimerism. *PLoS ONE*, *8*(7), e68114. https://doi.org/10.1371/journal.pone.0068114

Bakkour, S., Baker, C. A., Tarantal, A. F., Wen, L., Busch, M. P., Lee, T. H., & McCune, J. M. (2014). Analysis of maternal microchimerism in rhesus monkeys (Macaca mulatta) using real-time quantitative PCR amplification of MHC polymorphisms. *Chimerism*, *5*(1), 6–15. https://doi.org/10.4161/chim.27778

Bear, M. F., Paradiso, M. A., & Connors, B. W. (2015). *Neuroscience*. Wolters Kluwer.

Beksac, M. S., Fadiloglu, E., Cakar, A. N., Gurbuz, R. H., Atilla, P., Onbasilar, I., Beksac, K., Katlan, D. C., Mumusoglu, S., Calis, P., & Beksac, M. (2019). Fetal Cell Microchimerism; Normal and Immunocompromised Gestations in Mice. *Fetal and Pediatric Pathology*, *39*(4), 277–287. https://doi.org/10.1080/15513815.2019.1651803

Bianchi, D. W., Zickwolf, G. K., Weil, G. J., Sylvester, S., & DeMaria, M. A. (1996). Male fetal progenitor cells persist in maternal blood for as long as 27 years postpartum. *Proceedings of the National Academy of Sciences*, *93*(2), 705–708. https://doi.org/10.1073/pnas.93.2.705

Boddy, A. M., Fortunato, A., Wilson Sayres, M., & Aktipis, A. (2015). Fetal microchimerism and maternal health: A review and evolutionary analysis of cooperation and conflict beyond the womb. *BioEssays*, *37*(10), 1106–1118. https://doi.org/10.1002/bies.201500059

Broestl, L., Rubin, J. B., & Dahiya, S. (2017). Fetal microchimerism in human brain tumors. *Brain Pathology*, *28*(4), 484–494. https://doi.org/10.1111/bpa.12557

Byers, S. L., Wiles, M. V., Dunn, S. L., & Taft, R. A. (2012). Mouse estrous cycle identification tool and images. PLoS ONE, 7(4), 35538. https://doi.org/10.1371/journal.pone.0035538

Chan, W. F. N., Gurnot, C., Montine, T. J., Sonnen, J. A., Guthrie, K. A., & Nelson, J. L. (2012). Male Microchimerism in the Human Female Brain. *PLoS ONE*, *7*(9), e45592. https://doi.org/10.1371/journal.pone.0045592

Coward, F., & Grove, M. (2012). Rethinking phylogeny and ontogeny in hominin brain evolution. *Human Origins*, *1*, 65–91.

Dawe, G. S., Tan, X. W., & Xiao, Z. C. (2007). Cell Migration from Baby to Mother. *Cell Adhesion & Migration*, *1*(1), 19–27. https://doi.org/10.4161/cam.4082

Donà, F., & Houseley, J. (2014). Unexpected DNA Loss Mediated by the DNA Binding Activity of Ribonuclease A. *PLoS ONE*, *9*(12), e115008. https://doi.org/10.1371/journal.pone.0115008

Ferris, C. F., Kulkarni, P., Sullivan Jr, J. M., Harder, J. A., Messenger, T. L., & Febo, M. (2005). Pup Suckling Is More Rewarding Than Cocaine: Evidence from Functional Magnetic Resonance Imaging and Three-Dimensional Computational Analysis. *Journal of Neuroscience*, *25*(1), 149–156. https://doi.org/10.1523/jneurosci.3156-04.2005

Fujiki, Y., Johnson, K. L., Tighiouart, H., Peter, I., & Bianchi, D. W. (2008). Fetomaternal Trafficking in the Mouse Increases as Delivery Approaches and Is Highest in the Maternal Lung1. *Biology of Reproduction*, *79*(5), 841–848. https://doi.org/10.1095/biolreprod.108.068973

Gluckman, P. D., Beedle, A., Hanson, M., Buklijas, T., Low, F., & Director Academic Unit of Human Development and Health Director Institute of Developmental Sciences and British Heart Foundation Professor of Cardiovascular Science Mark Hanson. (2016). *Principles of Evolutionary Medicine*. Oxford University Press.

Guernsey, M. W., Chuong, E. B., Cornelis, G., Renfree, M. B., & Baker, J. C. (2017). Molecular conservation of marsupial and eutherian placentation and lactation. *ELife*, *6*. https://doi.org/10.7554/elife.27450

Herba, C. M., Roza, S., Govaert, P., Hofman, A., Jaddoe, V., Verhulst, F. C., & Tiemeier, H. (2012). Breastfeeding and early brain development: the Generation R study. *Maternal & Child Nutrition*, *9*(3), 332–349. https://doi.org/10.1111/mcn.12015

Kara, R. J., Bolli, P., Karakikes, I., Matsunaga, I., Tripodi, J., Tanweer, O., Altman, P., Shachter, N. S., Nakano, A., Najfeld, V., & Chaudhry, H. W. (2012). Fetal Cells Traffic to Injured Maternal Myocardium and Undergo Cardiac Differentiation. *Circulation Research*, *110*(1), 82–93. https://doi.org/10.1161/circresaha.111.249037

Khosrotehrani, K., Johnson, K. L., Guégan, S., Stroh, H., & Bianchi, D. W. (2005). Natural history of fetal cell microchimerism during and following murine pregnancy. *Journal of Reproductive Immunology*, *66*(1), 1–12. https://doi.org/10.1016/j.jri.2005.02.001

Kinder, J. M., Stelzer, I. A., Arck, P. C., & Way, S. S. (2017). Immunological implications of pregnancy-induced microchimerism. *Nature Reviews Immunology*, *17*(8), 483–494. https://doi.org/10.1038/nri.2017.38

Koetsier, G., & Cantor, E. (n.d.). *A Practical Guide to Analyzing Nucleic Acid Concentration and Purity with Microvolume Spectrophotometers*. Bioké. Retrieved 27 July 2021, from https://www.bioke.com/support/appnotes/1345/a-practical-guide-to-analyzing-nucleic-acid-concentration-and-purity-with-microvolume-spectrophotometers.html

Kolialexi, A., Tsangaris, G. T., Antsaklis, A., & Mavroua, A. (2004). Rapid Clearance of Fetal Cells from Maternal Circulation after Delivery. *Annals of the New York Academy of Sciences*, *1022*(1), 113–118. https://doi.org/10.1196/annals.1318.018

McGhee, G. R. (2011). *Convergent Evolution: Limited Forms Most Beautiful*. MIT Press.

McHenry, J. A., Otis, J. M., Rossi, M. A., Robinson, J. E., Kosyk, O., Miller, N. W., McElligott, Z. A., Budygin, E. A., Rubinow, D. R., & Stuber, G. D. (2017). Hormonal gain control of a medial preoptic area social reward circuit. *Nature Neuroscience*, *20*(3), 449–458. https://doi.org/10.1038/nn.4487

McKinley, M. J., Yao, S. T., Uschakov, A., McAllen, R. M., Rundgren, M., & Martelli, D. (2015). The median preoptic nucleus: front and centre for the regulation of body fluid, sodium, temperature, sleep and cardiovascular homeostasis. *Acta Physiologica*, *214*(1), 8–32. https://doi.org/10.1111/apha.12487

McLean, A. C., Valenzuela, N., Fai, S., & Bennett, S. A. (2012). Performing Vaginal Lavage, Crystal Violet Staining, and Vaginal Cytological Evaluation for Mouse Estrous Cycle Staging Identification. *Journal of Visualized Experiments*, *67*. https://doi.org/10.3791/4389

Meindertsma, H. J., Smit, J. R., & Elliot, M. G. (2021). Brain Microchimerism: Frequency and distribution of maternal and fetal microchimerism in the mouse brain. *Master Thesis - Research Project 2*. Published.

Moffett, A., & Loke, C. (2006). Immunology of placentation in eutherian mammals. *Nature Reviews Immunology*, *6*(8), 584–594. https://doi.org/10.1038/nri1897

Murphy, K., & Weaver, C. (2016). *Janeway's Immunobiology* (9th New edition). Ww Norton & Co.

New England Biolabs. (n.d.). *Silica Based Methods*. Retrieved 27 July 2021, from https://international.neb.com/applications/cloning-and-synthetic-biology/nucleic-acid-purification/silica-based-methods

Numan, M., Numan, M. J., Schwarz, J. M., Neuner, C. M., Flood, T. F., & Smith, C. D. (2005). Medial preoptic area interactions with the nucleus accumbens–ventral pallidum circuit and maternal behavior in rats. *Behavioural Brain Research*, *158*(1), 53–68. https://doi.org/10.1016/j.bbr.2004.08.008

Oftedal, O. T. (1984). Milk composition, milk yield and energy output at peak lactation: a comparative review. *Symposia of the Zoological Society of London*, *51*, 33–85.

Packer, H. (2013, September 16). *Double-quenched probes increase qPCR sensitivity and precision*. Integrated DNA Technologies. https://www.idtdna.com/pages/education/decoded/article/two-quenchers-are-better-than-one#:%7E:text=ZEN%E2%84%A2%20and%20TAO%E2%84%A2%20Double%2DQuenched%20Probes&text=Including%20a%20second%2C%20internal%20quencher,qPCR%20experiments%20(Figure%201A).

PrabhuDas, M., Bonney, E., Caron, K., Dey, S., Erlebacher, A., Fazleabas, A., Fisher, S., Golos, T., Matzuk, M., McCune, J. M., Mor, G., Schulz, L., Soares, M., Spencer, T., Strominger, J., Way, S. S., & Yoshinaga, K. (2015). Immune mechanisms at the maternal-fetal interface: perspectives and challenges. *Nature Immunology*, *16*(4), 328–334. https://doi.org/10.1038/ni.3131

Protocol Online. (2013, May 3). *DNA extraction using qiagen kit - General Lab Techniques*. http://www.protocol-online.org/biology-forums-2/posts/29353.html

QIAGEN. (2020, January). *DNeasy® Blood & Tissue Handbook*. https://www.qiagen.com/us/products/discovery-and-translational-research/dna-rna-purification/dna-purification/genomic-dna/dneasy-blood-and-tissue-kit/

QIAGEN. (n.d.). *DNeasy Blood & Tissue Kits*. Retrieved 24 June 2021, from https://www.qiagen.com/us/products/discovery-and-translational-research/dna-rna-purification/dna-purification/genomic-dna/dneasy-blood-and-tissue-kit/

Ritzel, R. M., Patel, A. R., Spychala, M., Verma, R., Crapser, J., Koellhoffer, E. C., Schrecengost, A., Jellison, E. R., Zhu, L., Venna, V. R., & McCullough, L. D. (2017). Multiparity improves outcomes after cerebral ischemia in female mice despite features of increased metabovascular risk. *Proceedings of the National Academy of Sciences*, *114*(28), 5673–5682. https://doi.org/10.1073/pnas.1607002114

Seppanen, E., Roy, E., Ellis, R., Bou-Gharios, G., Fisk, N. M., & Khosrotehrani, K. (2013). Distant Mesenchymal Progenitors Contribute to Skin Wound Healing and Produce Collagen: Evidence from a Murine Fetal Microchimerism Model. *PLoS ONE*, *8*(5), e62662. https://doi.org/10.1371/journal.pone.0062662

Smiley, K. O., Ladyman, S. R., Gustafson, P., Grattan, D. R., & Brown, R. S. E. (2019). Neuroendocrinology and Adaptive Physiology of Maternal Care. *Neuroendocrine Regulation of Behavior*, 161–210. https://doi.org/10.1007/7854_2019_122

Stervander, M. (2013, February 27). *Degradation of DNA during RNase A treatment of previously extracted DNA: I wonder if anyone here has had any* [ResearchGate]. ResearchGate. https://www.researchgate.net/post/Degradation_of_DNA_during_RNase_A_treatment_of_previously_extracted_DNA

Tan, X. W., Liao, H., Sun, L., Okabe, M., Xiao, Z. C., & Dawe, G. S. (2005). Fetal Microchimerism in the Maternal Mouse Brain: A Novel Population of Fetal Progenitor or Stem Cells Able to Cross the Blood-Brain Barrier? *Stem Cells*, *23*(10), 1443–1452. https://doi.org/10.1634/stemcells.2004-0169

The Jackson Laboratory. (n.d.-a). *006567 - C57BL/6-Tg(CAG-EGFP)131Osb/LeySopJ*. Retrieved 24 June 2021, from https://www.jax.org/strain/006567

The Jackson Laboratory. (n.d.-b). *Protocol 22182 - Generic GFP/EGFP qPCR*. Retrieved 28 July 2021, from https://www.jax.org/Protocol?stockNumber=008450&protocolID=22182

ThermoFisher Scientific. (n.d.-a). *GeneRuler 1 kb Plus DNA Ladder*. Retrieved 31 July 2021, from https://www.thermofisher.com/document-connect/document-connect.html?url=https%3A%2F%2Fassets.thermofisher.com%2FTFS-Assets%2FLSG%2Fmanuals%2FMAN0013047_GeneRuler_1kb_Plus_DNALadder_250ug_UG.pdf

ThermoFisher Scientific. (n.d.-b). *Mouse Haplotype Table*. Retrieved 27 July 2021, from https://www.thermofisher.com/document-connect/document-connect.html?url=https%3A%2F%2Fassets.thermofisher.com%2FTFS-Assets%2FLSG%2Fbrochures%2FMouse_Haplotype_Table.pdf&title=TW91c2UgSGFwbG90eXBlIFRhYmxl

ThermoFisher Scientific. (n.d.-c). *NanoDrop Nucleic Acid Handbook*. Retrieved 27 July 2021, from https://www.thermofisher.com/document-connect/document-

connect.html?url=https%3A%2F%2Fassets.thermofisher.com%2FTFS-Assets%2FCAD%2Fmanuals%2Fts-nanodrop-nucleicacid-olv-r2.pdf

Turin, L., Invernizzi, P., Woodcock, M., Grati, F. R., Riva, F., Tribbioli, G., & Laible, G. (2007). Bovine fetal microchimerism in normal and embryo transfer pregnancies and its implications for biotechnology applications in cattle. *Biotechnology Journal*, *2*(4), 486–491. https://doi.org/10.1002/biot.200600218

VanDerBilt University. (2019). *DNA EXTRACTION LAB*. https://cdn.vanderbilt.edu/vu-wp0/wp-content/uploads/sites/267/2019/06/19164057/Lab2_DNA_19June2019.pdf

Vojdani, Z., Bagheri, J., Talaei-Khozani, T., Azarpira, N., Salmannjad, M., & Farrokhi, A. (2018). Fetal microchimerism in mouse caerulein-induced pancreatitis model. *Iranian Journal of Basic Medical Sciences*, *21*, 889–895. https://doi.org/10.22038/IJBMS.2018.26976.6595

Wildman, D. E., Chen, C., Erez, O., Grossman, L. I., Goodman, M., & Romero, R. (2006). Evolution of the mammalian placenta revealed by phylogenetic analysis. *Proceedings of the National Academy of Sciences*, *103*(9), 3203–3208. https://doi.org/10.1073/pnas.0511344103

Zeng, X. X., Tan, K. H., Yeo, A., Sasajala, P., Tan, X., Xiao, Z. C., Dawe, G., & Udolph, G. (2010). Pregnancy-Associated Progenitor Cells Differentiate and Mature into Neurons in the Maternal Brain. *Stem Cells and Development*, *19*(12), 1819–1830. https://doi.org/10.1089/scd.2010.0046

Zhang, G., Zhao, Y., Li, X. M., & Kong, J. (2013). Fetal cell microchimerism in the maternal mouse spinal cord. *Neuroscience Bulletin*, *30*(1), 81–89. https://doi.org/10.1007/s12264-013-1392-1

7. Appendixes

7.1 Datasheet – Animal ID and Tissues

Animal ID	Genetic background	Model	Age	Mate		Litter			Termination		Organs			Purpose
	Animal		(days)	ID	Genotype	Genotype	Size	Date of birth	Date	Days since weaning	Brain	Spleen	Lung	
D	KO TNF-R1(C57BL/6J)	C	106	X	X	X	4	17/11/20	8/12/20	1	X			Optimization
E	C57BL/6J (Backcross)	C	141	X	X	X	5	17/11/20	8/12/20	1	X			Optimization
F	tg Camk2a-tTA(C57NL/6J)	C	204	X	X	X	10	11/11/20	8/12/20	1	X			Optimization
G	C57BL/6J (Backcross)	C	141	X	X	X	8	16/11/20	8/12/20	1	X			Optimization
H	KO TNF-R2(C57BL/6J)	C	103	X	X	X	9	17/11/20	8/12/20	1	X			Optimization
I	Pcdh9 KO(C57BL/6J)	C	188	X	X	X	X	X	10/12/20	X	X			Optimization
J	Pcdh9 KO(C57BL/6J)	C	188	X	X	X	X	X	10/12/20	X	X			Optimization
K	Pcdh9 KO(C57BL/6J)	C	136	X	X	X	X	X	10/12/20	X	X			Optimization
L	Pcdh9 KO(C57BL/6J)	C	136	X	X	X	X	X	10/12/20	X	X			Optimization
M	tg J20 B(C57BL/6J)	C	192	X	X	X	X	X	26/1/21	X	X			Optimization
1	C57BL/6J	A-2	253	8	C57BL/6-Tg(CAG-EGFP)131Osb/LeySopJ	C5BL/6J-eGFP(+,-)	8	11/11/20	25/3/21	105	X	X	X	qPCR-pilot
2	C57BL/6J	A-2	253	8	C57BL/6-Tg(CAG-EGFP)131Osb/LeySopJ	C5BL/6J-eGFP(+,-)	7	25/12/20	25/3/21	63	X	X	X	qPCR-pilot
9	C57BL/6J	A-1	138	4	C57BL/6-Tg(CAG-EGFP)131Osb/LeySopJ	C5BL/6J-eGFP(+,-)	10	X	30/11/20	X	X	X	X	qPCR-pilot

11	C57BL/6J	C	253	X	X	X	X	X	25/3/21	X	X			Optimization
12	C57BL/6J	A-1	138	8	C57BL/6-Tg(CAG-EGFP)131Osb/LeySopJ	C5BL/6J-eGFP(+,-)	8	X	30/11/20	X	X			qPCR-pilot
13	BALB/c	B-1	132	4	C57BL/6-Tg(CAG-EGFP)131Osb/LeySopJ	BALB/c-eGFP(+,-)	11	X	26/1/21	X	X	X	X	qPCR-pilot
14	BALB/c	B-1	132	3	C57BL/6-Tg(CAG-EGFP)131Osb/LeySopJ	BALB/c-eGFP(+,-)	9	X	26/1/21	X	X			qPCR-pilot
15	BALB/c	B-2	175	5	C57BL/6-Tg(CAG-EGFP)131Osb/LeySopJ	BALB/c-eGFP(+,-)	8	28/1/21	25/3/21	35	X	X	X	qPCR-pilot
30	C57BL/6J	A-2	175	8	C57BL/6-Tg(CAG-EGFP)131Osb/LeySopJ	C5BL/6J-eGFP(+,-)	8	28/1/21	25/3/21	28	X	X	X	qPCR-pilot
33 (M)	C5BL/6J-eGFP(+,-)	C	79	X	X	X	X	X	28/1/21	X	X			Optimization
39 (M)	C5BL/6J-eGFP(+,-)	C	84	X	X	X	X	X	17/3/21	X	X			Optimization
40 (M)	C5BL/6J-eGFP(+,-)	C	84	X	X	X	X	X	17/3/21	X	X			Optimization
41 (M)	C5BL/6J-eGFP(+,-)	C	84	X	X	X	X	X	17/3/21	X	X			Optimization
46 (M)	C5BL/6J-eGFP(+,-)	C	84	X	X	X	X	X	21/4/21	X	X			Optimization
49 (M)	C5BL/6J-eGFP(+,-)	C	84	X	X	X	X	X	21/4/21	X	X			Optimization

7.2 Protocol – Estrus Checks

Solutions:

- ✓ 50mM Tris-HCl (pH=7,0-7,4)
  - 7,88 g Tris-base in 900 mL MilliQ
  - Set pH to 7,0-7,4
  - Complete to 1L with MilliQ
  - Measure pH again → Set it to pH=7,0-7,4 if needed
- ✓ Filtered Giemsa (~70-80 mL)
- ✓ Giemsa Solution (for one staining basin)
  - 8,75 mL filtered Giemsa
  - 119 mL 50mM Tris-HCl

Protocol:

- Make an estrus swipe:
  - *Vaginal lavage:* pipette one droplet of autoclaved demi water up and down at the surface of the vagina using 300µl filter pipette tips and a latex bulb. Place the droplet from the vaginal lavage on a microscope slide.
  - *Inoculating loop:* Dip the inoculating loop in autoclaved demi water. Insert the inoculating loop superficially into the vagina, and slightly turn it inside the vagina. Smear the sample out on a microscope slide.
- Let the droplet on the microscope slide dry
- Place the microscope slide in the staining basin with the cells facing towards you.
- Poor the staining solution in the basin. Do not poor it over the cells.
- Leave the slides in the staining for 10 minutes.
- Carefully rinse the backside of the slide under a slow running tap.
- Rinse the backside again with demi water.
- Use paper to dry the backside of the slide.
- Let the slide dry, with the cell to the top.
- Cif can be used to clean your instruments from the Giemsa staining.
- Analyse the dry microscope slides under the microscope to check for estrus phase.

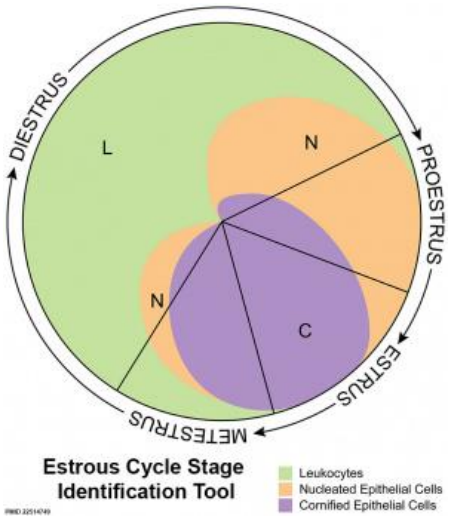

Figure A: An overview of cell types found in each phase of the estrus cycle. The estrus phase consist mainly of cornified epithelial cells. *Figure borrowed from Byers et al., (2012).*

7.3 Protocol – Termination

Materials:

- ✓ Dissection kit
  - Termination forms
  - Toolbox
  - Permanent markers (red & black; waterproof)
  - Boxes with empty cups
  - Needles
- ✓ Storage of organs in freezer (-80):
  - Liquid nitrogen
  - Aluminium foil
  - Dry ice
- ✓ Storage of blood:
  - *EDTA cups*
  - Ice
- ✓ Other materials:
  - Petri dishes (10x)

Solutions:

- ✓ 70% ethanol (bottle)
- ✓ Demi water (Erlenmeyer)
- ✓ Rinsing Solution (Erlenmeyer)
- ✓ Washing Solution (0.01M PB) (bottle)

Protocol:

Steps (short version):

1. Clean perfusion pump with demi water
2. Fill the system with rinsing solution
3. Anaesthesia – Isoflurane (box → nose)
4. Cardiac puncture (on table)
5. Uterus removed
6. Perfusion (saline)
7. Decapitation
8. Collection of organs (mother first)
9. Pups:
   1. Placenta
   2. Tails
   3. Organs

Perfusion:

Rinsing/fixation speed:

Check on graph the pumps settings (hanging above the pump in the perfusion room)
For Mouse : 15 ml/ min (~ 8 on the pump scale/ left pump)

Perfusion:

- Clean the pump tubes with demi water and fill the system with rinsing solution.
- Anesthetize the animal with isoflurane in the box
- Move animal to the table & perform cardiac puncture
- Move animal to perfusion room
- Cut the animal open
  - Above muscle layer
  - Tear of skin

    - Cut through muscle & open the animal
    - Cut the ribs at the sides
    - Cut the diaphragm
    - Pull up the ribs
- Insert the needle into the left ventricle and cut the right atrium of the heart (the rinsing solution goes into the blood vessels but not in the lungs.).
- Rinse the animal with rinsing solution
- After perfusion, take out the brain & other organs

Collection of organs:

Organs are snap frozen with liquid nitrogen. Use the mother/pup dissection form(s). Write down animal number, amount of pups L and R, date & your name.

IMPORTANT:

- Blood must be washed from the organs before freezing! You can use the WASH bottles & petri dishes to do so. Dry the organs in tissue before freezing! WEIGH each organ!
- Fat cups are NOT labelled (write type of fat down):
    - Retro-peritoneal = RP
    - Mesenteric = M
    - Posterior subcutaneous = PS
    - Axillary = A
- Placentas & pup organs are NOT labelled (write animal number down!)
- Tails are collected in normal eppendorfs (no hole)
- Organs for freezing are collected in punctured eppendorfs.
- CLEAN your dissection tools with 70% ethanol & tissue between animals

Solutions:

Rinsing Solution – 0.9% NaCl + Heparin solution for (150 mL)

- *Dissolve 1.35 gr NaCl in 135 mL demi water*
- *Add 0.6 mL Heparin 500 U/mL*
  (Or 0.75 mL Heparin 400 U/mL)
- *Complete to 150 mL with demi water*
- *Amount for 1 mouse: 150 mL solution*

Washing Solution - 0.01M PB for (1 L)

- *Take 100 mL 0.2M PB*
- *Complete to 1900 mL with demi water*

7.4 Protocol – Tissue Cutting in Cryostat

Materials

- Frozen (Brain) Sample for -80°C
- Brain Matrix (1mm slots)
- Cryostat (-20°C)
- Razor Blade
- Tweezers
- Spatula
- Petri dish (glass)
- 2ml Eppendorf cups
- Waterproof fine liner
- Highly sensitive scale
- Dry Ice
- Lab Journal + Pencil

Reagents

- Ethanol (70%) for cleaning afterwards

General

- Preferably work with two persons to cut tissue with this protocol
- Put all the instruments in the cryostat (-20°C) beforehand, so they can cool down and do not melt your tissue
- Weigh and write the cups before starting to cut the tissue. Additionally, it is wise to put the cups in the cryostat beforehand as well.
- Never clean the Brain Matrix with paper towel because the fibres will get stuck
- Clean the Brain Matrix before use, between brains and after use with hot water and ethanol. Make sure the Brain Matrix is dry before putting it back in the cryostat, to prevent frosting. Additionally, it is important to cool the Brain Matrix down before putting the new tissue on the Brain Matrix.
- Cut one piece at the time, weigh it, make sure it is within the right proportions before continuing with another piece. If the piece is too big you can cut it smaller in the Petri dish. If cutting a piece of brain in smaller fractions, preferably split the hemispheres (sagittal cut).

Protocol: Cutting Tissue in the Brain Matrix

1. Set the chamber temperature of the cryostat to -20°C and place the instruments in the cryostat, so they can cool off.
    a. Brain Matrix
    b. Razor Blade
    c. Tweezers
    d. Spatula
    e. Petri dish
2. Weigh and write the expected number of cups needed for cutting your tissue. When finished, put the cups in the cryostat so they can cool off as well.
    a. Expected cups for whole brain cutting is ~25 cups, if the weight of the pieces is between 15-23 mg.
3. If all the instruments are cooled down enough and the cups are prepared, the tissue can be taken from the dry ice and positioned on the brain matrix inside the cryostat.
    a. It is wise to put the brain with the dorsal side down, as the matrix is formed in that way. This will reduce tissue movement and refine the cutting of the tissue.

4. Position the razor blade above one of the slots with one hand and keep the tissue in place using the spatula with the other.
    a. Preferably, when cutting a brain, start with the olfactory bulb and make sure that the entire olfactory bulb is the first section.
5. Put force on the razor blade and push it down in the slot to cut one slice of your tissue.
6. After cutting you can use the tweezers to carefully pick up the piece and put it in the right cup.
    a. Sometimes it helps to keep the razorblade in place. It will make it easier to pick up the piece and if other scraps occur due to the cutting, you can distinguish them as well. This way you can make sure you pick up every single piece of the cut slice.
7. Weigh the cup with the tissue and put it back on dry ice as fast as possible. If the piece turns out to be too heavy, cut the piece in smaller sections in the Petri dish inside the cryostat. Do this before continuing with a new slice of the tissue.
    a. Wait for cutting a new piece until you are sure the previous piece was the right size
    b. If cutting brain cut the bigger pieces sagittal.
8. Continue this protocol until you have cut up the entire organ. At the end you can fill a cup with left over scraps of tissue in the matrix.
9. Clean the Brain Matrix after finishing one piece of tissue. Wash it with hot water and ethanol. Also, clean out the cryostat and the instruments used with ethanol.
    a. If you cut another organ, make sure all the tools are dry and put them back in the cryostat to cool them down again. Do not place the new organ on the matrix until you are certain it is cooled down enough.
10. Place the cut tissue in the -80°C until further use.

7.5 Protocol – Bead Cleaning

Solutions:

- ✓ 1L MilliQ
  - 1000 mL MilliQ

  ➔ Autoclave (20 min, 121°C)
- ✓ 1L DEPC treated MilliQ
  - 1000 mL MilliQ
  - 1 mL DEPC (fridge)

  ➔ Shake
  ➔ Overnight at 37°C
  ➔ Autoclave (20 min, 121°C)
- ✓ 1L DEPC treated 0.1M NaOH
  - 990 mL MilliQ
  - 10 mL NaOH
  - 1 mL DEPC (frigde)

  ➔ Shake
  ➔ Overnight at 37°C
  ➔ Autoclave (20 min, 121°C)

Protocol:

- Wash three times in autoclaved MilliQ
- Overnight in DEPC treated 0.1M NaOH on shaker
- Wash three times in DEPC treated MilliQ
- Dry in stove at 37°C
- Store in plastic 50 mL cup

7.6 Protocol – qPCR

Protocol:

- Prepare your run in the StepOnePlus-software. Run it at: Relative Standard Curve, with the standard settings (a run of ~2 hrs). Assign your samples to the wells, determine your standards. Install your run method.
- Prepare the centrifuge: Set the temperature to 4°C.
- Make the Master Mix and prepare the samples. Make enough Master Mix for all your wells +10%. While preparing the Master Mix make sure you place the solutions on ice.

Table A: Master Mix volumes for one well. Multiply each amount with the number of wells + 10%.

Mastermix	1x
UltraPure H2O	6 µL
iTaq mastermix	10 µL
GFP assay	1 µL
Apob assay	1 µL
DNA (x ng/µL)	2 µL
Total	**20 µL**

- Plate the well plate in a cooler or on ice.
- Vortex the Master Mix.
- Reverse pipette 18 µl the Master Mix onto the qPCR-plate
- Add 200 ng (in 2µl) DNA of your samples to the correct wells. Also include a NTC of 2µl UltraPure H2O. Make sure to pipette your sample into the Master Mix. Furthermore, vortex your sample before pipetting it onto the plate.

Table B: Example of sample dilution needed to load 200 ng of sample.

Dilution	Organ DNA	ng/uL	DNA when add 2 uL (ng)	Total concentration in MM (ng/uL)
	1	100,0	200	10

- Seal the plate:
  - Get the cover seal.
  - Take off the coverslip.
  - Apply the cover to the well plate. Make sure you align it with the well plate and secure all the borders with your nail. Remove the slips on the side.
- Spin the well plate at 1500 xg (rcf), 4°C for 2 min.
- Place the well plate in the StepOnePlus and run the following program:
  - 2 min, 95°C
  - 45 cycles of 30 sec, 95°C; 30 sec, 60°C; 36 sec, 72°C.
  - 7 min, 72°C
  - 4°C, ∞
- Analyse your data in the StepOnePlus-software and LinRegPCR

7.7 Protocol – Gel Electrophoresis

Protocol:

- Prepare the mould for the gel.
- Mix x g agarose with x mL TAE buffer.
- Put on scale → TARE
- Heat in microwave until bubbles appear.
- Mix solution and make sure all the agarose is gone and the solution is clear
- Add x µl of SYBR safe.
- Put on scale and fill up to 0 g with demi water.
- Add x mL TAE and let the solution cool down a bit.
- Poor the solution in the corner of the mould, remove any bubbles with the slots.
- Let the mould and solution stand for 30-45 min until the gel is dry and hard.
- Remove slot mould.
- Place the gel in the TAE buffer.
- Load 5µl of your sample including loading dye to the assigned wells, together with your DNA ladder. (GeneRuler 1Kb Plus DNA ladder, ThermoFisher Scientific, USA).
- Run the electrophoresis.

Table A: Instructions for 0,8% and 2,0% agarose gels in middle size mould.

Gel	Size	Agarose	TAE	SYBR Safe	Settings
0.8%	Middle	0,92 g	115 mL (85 + 30 mL)	5,75 µl	110V, 1 hr
2.0%	Middle	2,3 g	115 mL (85 mL + 30 mL)	5,75 µl	110V, 25 min

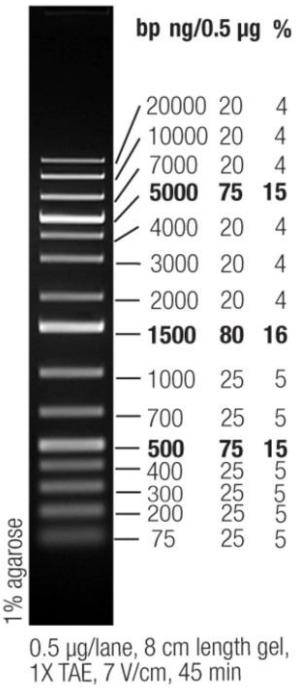

Figure A: The GeneRuler 1Kb Plus DNA Ladder from ThermoFisher Scientific, which was used in this project. (*ThermoFisher Scientific, n.d.-a*).

7.8 Protocol – QIAGEN DNeasy Blood and Tissue Kit

The handbook of the DNeasy Blood and Tissue Kit provided us with a protocol for the use of the mini-spin columns. Additionally, QIAGEN provided us with a user-protocol, which implemented the use of the TissueLyser II (QIAGEN, Germany). Before we started the optimization, we tried both protocols, with and without TissueLyser. The protocol can be found below (QIAGEN, 2020):

Preparations:

- Warm Buffer ATL and Buffer AL to 56 °C in case of precipitates.
- Add the appropriate amount of ethanol (96-100%) to Buffer AW1 and Buffer AW2.
- Preheat water bath to 56 °C.

Protocol:

1. Pipet 180 µl Buffer ATL into a 2 ml Safe-Lock microtube containing the sample.

In case of the use of the TissueLyser:

a. *Add one stainless steel bead to each tube. For best results, use 5 mm (mean diameter) stainless steel beads.*

b. *Add 10 mg tissue to the tube and assemble the TissueLyser.*

c. *Homogenize on the TissueLyser for 20 s at 15 Hz. Do not exceed this time as it may result in DNA shearing.*

d. *Centrifuge the sample briefly to ensure that all the tissue debris is on the bottom of the tube*.

2. Add 20 µl proteinase K to the tube. Incubate for 56°C for 1 h in a shaker incubator.

* Note: Add 40 µl proteinase K if using RNAlater stabilized tissues.

Lysis time varies depending on the sample processed. In general, samples are lysed in 1 h. If it is more convenient, samples can be lysed overnight; this will not affect them adversely.

* Optional: If RNA-free genomic DNA is required, add 4 µl RNase (100 mg/ml) and incubate for 5 min at room temperature before continuing with step 9.

3. Add 200 µl Buffer AL to the sample (* 220 µl Buffer AL if using RNAlater stabilized tissues) and mix thoroughly by vortexing. Then add 200 µl ethanol (96–100%) and mix again thoroughly by vortexing.

It is essential that the sample, Buffer AL, and ethanol are mixed immediately and thoroughly by vortexing or pipetting to yield a homogeneous solution. Buffer AL and ethanol can be premixed and added together in one step to save time when processing multiple samples.

A white precipitate may form on addition of Buffer AL and ethanol. This precipitate does not interfere with the DNeasy procedure. Some sample types may form a gelatinous lysate after addition of Buffer AL and ethanol. In this case, vigorously shaking or vortexing the preparation is recommended.

4. Pipet the mixture from step 3 (including any precipitate) into the DNeasy Mini spin column placed in a 2 ml collection tube (provided). Centrifuge at ≥6000 x g (8000 rpm) for 1 min. Discard flow-through and collection tube. *

5. Place the DNeasy Mini spin column in a new 2 ml collection tube (provided), add 500 µl Buffer AW1, and centrifuge for 1 min at ≥6000 x g (8000 rpm). Discard flow- through and collection tube. *

6. Place the DNeasy Mini spin column in a new 2 ml collection tube (provided), add 500 µl Buffer AW2, and centrifuge for 3 min at 20,000 x g (14,000 rpm) to dry the DNeasy membrane. Discard flow-through and collection tube.

It is important to dry the membrane of the DNeasy Mini spin column since residual ethanol may interfere with subsequent reactions. This centrifugation step ensures that no residual ethanol will be carried over during the following elution.

Following the centrifugation step, remove the DNeasy Mini spin column carefully so that the column does not come into contact with the flow-through, since this will result in carryover of ethanol. If carryover of ethanol occurs, empty the collection tube, then reuse it in another centrifugation for 1 min at 20,000 x g (14,000 rpm).

7. Place the DNeasy Mini spin column in a clean 1.5 ml or 2 ml microcentrifuge tube (not provided), and pipet 200 µl Buffer AE directly onto the DNeasy membrane. Incubate at room temperature for 1 min, and then centrifuge for 1 min at ≥6000 x g (8000 rpm) to elute.

* Elution with 100 µl (instead of 200 µl) increases the final DNA concentration in the eluate, but also decreases the overall DNA yield (see DNeasy Blood & Tissue Handbook).

8. Recommended: For maximum DNA yield, repeat elution once as described in step 7. This step leads to increased overall DNA yield.

A new microcentrifuge tube can be used for the second elution step to prevent dilution of the first eluate. Alternatively, to combine the eluates, the microcentrifuge tube from step 7 can be reused for the second elution step.

* Note: Do not elute more than 200 µl into a 1.5 ml microcentrifuge tube because the DNeasy Mini spin column will come into contact with the eluate.

7.9 Protocol – Optimized DNA Extraction

The following protocol was specifically optimized for the extraction of DNA from murine brain tissue.

Preparations:

- When using the kit for the first time: Add the appropriate amount of ethanol (96-100%) to the AW1 and AW2 buffers, as indicated on the bottles.
- Heat the stove to 56°C (pre-incubation).
- Heat the water bath to 70°C (post-incubation).
- Check AL and ATL buffers for precipitates. If precipitates are in the buffers, heat them to 56°C until the precipitates disappear. Cool the buffers to room temperature before use.
- Optional: Prepare the columns for each sample and write the sample numbers on them (post-incubation).
- Optional: Place two collection tubes for each sample in your microtube rack (post-incubation).
- Optional: Prepare the 2ml microcentrifuge tubes (RNase/DNase free) for each sample and write the sample number on them (post-incubation).

Protocol:

1. Take the whole mount of brain tissue from -80°C and cut it in the cryostat at -20°C in sections of approximately ~25mg (± 10 mg) (See Appendix 7.4: Protocol – Tissue cutting in Cryostat). Store the sections in dry ice until further use or place them back in -80°C if there will be no immediate extraction.

2. Keep the sections on dry ice. Pipet 180 µl Buffer ATL into a 2 ml Safe-Lock microtube containing the sample, after which the samples can be kept at room temperature.

3. Add one stainless steel bead to each tube, use 5 mm (mean diameter) stainless steel beads. Homogenize on the TissueLyser for 2 x 15 s at 30 Hz.

4. Spin your sample briefly to form a cell pellet. Use tweezers to take the bead out, clean them thoroughly between each sample with 70% ethanol. Vortex the sample afterwards.

5. Add 20 µl proteinase K to the tube. Vortex your sample briefly. Spin the sample for 5 seconds, after which you vortex the sample again briefly. Incubate for 56°C for 3-6hrs in a stove. Vortex the samples regularly during the incubation. Additionally, if more convenient, the samples can be incubated overnight without danger to damaging your samples.

6. Perform this entire step for each sample before proceeding to the next. Vortex your sample thoroughly after the incubation. Add 200 µl Buffer AL to the sample and mix thoroughly by vortexing. Then add 200 µl ethanol (96–100%) and mix again thoroughly by vortexing. Then proceed to the next sample.

*A white precipitate may form on addition of Buffer AL and ethanol. This precipitate does not interfere with the DNeasy procedure. However, if it happens, try vortexing for some while longer. Precipitates often disappear with brain tissue. It is important to get rid of the precipitates, as they can clod the membrane, which will adversely affect the extraction later on.

7. Pipet ~350µl of the mixture from step 6 into the DNeasy Mini spin column placed in a 2 ml collection tube. Centrifuge at ≥6000 x g (8000 rpm) for 1 min. Pipet the additional ~350µl of the mixture onto the membrane. Centrifuge again at ≥6000 x g (8000 rpm) for 1 min. Discard flow-through and collection tube. Place the column in a new collection tube.

5. Add 500 µl Buffer AW1, and centrifuge for 1 min at ≥6000 x g (8000 rpm). Discard flow- through and collection tube. Place the column in a new collection tube.

6. Add 500 µl Buffer AW2, and centrifuge for 3 min at 20,000 x g (14,000 rpm) to dry the DNeasy membrane. Discard flow-through and place the column back in the empty collection tube. Add 500 µl Buffer AW2 again, and centrifuge for 3 min at 20,000 x g (14,000 rpm). Discard the flow-through and collection tube. Place the column in a clean 2ml microcentrifuge tube (RNase and DNase free).

7. Pipet 200 µl Buffer AE directly onto the DNeasy membrane. Incubate at 70°C in a water bath for 1 min, and then centrifuge for 1 min at ≥6000 x g (8000 rpm) to elute. Do not switch the microcentrifuge tube. Both elutions will be collected in the same cup for this experiment.

8. Pipet 100 µl Buffer AE directly onto the DNeasy membrane. Incubate at 70°C in a water bath for 1 min, and then centrifuge for 1 min at ≥6000 x g (8000 rpm) to elute.

9. Store at 4°C until further use for a short period of time (± 24 hours). Store at -20°C until further use for a longer period of time.

7.10 Protocol – NucleoSpin Kit and NucleoSpin XS

DNA extraction NucleoSpin

1. **Prepare samples → Tissue Lyser II**
   - Add **180 µL T1**
   - Add bead
   - Homogenize samples at ***30 Hz for 30 sec***
   - **Centrifuge** sample (pellet)
   - Remove bead

2. **Pre-Lysis**
   - Vortex
   - Add **25 µL Proteinase K**
   - Vortex (!!!)
   - Incubate at **56 °C** (vortex occasionally)
   - ➔ ~1-3 hours
   - Incubate at **RT for 5 min**

3. **Lyse Sample**
   - Vortex
   - Add **200 µL B3**
   - Vortex
   - Incubate **70°C for 10 min**
   - Vortex briefly

4. **Adjust DNA binding conditions**
   - Add **210 µL Ethanol** (96-100%)
   - Vortex (!!!)

5. **Bind DNA**
   - NucleoSpin Tissue Column in Collection Tube
   - **Load all sample** to the Column
   - Centrifuge at ***11,000 x g for 1 min***
   - Discard flow through and Collection Tube
   - New Collection Tube

6. **Washing I**
   - Add **500 µL BW**
   - Centrifuge at ***11,000 x g for 1 min***
   - Discard flow through
   - Place Column back in Tube

7. **Washing II**
   - Add **600 µL B5**
   - Centrifuge at ***11,000 x g for 1 min***
   - Discard flowthrough
   - Place Column back in Tube
   - Centrifuge at ***11,000 x g for 1 min***
   - Discard flow through & tube

8. **Elution**
   - Column in NEW Eppendorf
   - Add **100 µL BE**
   - Incubate **1 min at RT**
   - Centrifuge at ***11,000 x g for 1 min***
   - Store flowthrough (DNA!) in -20 °C

DNA extraction with NucleoSpin XS

1. **Prepare samples → Tissue Lyser II**
   - Add **80 µL T1**
   - Add bead
   - Homogenize samples at ***30 Hz for 30 sec***
   - **Centrifuge** sample (pellet)
   - Remove bead

2. **Pre-Lysis**
   - Vortex
   - Add **8 µL Proteinase K**
   - Vortex
   - Incubate at **56 °C** (vortex occasionally)
   - ➔ ~1-4 hours
   - RNA-free DNA: Add **20 µL RNAse A**
   - Incubate at **RT for 5 min**

3. **Lyse Sample**
   - Add **80 µL B3**
   - Vortex 2x5s
   - Incubate **70°C for 5 min**
   - Vortex briefly
   - Let cool down to **RT**

4. **Adjust DNA binding conditions**
   - Add **80 µL Ethanol** (96-100%)
   - Vortex 2x5s
   - Spin briefly

5. **Bind DNA**
   - NucleoSpin Tissue XS Column in Collection Tube
   - **Load all sample** to the Column
   - Centrifuge at ***11,000 x g for 1 min***
   - Discard flow through and Collection Tube
   - New Collection Tube

6. **Washing I**
   - Add **50 µL BW**
   - Centrifuge at ***11,000 x g for 1 min***
   - Discard flow through
   - Place Column back in Tube

7. **Washing II**
   - Add **50 µL B5**
   - Centrifuge at ***11,000 x g for 2 min***
   - Discard flow through & tube

8. **Elution**
   - Column in NEW Eppendorf
   - Add **20 µL BE** on center of the silica
   - Centrifuge at ***11,000 x g for 1 min***

9. **Remove Residual ethanol**
   - Incubate elution with open lid for **8 min at 90°C**
   - Store flowthrough (DNA!) in -20 °C

7.11 Datasheet – DNA Extraction Optimization

In the Excel-file 'Datasheet – DNA Extraction Optimization' the full dataset of the DNA extraction optimization can be found. This file includes the data of each separate extraction, including the used protocol. Furthermore, a sheet with all the results collected together can be found. Important data include sample weight (mg), concentration (ng/µl), yield (µg), yield/weight (µg/mg), and the A260/A280- and A260/A230-ratios.

7.12 Graphs – DNA Extraction Optimization

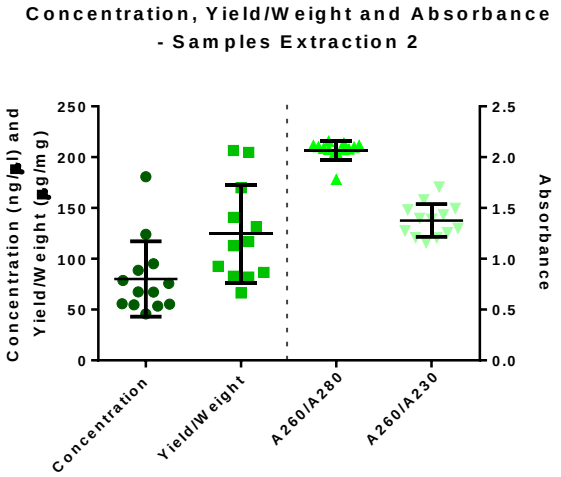

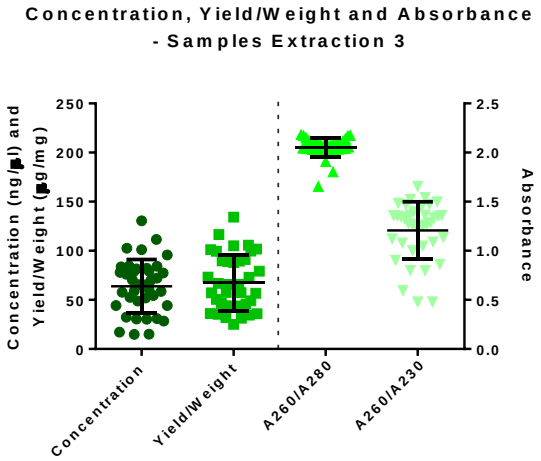

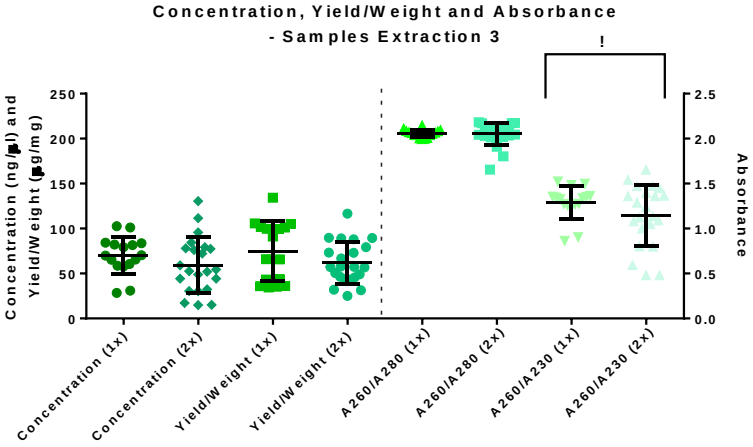

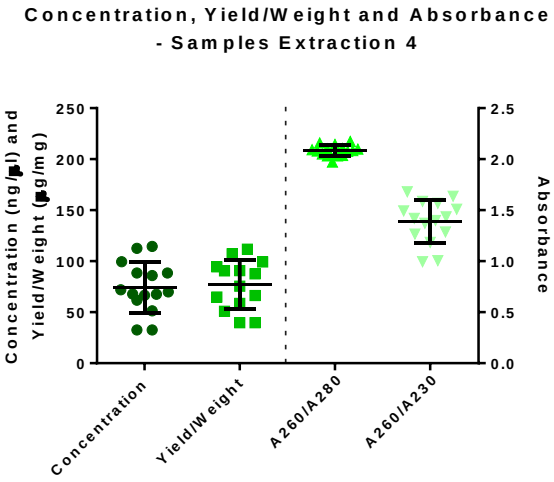

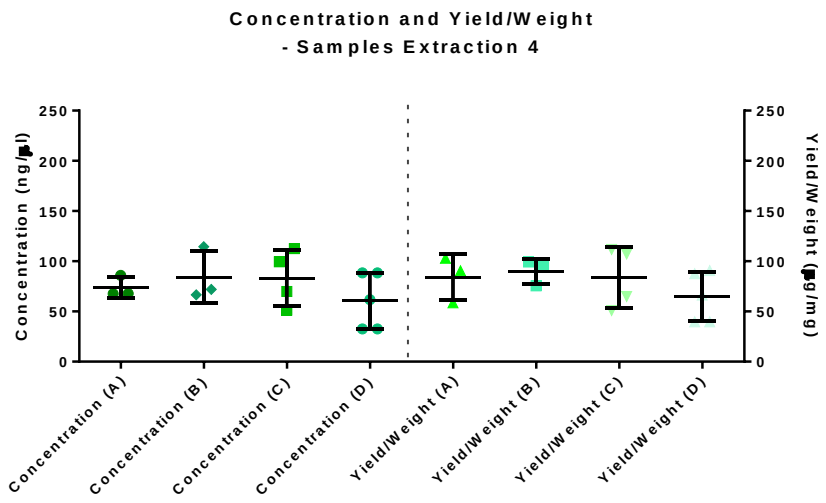
Concentration and Yield/Weight
- Samples Extraction 4
Concentration (ng/µl)
Yield/Weight (µg/mg)
250
200
150
100
50
0
Concentration (A)
Concentration (B)
Concentration (C)
Concentration (D)
Yield/Weight (A)
Yield/Weight (B)
Yield/Weight (C)
Yield/Weight (D)

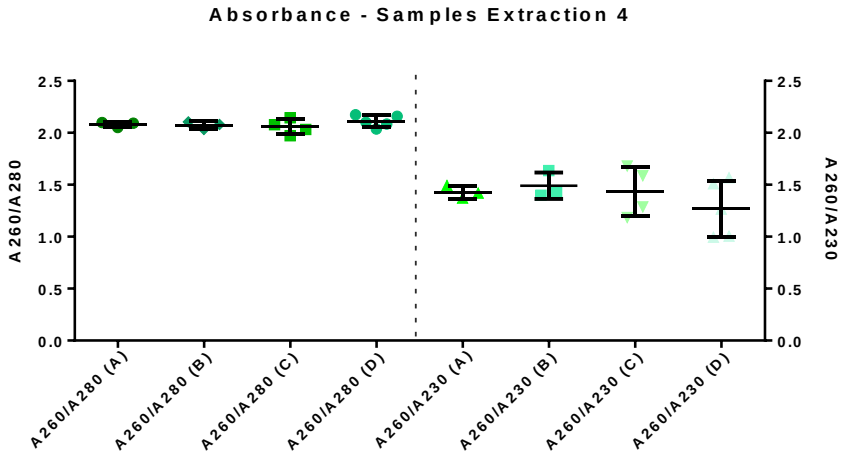
Absorbance - Samples Extraction 4
A260/A280
A260/A230
2.5
2.0
1.5
1.0
0.5
0.0
A260/A280 (A)
A260/A280 (B)
A260/A280 (C)
A260/A280 (D)
A260/A230 (A)
A260/A230 (B)
A260/A230 (C)
A260/A230 (D)

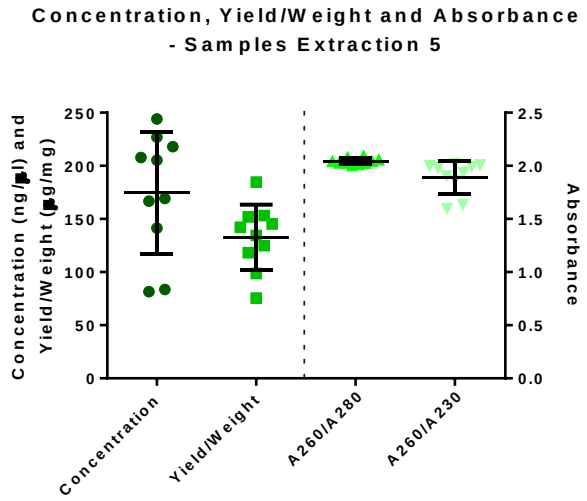
Concentration, Yield/Weight and Absorbance
- Samples Extraction 5
Concentration (ng/µl) and
Yield/Weight (µg/mg)
Absorbance
250
200
150
100
50
0
2.5
2.0
1.5
1.0
0.5
0.0
Concentration
Yield/Weight
A260/A280
A260/A230

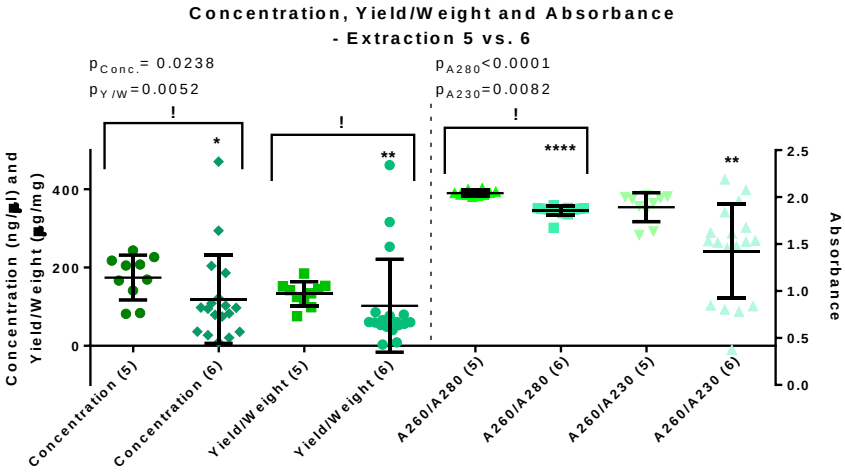

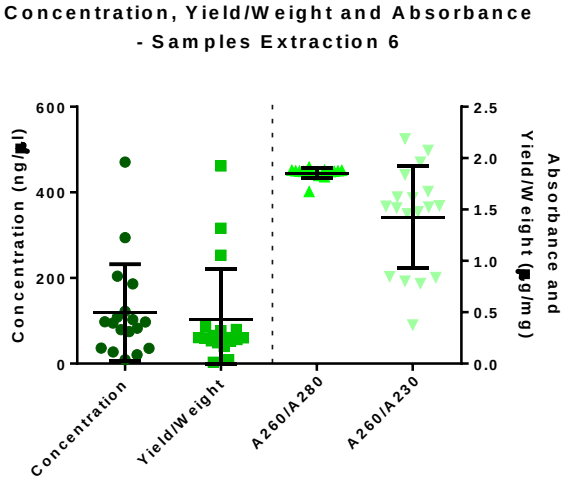

Only the first elutions are in the data

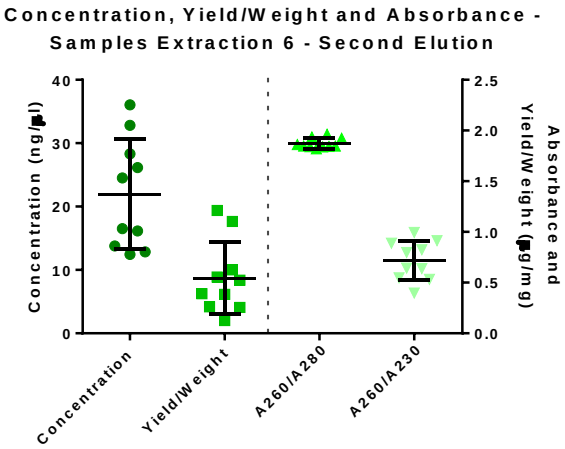

Only the second elutions are in this data

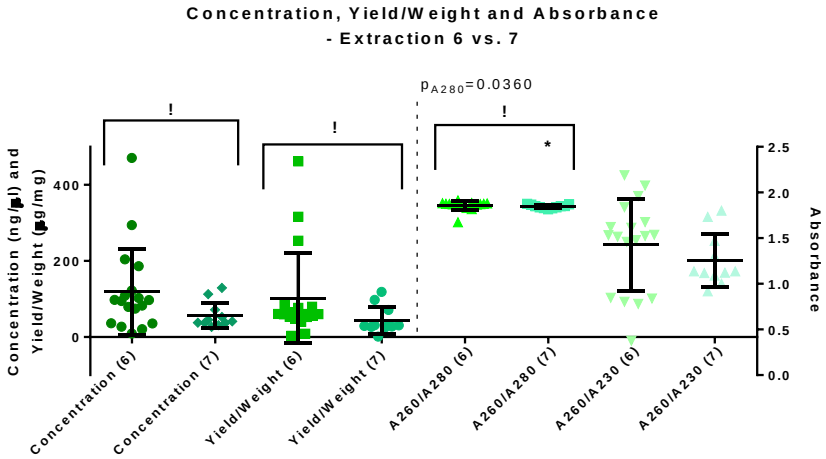

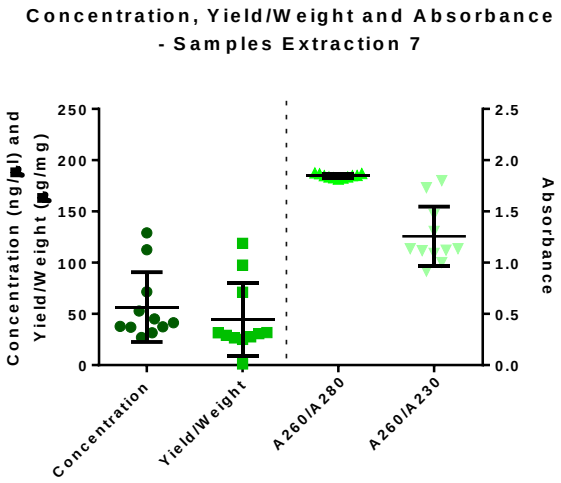

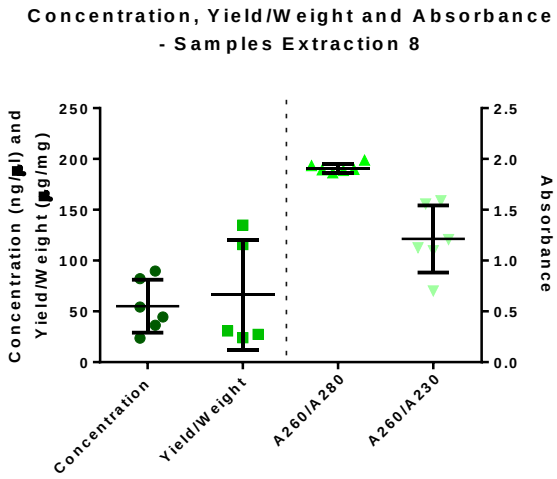

Only the first elutions are in this data

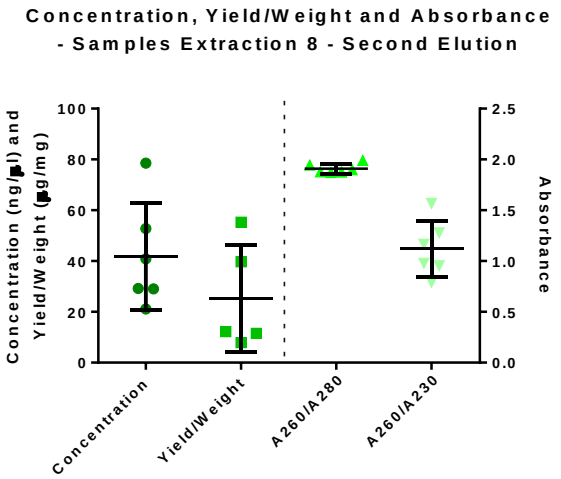

Only the second elutions are in this data

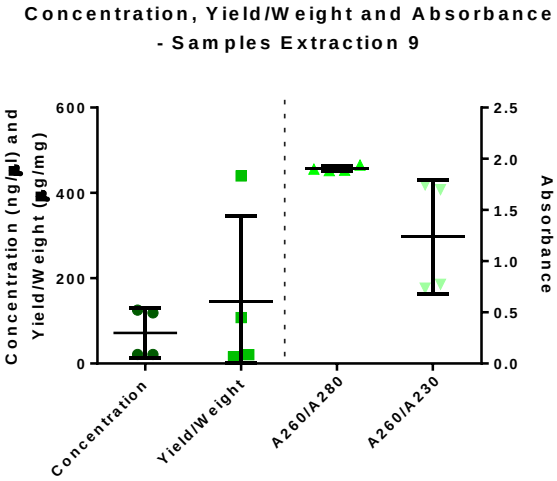

Only the first elutions are in the data

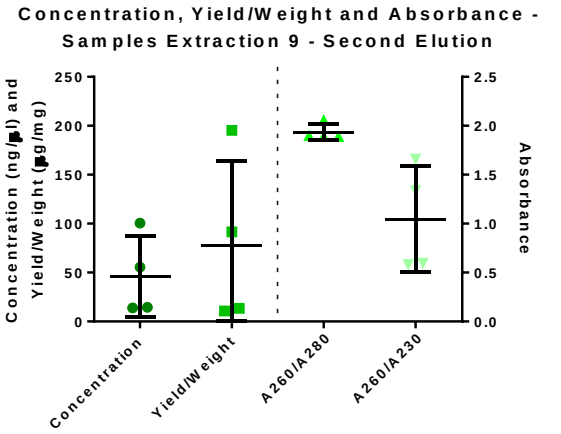

Only the second elutions are in this data

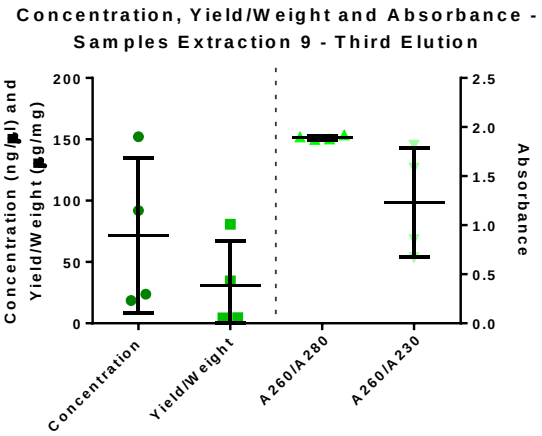

Only the third elutions are in this data

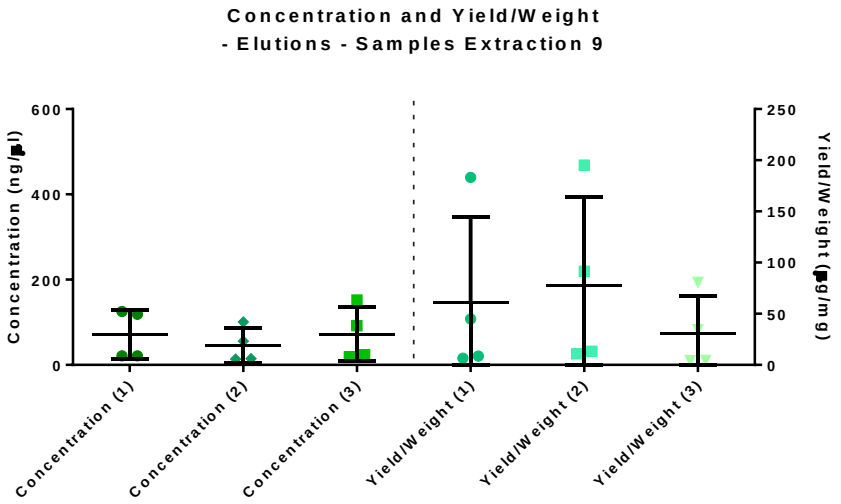

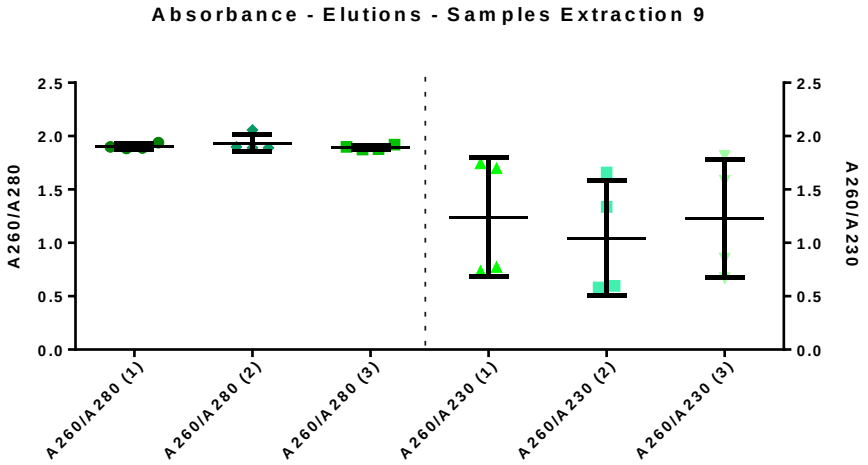

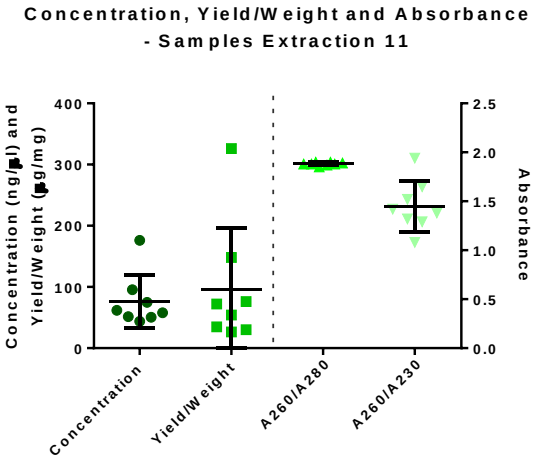

Only the first elutions are in this data

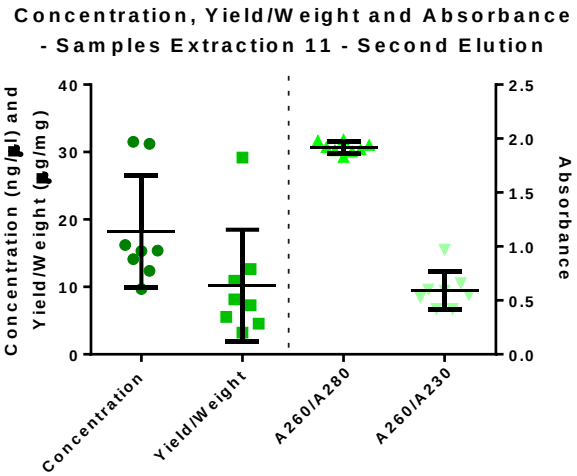

Only the second elutions are in this data

Concentration, Yield/Weight and Absorbance
- Samples Extraction 12

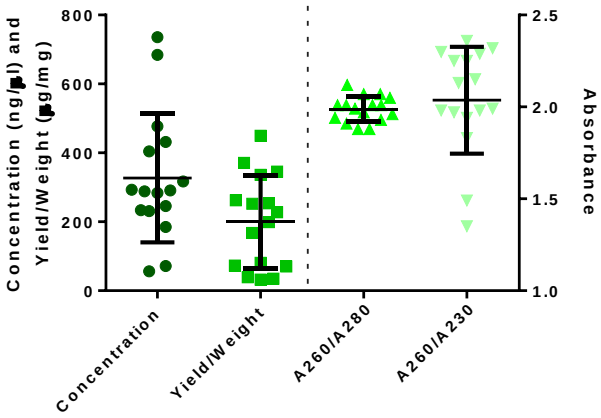

Concentration and Yield/Weight
- Groups Extraction 12

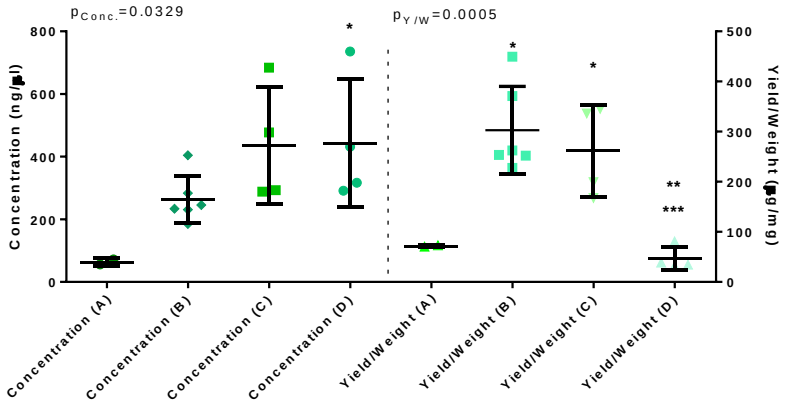

Absorbance
- Groups Extraction 12

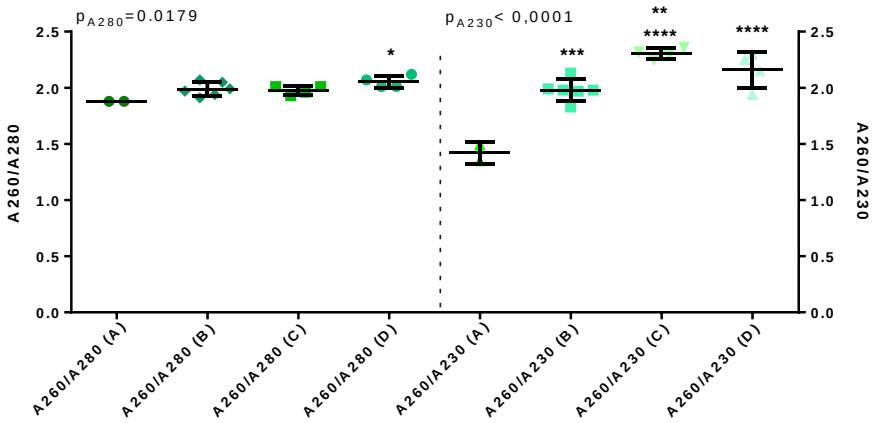

Concentration, Yield/Weight and Absorbance
- Samples Extraction 13

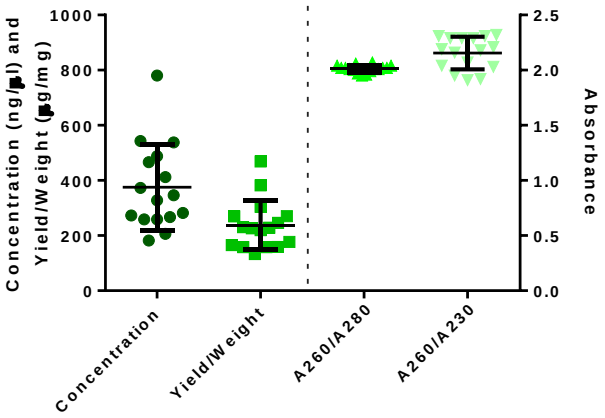

Concentration and Yield/Weight
- Groups Extraction 13

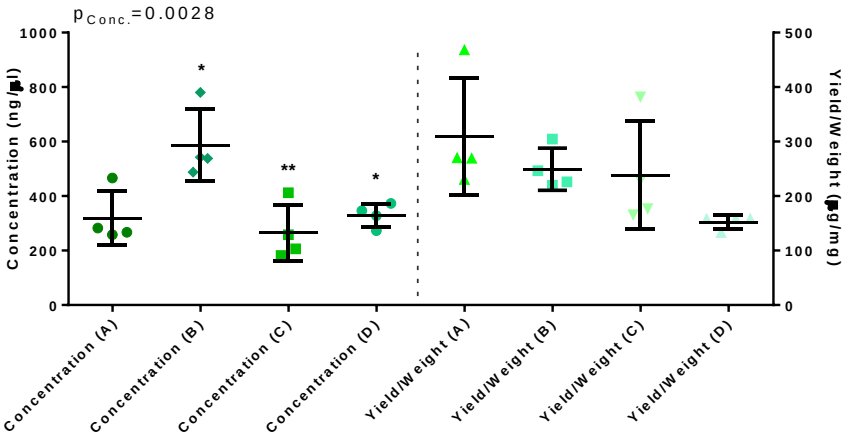

Absorbance
- Groups Extraction 13

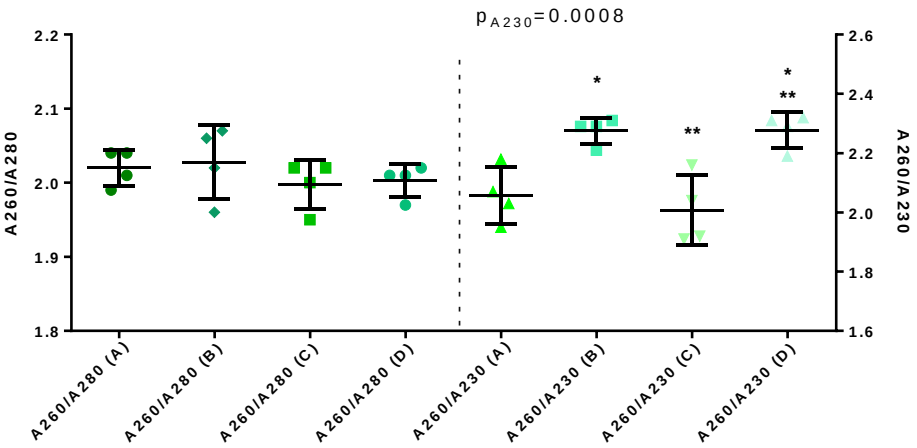

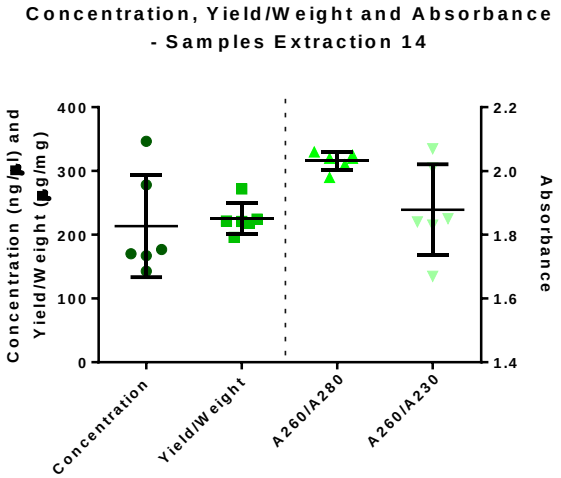
Concentration, Yield/Weight and Absorbance
- Samples Extraction 14
Concentration (ng/µl) and
Yield/Weight (µg/mg)
Absorbance
400
300
200
100
0
2.2
2.0
1.8
1.6
1.4
Concentration
Yield/Weight
A260/A280
A260/A230

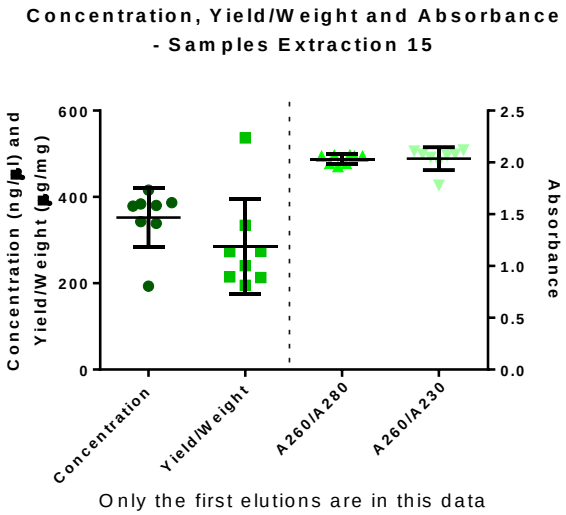
Concentration, Yield/Weight and Absorbance
- Samples Extraction 15
Concentration (ng/µl) and
Yield/Weight (µg/mg)
Absorbance
600
400
200
0
2.5
2.0
1.5
1.0
0.5
0.0
Concentration
Yield/Weight
A260/A280
A260/A230
Only the first elutions are in this data

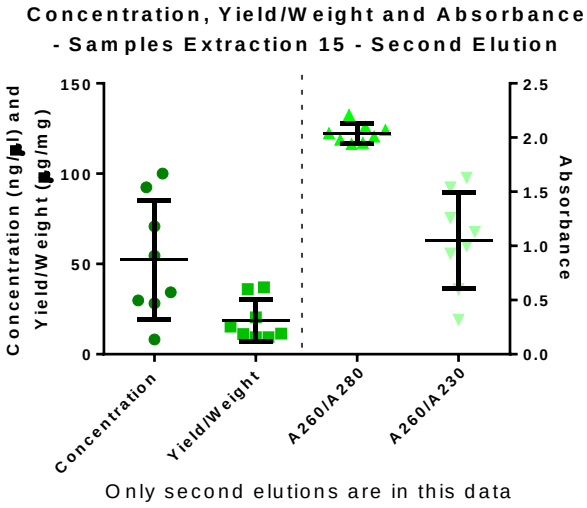
Concentration, Yield/Weight and Absorbance
- Samples Extraction 15 - Second Elution
Concentration (ng/µl) and
Yield/Weight (µg/mg)
Absorbance
150
100
50
0
2.5
2.0
1.5
1.0
0.5
0.0
Concentration
Yield/Weight
A260/A280
A260/A230
Only second elutions are in this data

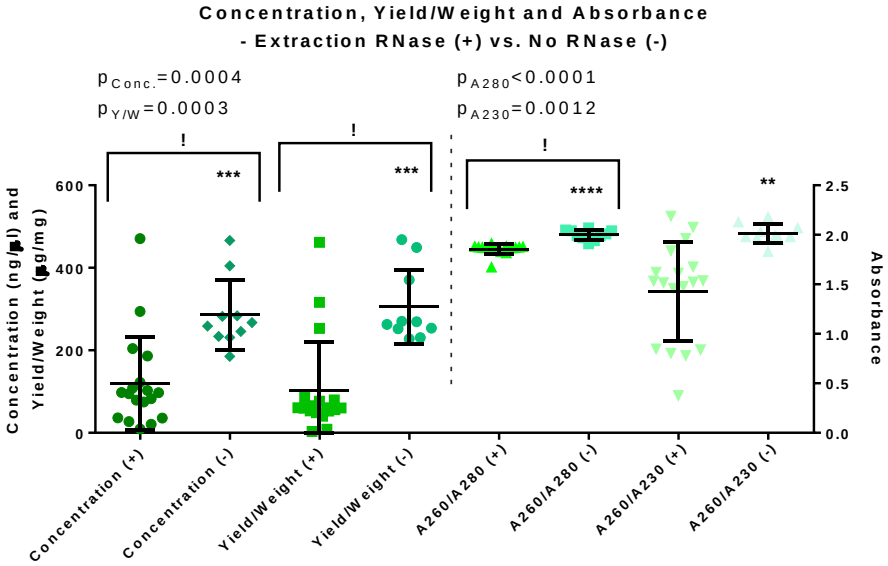
Concentration, Yield/Weight and Absorbance
- Extraction RNase (+) vs. No RNase (-)
pConc.=0.0004
pY/W=0.0003
pA280<0.0001
pA230=0.0012
!
***
!
***
!
****
**
Concentration (ng/µl) and
Yield/Weight (µg/mg)
Absorbance
600
400
200
0
2.5
2.0
1.5
1.0
0.5
0.0
Concentration (+)
Concentration (-)
Yield/Weight (+)
Yield/Weight (-)
A260/A280 (+)
A260/A280 (-)
A260/A230 (+)
A260/A230 (-)

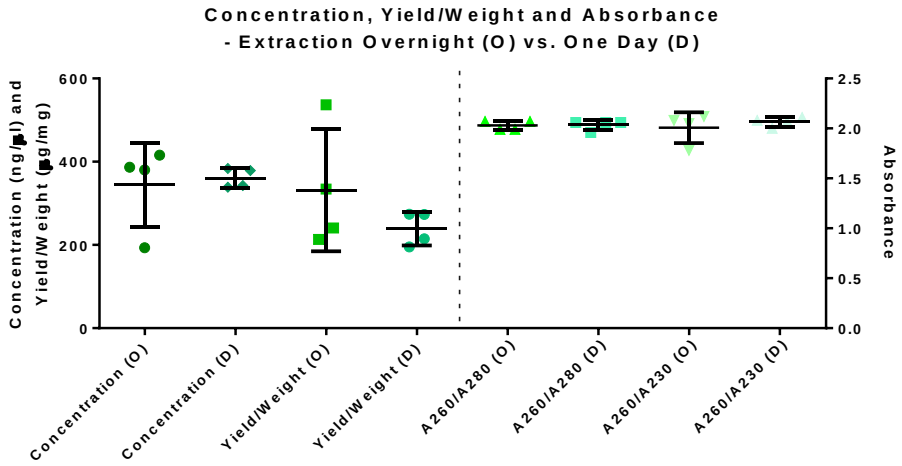
Concentration, Yield/Weight and Absorbance
- Extraction Overnight (O) vs. One Day (D)
Concentration (ng/µl) and Yield/Weight (µg/mg)
Absorbance
Concentration (O)
Concentration (D)
Yield/Weight (O)
Yield/Weight (D)
A260/A280 (O)
A260/A280 (D)
A260/A230 (O)
A260/A230 (D)

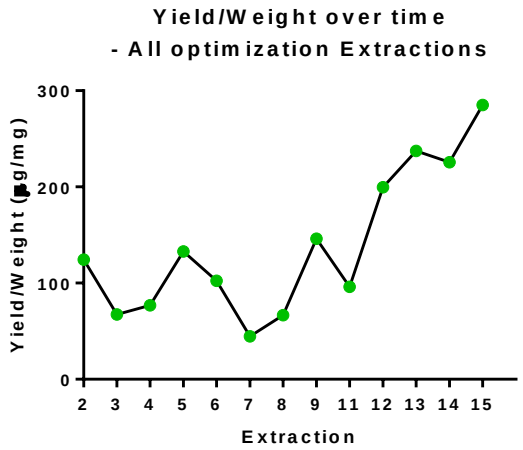
Yield/Weight over time
- All optimization Extractions
Yield/Weight (µg/mg)
Extraction

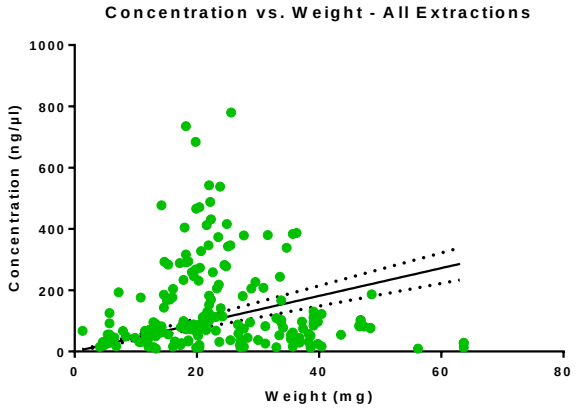
Concentration vs. Weight - All Extractions
Concentration (ng/µl)
Weight (mg)

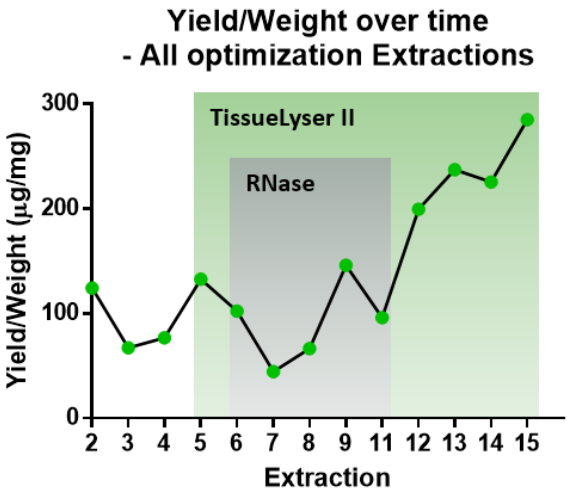
Yield/Weight over time
- All optimization Extractions
TissueLyser II
RNase
Yield/Weight (µg/mg)
Extraction

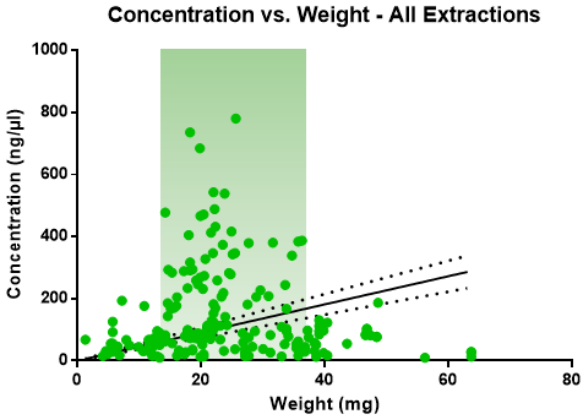
Concentration vs. Weight - All Extractions
Concentration (ng/µl)
Weight (mg)

7.13 DNA Extraction Gels

Extraction 5

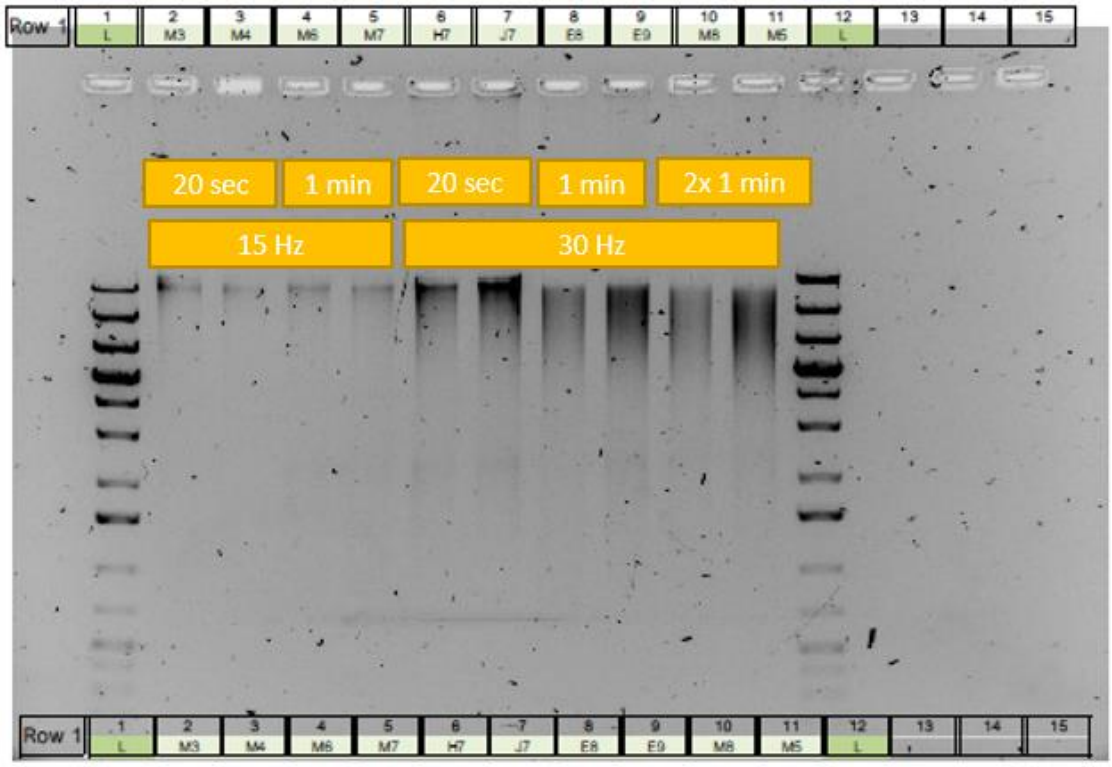

Extraction 7

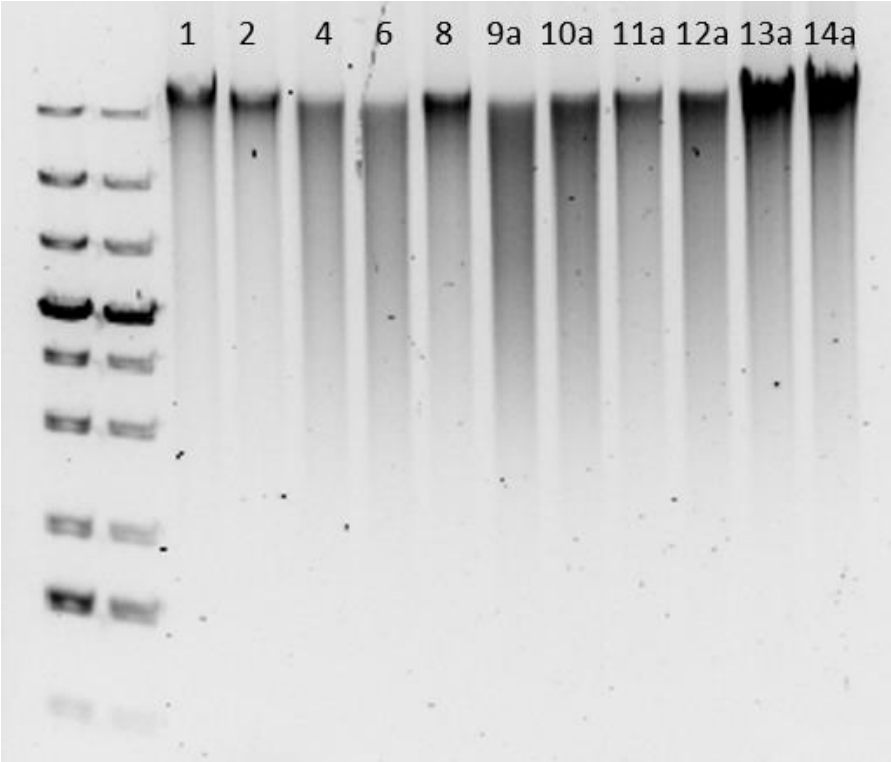

Extraction 8

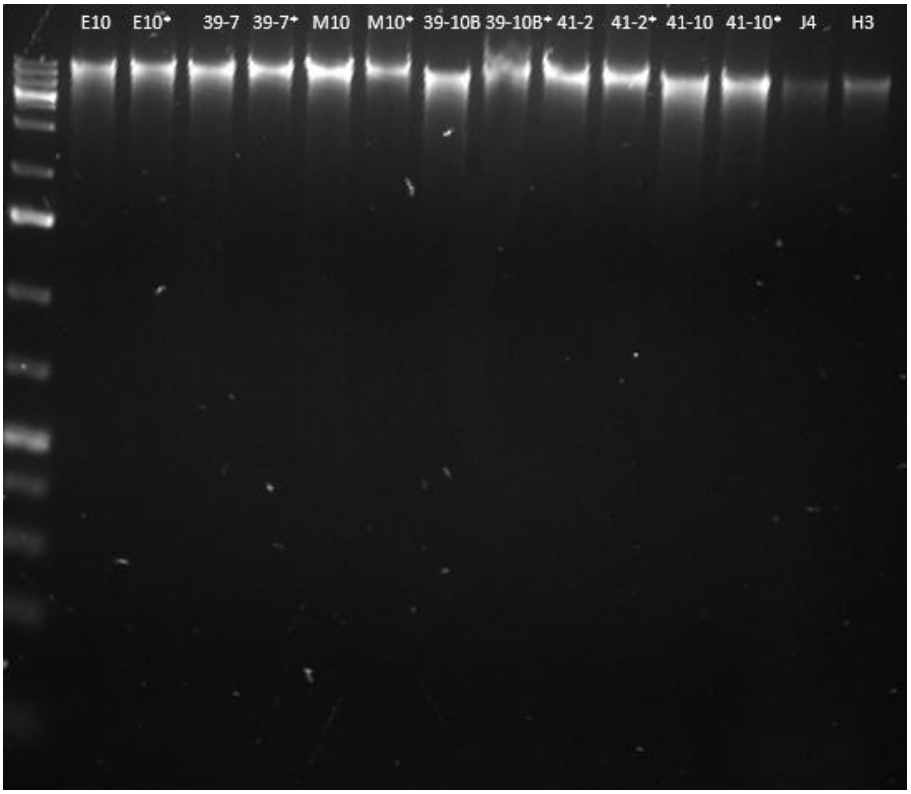

Samples from various extractions

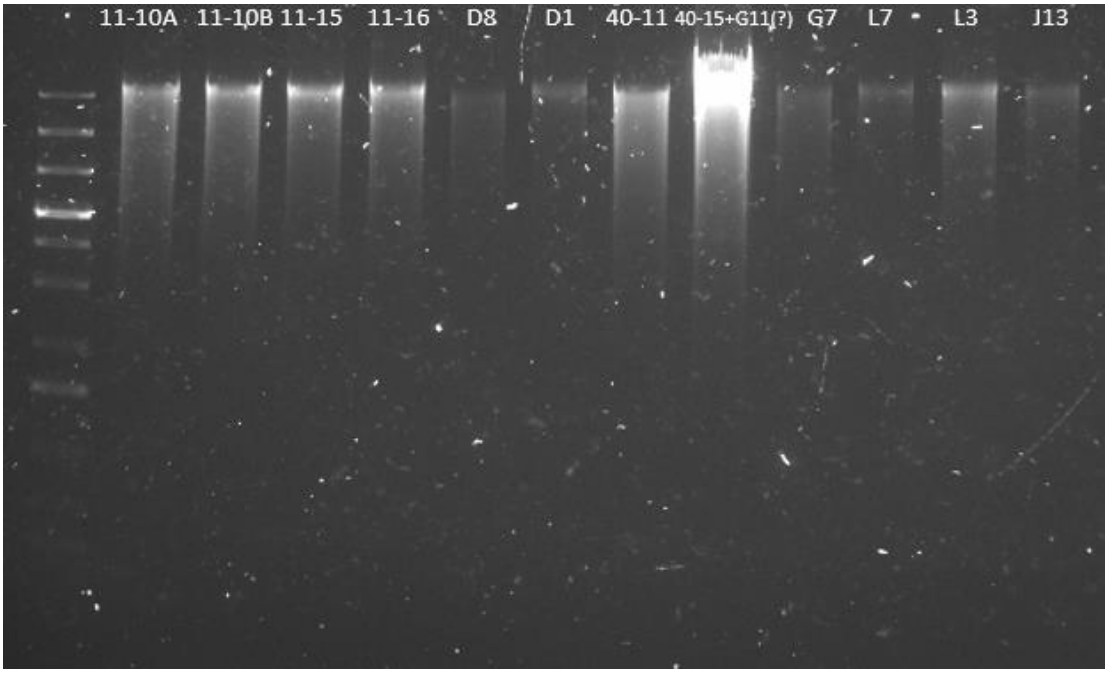

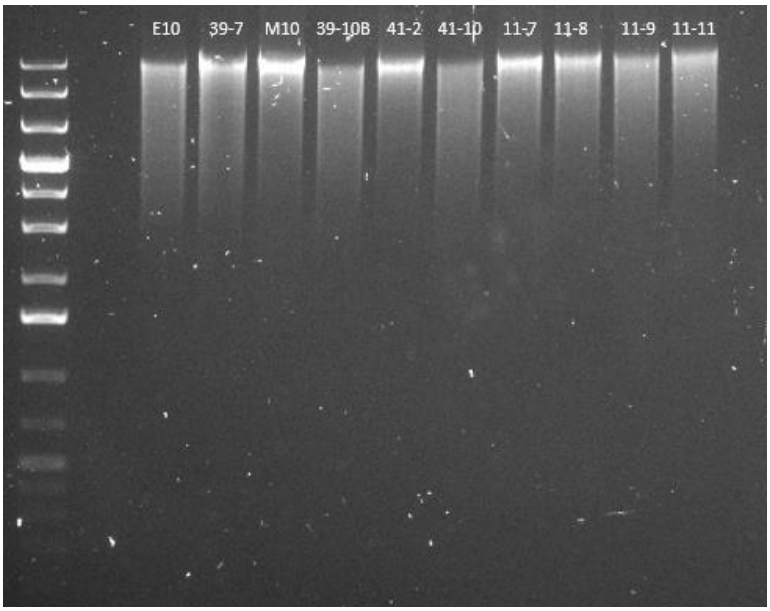

Extraction 12

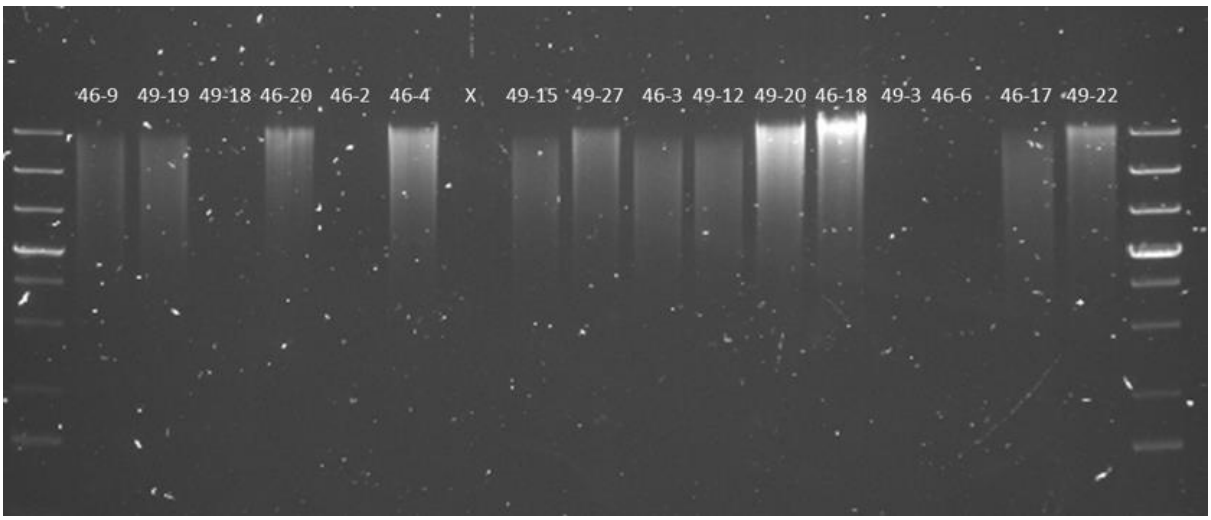

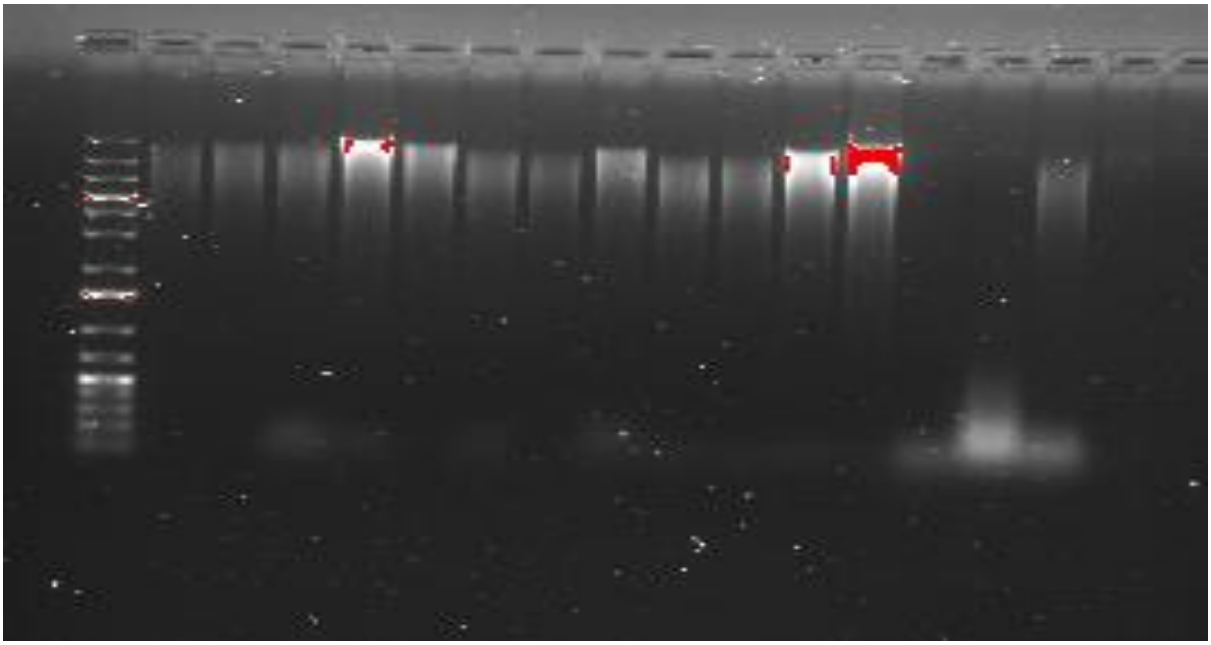

Extraction 13

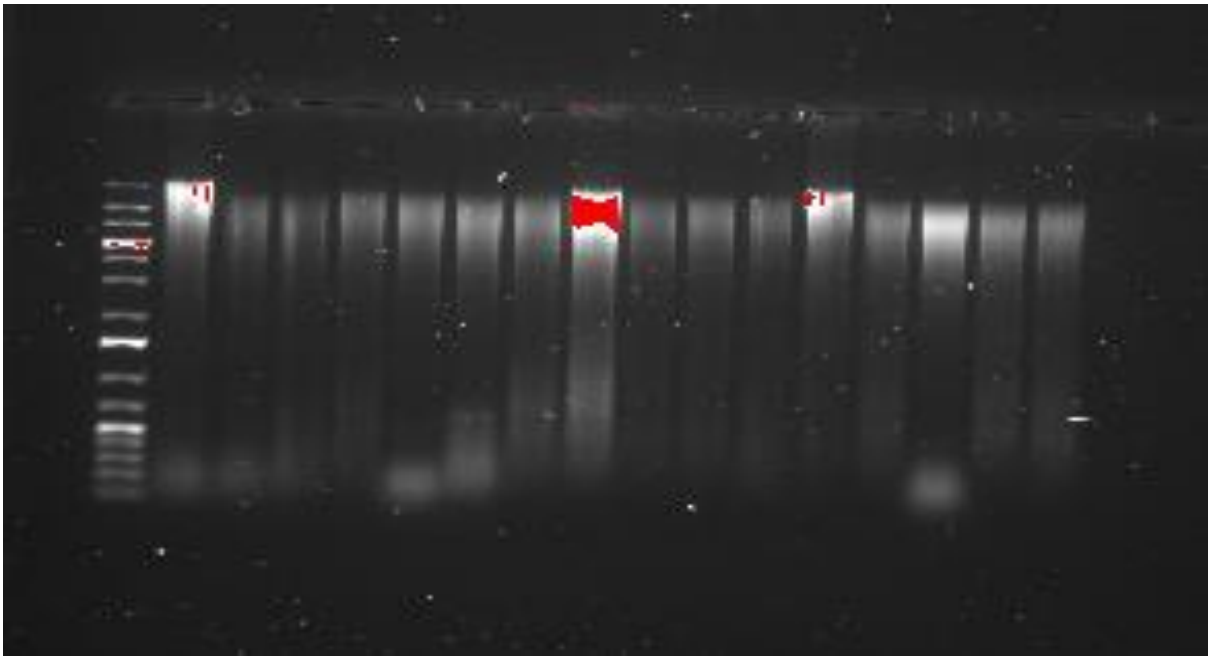

Contamination test

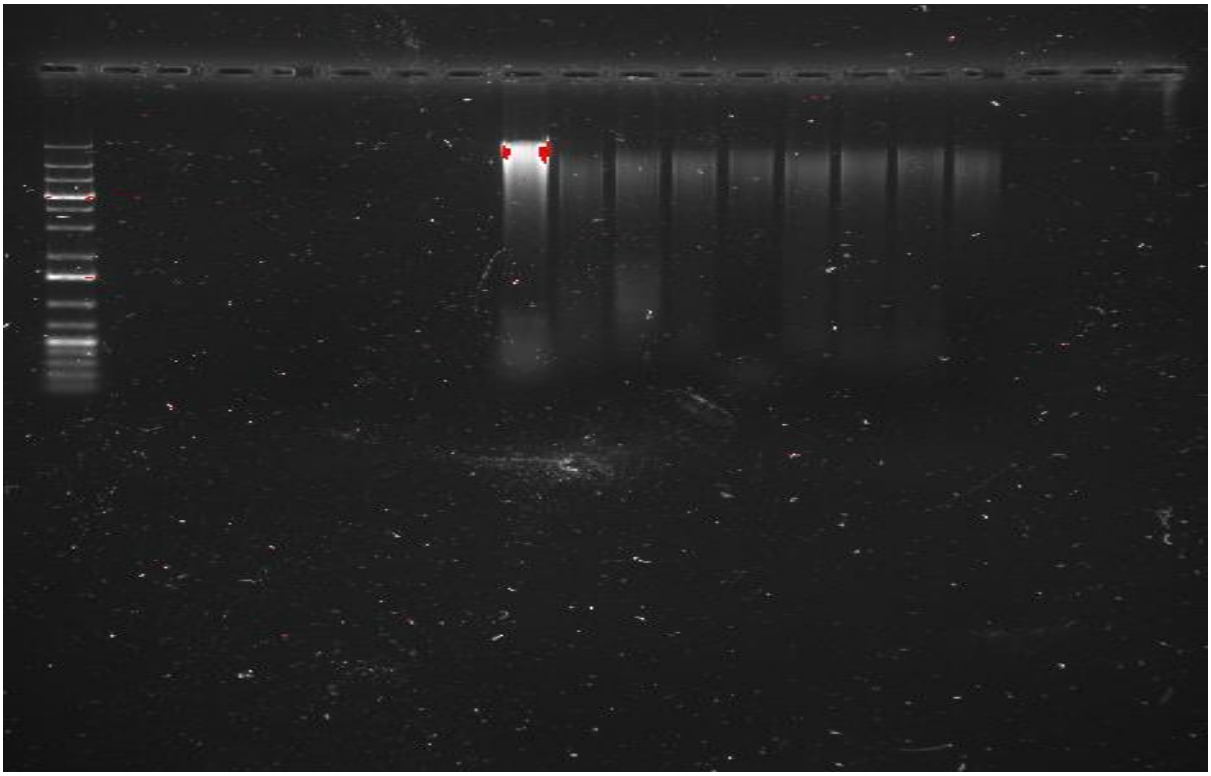

Extraction 14

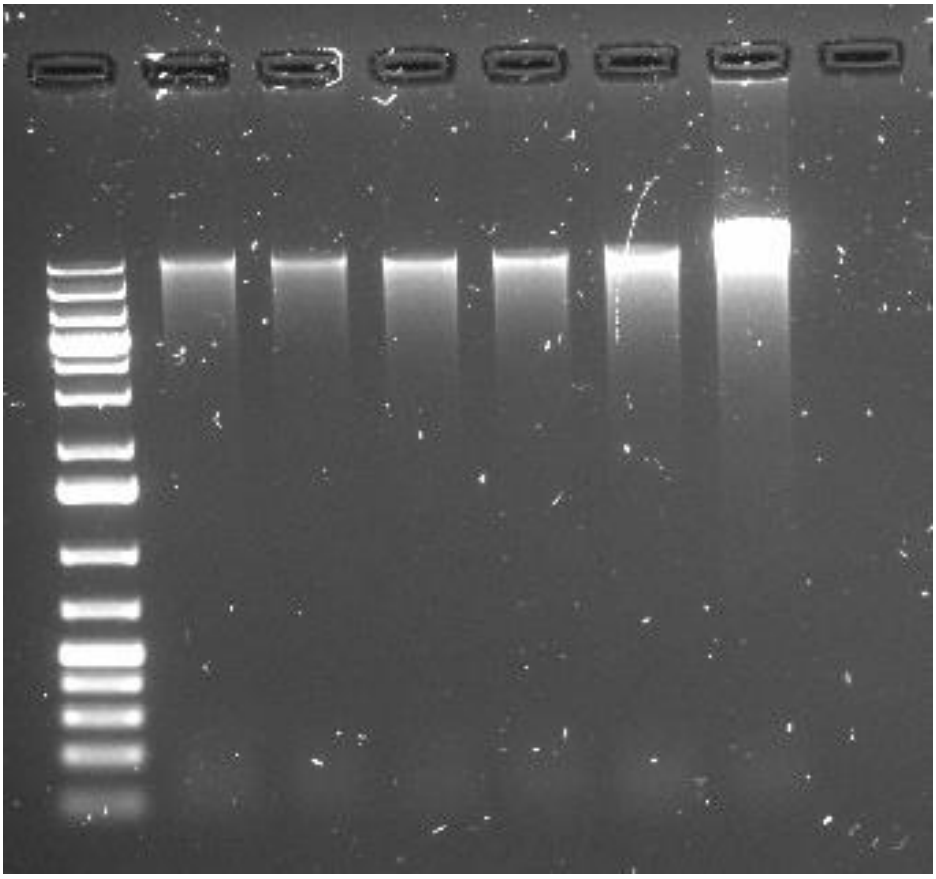

DNeasy contamination test

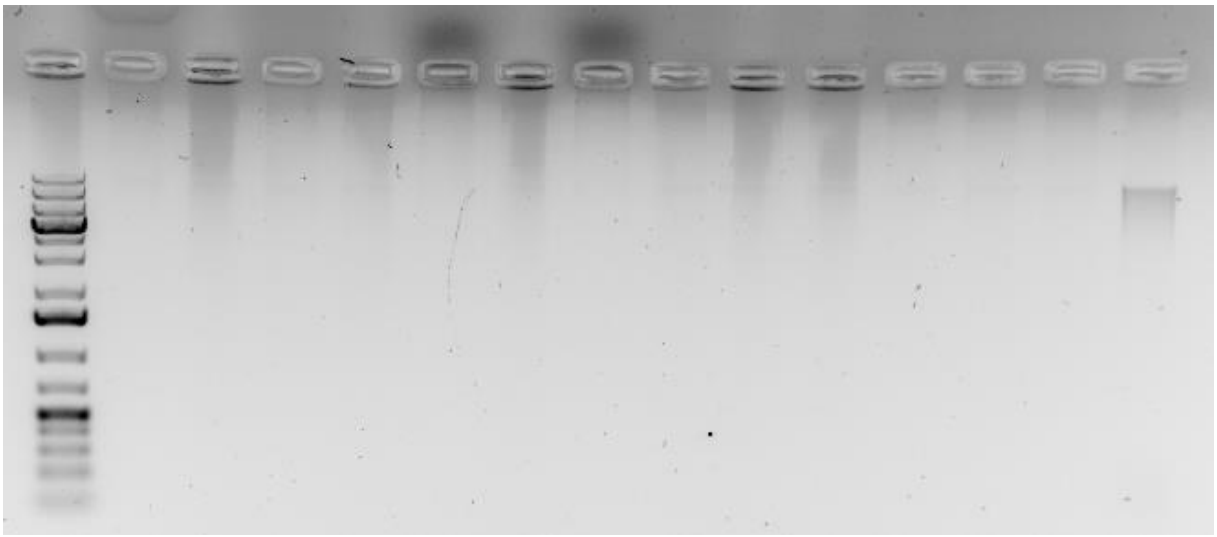

7.14 Datasheet – DNA Extraction Samples

In the Excel-file ‘Datasheet – DNA Extraction Samples’ the full dataset from the DNA extractions of our experimental samples can be found. Sheets are ordered for each organ, containing the data for each animal number separately. Important data include sample weight (mg), concentration (ng/µl), yield (µg), yield/weight (µg/mg), and the A260/A280- and A260/A230-ratios.

7.15 Graphs – DNA Extraction Samples

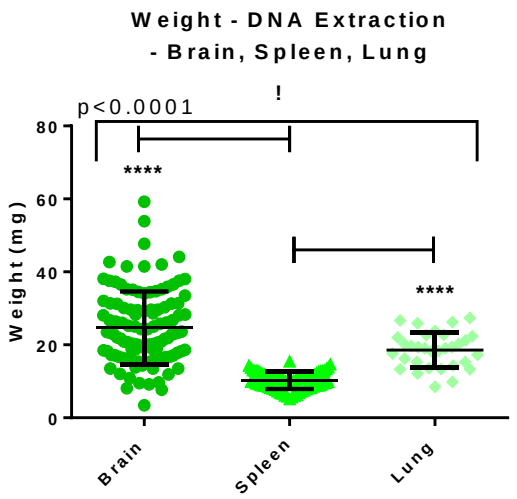

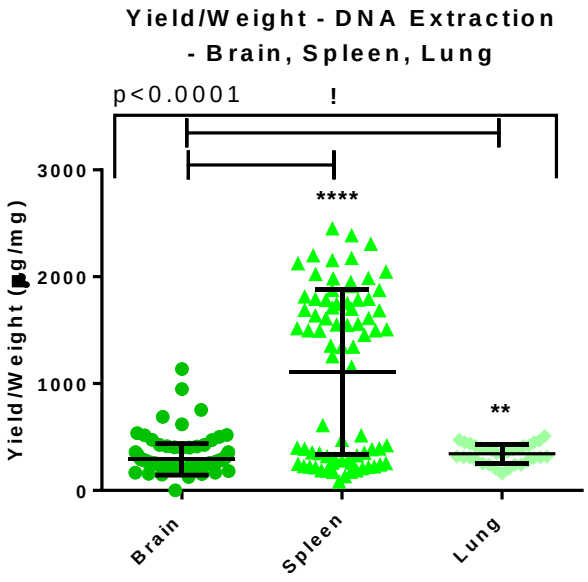

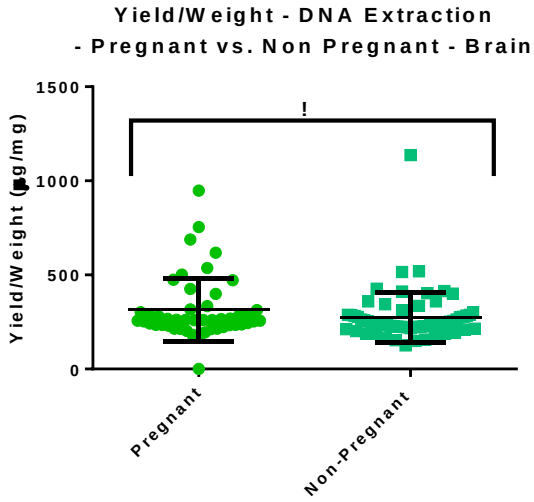

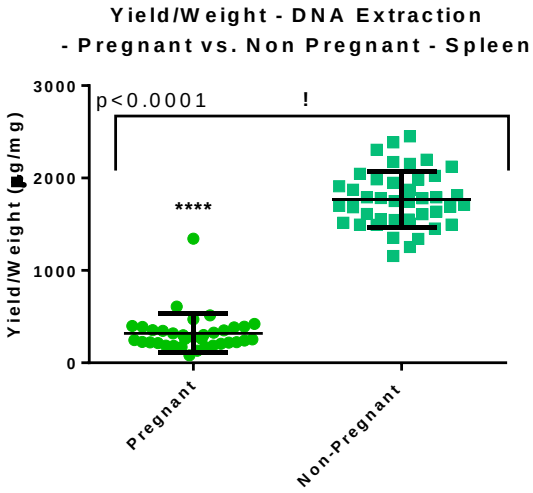

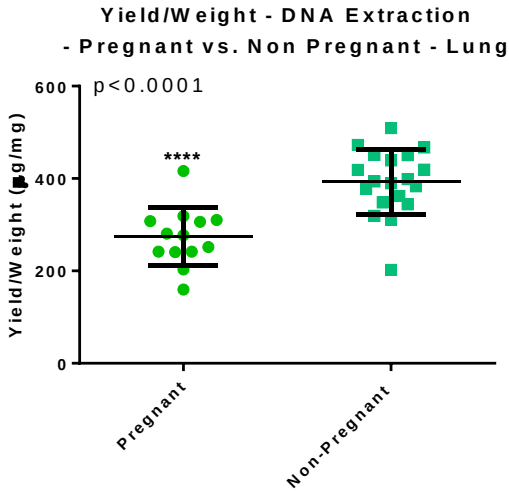

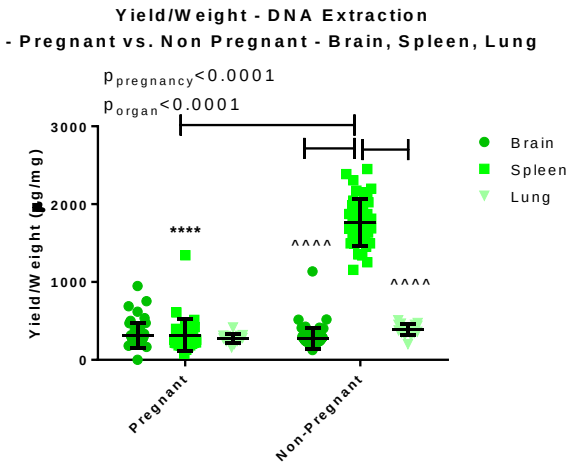

7.16 qPCR Plate Set-ups

Plate 1

	1	2	3	4	5	6	7	8	9	10	11	12
A	gB 6	B9-1	L9-5	B12-1	B13-1	L13-5	B14-1	B1-1	L1-5	B2-1	L2-4	B33-3
B	gB 7	B9-4	S9-2	B12-4	B13-4	S13-6	B14-3	B1-5	S1-1	B2-4	S2-1	L35-1
C	gB 8	B9-6	S9-7	B12-8	B13-6	S13-11	B14-6	B1-7	S1-4	B2-9	S2-4	S35-2
D	gB 9	B9-10	S9-9	B12-11	B13-8	S13-16	B14-9	B1-12	S1-7	B2-13	S2-7	
E	gB 10	B9-12	S9-12	B12-14	B13-9	S13-19	B14-11	B1-15	S1-9	B2-16	S2-11	
F	NTC	L9-2	M9-2	M12-2	L13-2	M13-3	M14-1	L1-1	M1-3	L2-1	M2-2	
G		L9-3	M9-3	M12-3	L13-3	M13-4	M14-2	L1-2	M1-6	L2-2	M2-3	
H		L9-4			L13-4			L1-3		L2-3		

Cq

	1		2		3		4		5		6		7		8		9		10		11		12	
	GFP	Apob	GFP	Apob	GFP	Apob	GFP	Apob	GFP	Apob	GFP	Apob	GFP	Apob	GFP	Apob	GFP	Apob	GFP	Apob	GFP	Apob	GFP	Apob
A	16,808	18,643	11,022	20,108	3,365	18,988	3,627	20,243	25,465	19,535	23,040	18,910	2,817	19,493	5,939	19,341	24,455	19,306	14,503	19,221	3,830	19,173	18,153	19,994
B	23,305	24,749	-0,286	19,646	3,282	19,618	1,839	20,713	26,765	20,277	25,350	19,042	22,396	20,493	1,908	20,224	25,436	19,121	23,758	20,252	18,968	19,105	19,921	19,262
C	26,216	27,431	2,655	20,580	25,896	18,979	21,610	20,450	25,337	20,281	25,429	19,137	18,639	20,488	25,277	20,310	15,466	19,329	21,223	20,123	23,260	19,031	19,909	18,735
D	-1,000	31,357	25,804	19,994	21,215	19,121	23,014	20,436	31,456	19,303	25,752	19,195	24,843	20,442	25,761	20,301	25,204	19,334	20,889	20,528	2,444	19,030		
E	3,801	33,090	6,750	18,370	29,363	24,745	25,207	19,372	25,918	19,619	27,366	20,941	25,506	19,098	23,743	19,407	26,976	18,545	25,583	19,629	5,765	21,585		
F	3,037	0,167	2,553	18,927	19,786	6,174	19,499	7,592	19,472	25,924	20,166	26,451	19,847	-2,693	19,004	-1,795	18,642	21,562	18,889	18,170	4,043	18,454		
G			4,197	19,144	4,816	19,451	3,577	19,520	24,458	19,046	24,492	20,221	-1,000	19,805	18,844	1,115	18,716	-4,660	19,306	4,395	18,195	6,156		
H			19,405	-2,544					-1,000	18,919					-0,148	19,129			4,382	18,848				

Individual Efficiency

	1		2		3		4		5		6		7		8		9		10		11		12	
	GFP	Apob	GFP	Apob	GFP	Apob	GFP	Apob	GFP	Apob	GFP	Apob	GFP	Apob	GFP	Apob	GFP	Apob	GFP	Apob	GFP	Apob	GFP	Apob
A	1,672	1,675	1,241	1,694	1,355	1,832	1,562	1,865	1,383	1,864	1,111	1,783	1,164	1,735	1,030	1,692	1,427	1,842	1,045	1,687	1,413	1,787	1,903	1,899
B	1,811	1,972	1,227	1,822	1,410	1,937	1,316	1,886	1,064	1,785	1,093	1,761	1,098	1,808	1,027	1,730	1,061	1,801	1,094	1,851	1,053	1,892	1,889	1,841
C	2,095	2,042	1,593	1,896	1,099	1,745	1,097	1,809	1,232	1,825	1,346	1,876	1,093	1,742	1,322	1,701	1,070	1,849	1,060	1,822	1,258	1,779	1,853	1,803
D	1,000	1,835	1,424	1,707	1,097	1,730	1,101	1,799	1,068	1,806	1,402	1,818	1,267	1,854	1,404	1,903	1,091	1,713	1,080	1,839	1,335	1,799		
E	1,252	1,741	1,052	1,832	1,496	1,772	1,086	1,808	1,323	1,797	1,387	1,742	1,336	1,599	1,274	1,788	1,094	1,758	1,410	1,848	1,252	1,557		
F	1,274	1,048	1,350	1,829	1,897	1,066	1,714	1,042	1,790	1,379	1,875	1,066	1,926	1,025	1,767	1,019	1,701	1,066	1,856	1,107	1,127	1,581		
G			1,323	1,553	1,422	1,911	1,383	1,785	1,250	1,823	1,267	1,771	1,000	1,692	1,751	1,374	1,819	1,046	1,804	1,542	1,713	1,262		
H			1,715	1,102					1,000	1,816					1,215	1,711			1,487	1,822				

Plate 2

	1	2	3	4	5	6	7	8	9	10	11	12
A	gB 6	B15-14	L15-5	B30-1	L30-5	B33-3						
B	gB 7	B15-10	S15-1	B30-4	S30-2	L35-1						
C	gB 8	B15-7	S15-4	B30-8	S30-4	S35-2						
D	gB 9	B15-4	S15-8	B30-12	S30-9	B9-2						
E	gB 10	B15-2	S15-11	B30-16	S30-11	B12-2						
F	NTC	L15-1	M15-1	L30-1	M30-1							
G		L15-2		L30-2	M30-2							
H		L15-4		L30-4								

Cq

	1		2		3		4		5		6		7		8		9		10		11		12	
	GFP	Apob	GFP	Apob	GFP	Apob	GFP	Apob	GFP	Apob	GFP	Apob	GFP	Apob	GFP	Apob	GFP	Apob	GFP	Apob	GFP	Apob	GFP	Apob
A	16,826	18,842	14,365	20,494	25,439	19,432	19,305	24,769	25,581	19,164	18,383	20,509												
B	20,527	22,283	6,005	20,599	29,300	19,233	20,163	30,666	18,613	30,501	19,686	19,613												
C	27,011	26,164	25,828	20,598	32,149	19,023	20,680	29,962	19,113	31,619	19,323	19,005												
D	28,391	29,460	7,874	21,135	22,215	19,109	32,539	19,822	30,797	18,689	37,120	20,584												
E	28,490	28,117	8,174	19,291	31,489	19,004	29,407	19,200	29,343	18,717	31,903	19,518												
F	32,103	31,077	18,280	19,136	19,039	28,940	19,177	6,104	18,807	30,411														
G			8,337	18,918			29,111	19,501	28,743	18,813														
H			19,145	25,257			26,3506	19,268																

Individual Efficiency

	1		2		3		4		5		6		7		8		9		10		11		12	
	GFP	Apob	GFP	Apob	GFP	Apob	GFP	Apob	GFP	Apob	GFP	Apob	GFP	Apob	GFP	Apob	GFP	Apob	GFP	Apob	GFP	Apob	GFP	Apob
A	1,614	1,689	1,137	1,767	1,347	1,846	1,857	1,379	1,357	1,848	1,949	1,950												
B	1,734	1,826	1,237	1,764	1,081	1,985	1,824	1,074	1,779	1,074	1,910	1,763												
C	1,896	2,100	1,362	1,683	1,056	1,715	1,917	1,082	1,860	1,070	1,847	1,815												
D	1,684	1,945	1,084	1,810	1,175	1,685	1,068	1,877	1,068	1,752	1,061	1,870												
E	1,602	1,887	1,088	1,807	1,062	1,737	1,078	1,876	1,079	1,787	1,069	1,880												
F	1,776	1,674	1,048	1,837	1,877	1,079	1,976	1,066	1,734	1,074														
G			1,170	1,649			1,081	1,739	1,085	1,800														
H			1,740	1,272			1,3147	1,832																

7.17 Datasheet – qPCR Results

In the Excel-file ‘qPCR – all results – LinReg’ the full dataset of the qPCR data generated from LinRegPCR can be found. This data includes both pilot plates. The data is ordered per plate (well and sample) and per organ. Important data include the Cq-values and Individual Efficiency (IE) calculated by LinRegPCR. Both parameters also have been visualized for each plate. In the Excel-file ‘qPCR – all results – StepOnePlus’ the full dataset from the StepOnePlus-software can be found. This data includes both pilot plates, as well as an earlier qPCR-pilot. The data is ordered per plate (well and sample) and per organ. Important data includes the quantity calculated based on the gBlock dilution series by the StepOnePlus. Furthermore, Ct-values calculated by the StepOnePlus itself can be found. Further calculations for frequency and scaled GFP quantities also can be found in the datasheets for each organ. The quantities of both Apob and GFP have been visualized in this file as well.

7.18 Graphs – qPCR Results

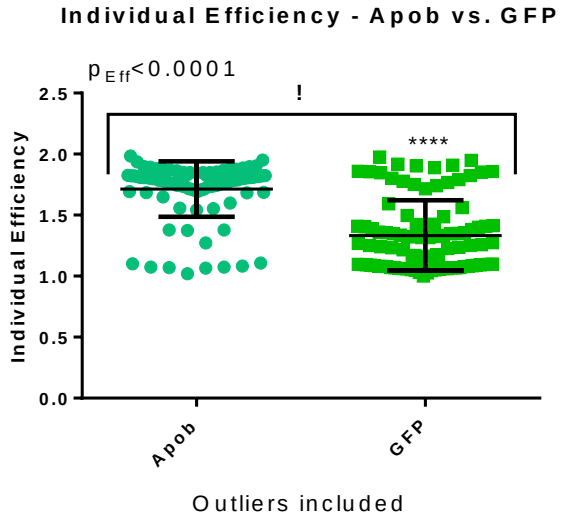

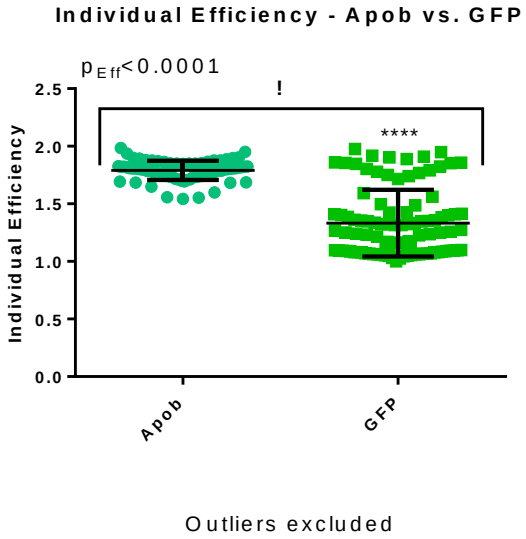

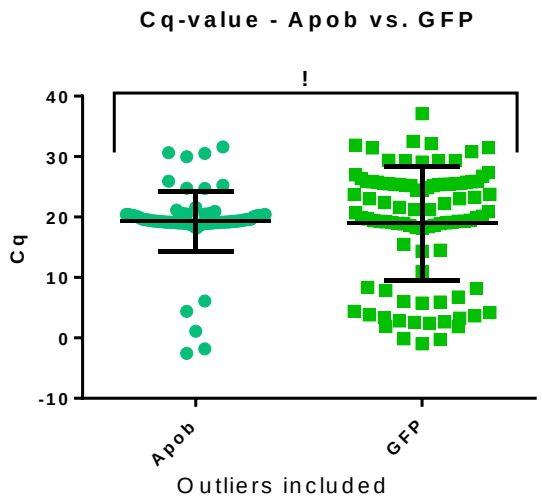

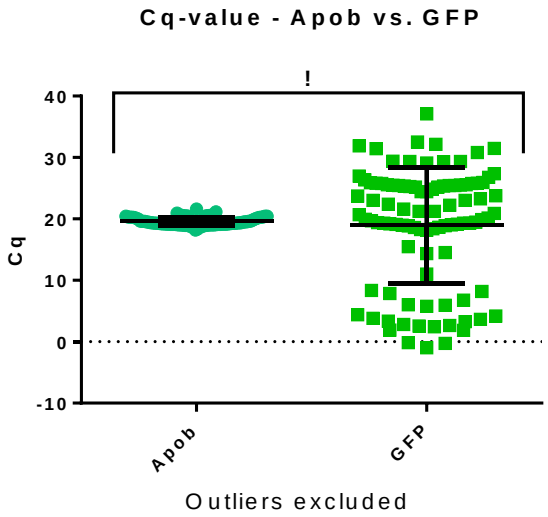

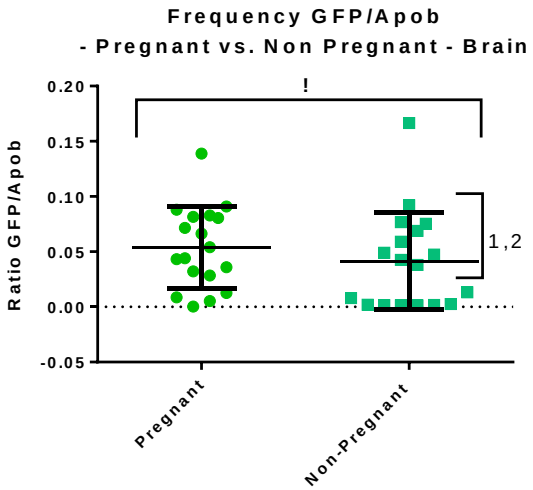

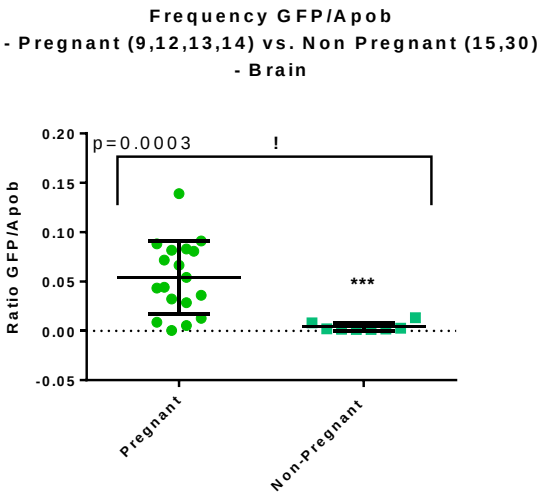

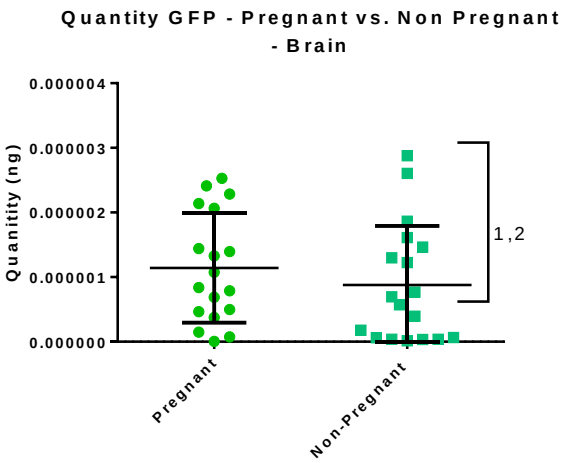
Quantity GFP - Pregnant vs. Non Pregnant
- Brain
Quanitity (ng)
0.000004
0.000003
0.000002
0.000001
0.000000
1,2
Pregnant
Non-Pregnant

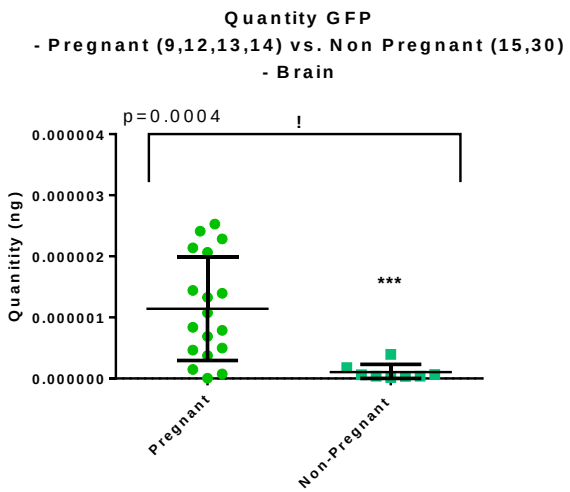
Quantity GFP
- Pregnant (9,12,13,14) vs. Non Pregnant (15,30)
- Brain
p=0.0004
!
***
Quanitity (ng)
0.000004
0.000003
0.000002
0.000001
0.000000
Pregnant
Non-Pregnant

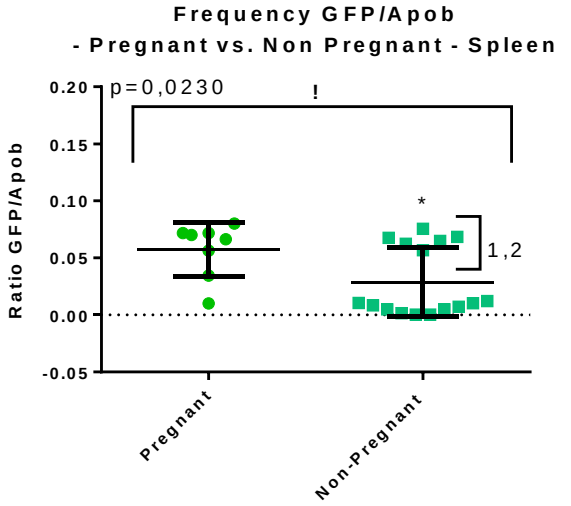
Frequency GFP/Apob
- Pregnant vs. Non Pregnant - Spleen
p=0,0230
!
*
1,2
Ratio GFP/Apob
0.20
0.15
0.10
0.05
0.00
-0.05
Pregnant
Non-Pregnant

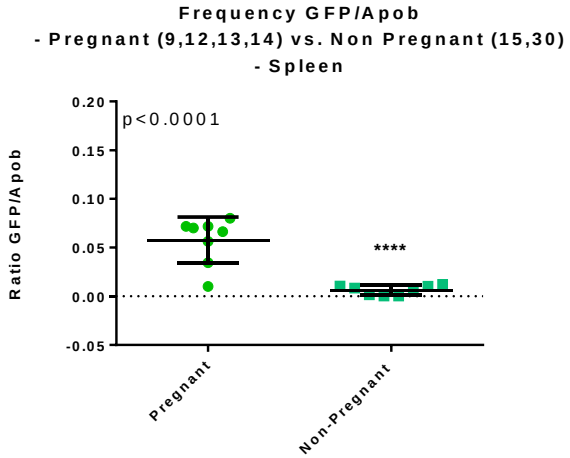
Frequency GFP/Apob
- Pregnant (9,12,13,14) vs. Non Pregnant (15,30)
- Spleen
p<0.0001
****
Ratio GFP/Apob
0.20
0.15
0.10
0.05
0.00
-0.05
Pregnant
Non-Pregnant

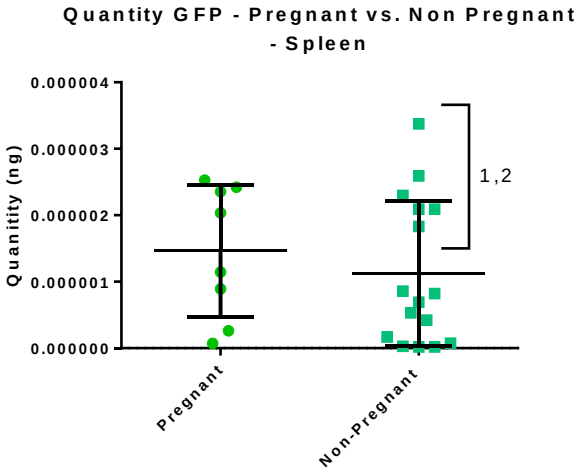
Quantity GFP - Pregnant vs. Non Pregnant
- Spleen
Quanitity (ng)
0.000004
0.000003
0.000002
0.000001
0.000000
1,2
Pregnant
Non-Pregnant

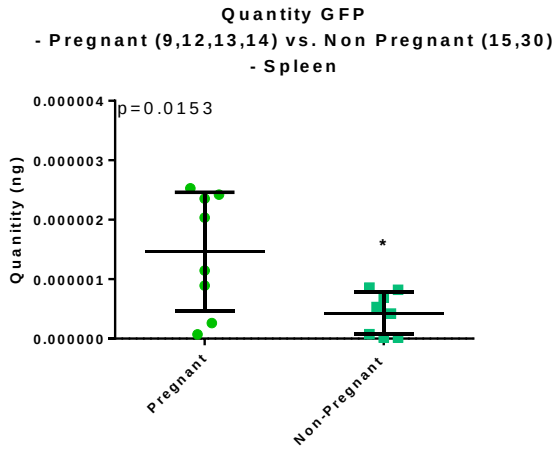
Quantity GFP
- Pregnant (9,12,13,14) vs. Non Pregnant (15,30)
- Spleen
p=0.0153
*
Quanitity (ng)
0.000004
0.000003
0.000002
0.000001
0.000000
Pregnant
Non-Pregnant

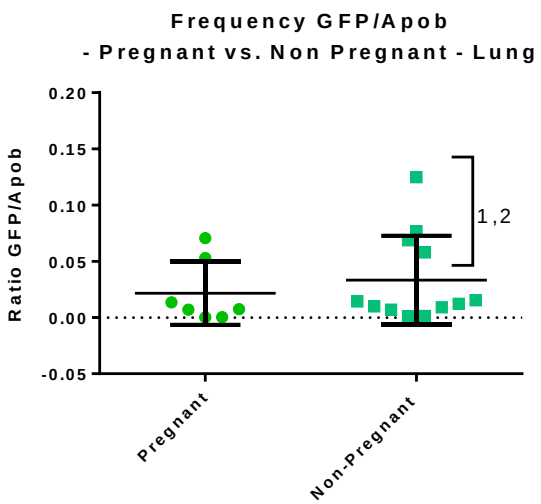
Frequency GFP/Apob
- Pregnant vs. Non Pregnant - Lung
Ratio GFP/Apob
0.20
0.15
0.10
0.05
0.00
-0.05
1,2
Pregnant
Non-Pregnant

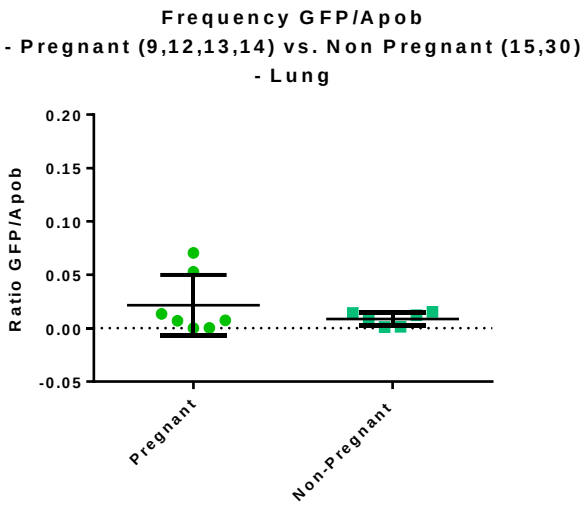
Frequency GFP/Apob
- Pregnant (9,12,13,14) vs. Non Pregnant (15,30)
- Lung
Ratio GFP/Apob
0.20
0.15
0.10
0.05
0.00
-0.05
Pregnant
Non-Pregnant

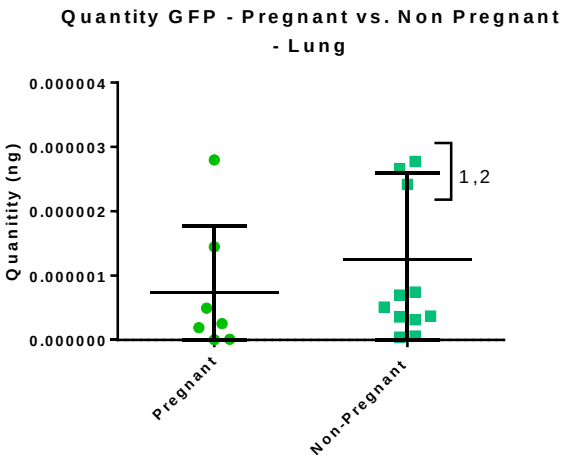
Quantity GFP - Pregnant vs. Non Pregnant
- Lung
Quanitity (ng)
0.000004
0.000003
0.000002
0.000001
0.000000
1,2
Pregnant
Non-Pregnant

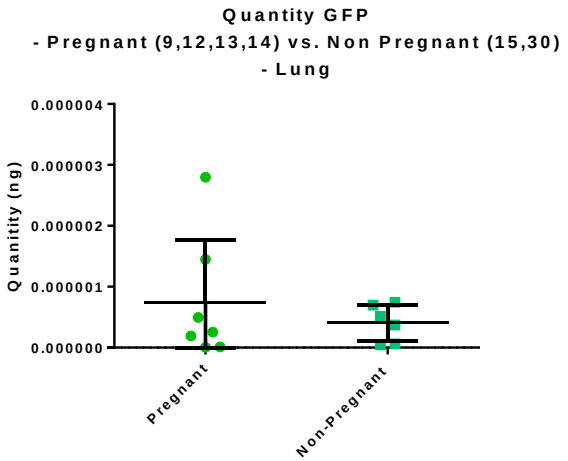
Quantity GFP
- Pregnant (9,12,13,14) vs. Non Pregnant (15,30)
- Lung
Quanitity (ng)
0.000004
0.000003
0.000002
0.000001
0.000000
Pregnant
Non-Pregnant

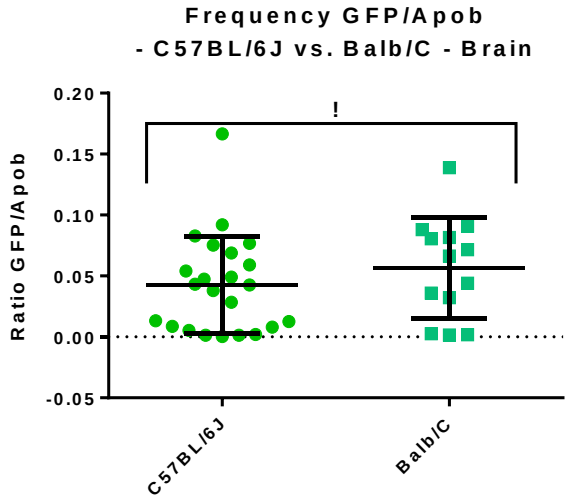
Frequency GFP/Apob
- C57BL/6J vs. Balb/C - Brain
Ratio GFP/Apob
0.20
0.15
0.10
0.05
0.00
-0.05
!
C57BL/6J
Balb/C

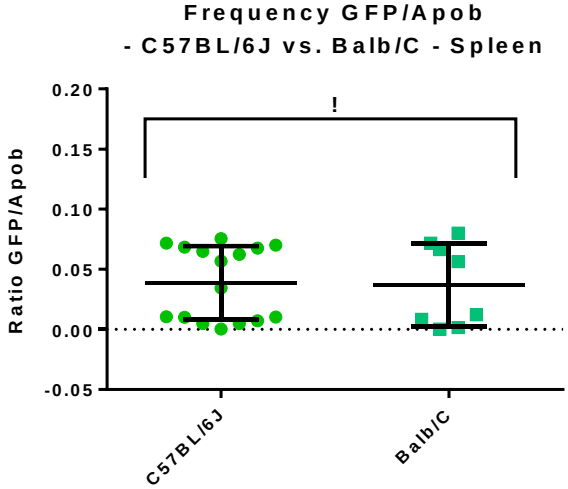
Frequency GFP/Apob
- C57BL/6J vs. Balb/C - Spleen
Ratio GFP/Apob
0.20
0.15
0.10
0.05
0.00
-0.05
!
C57BL/6J
Balb/C

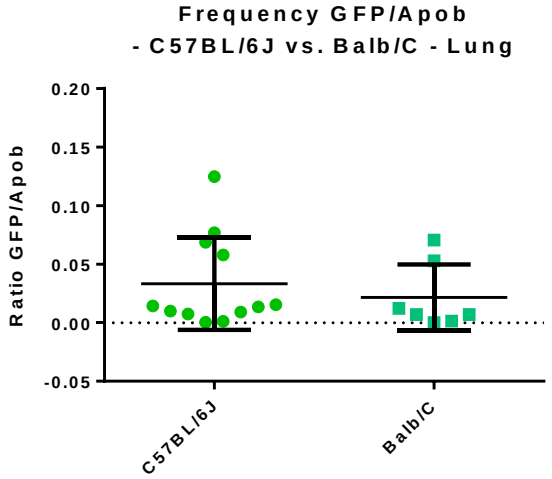
Frequency GFP/Apob
- C57BL/6J vs. Balb/C - Lung
Ratio GFP/Apob
0.20
0.15
0.10
0.05
0.00
-0.05
C57BL/6J
Balb/C

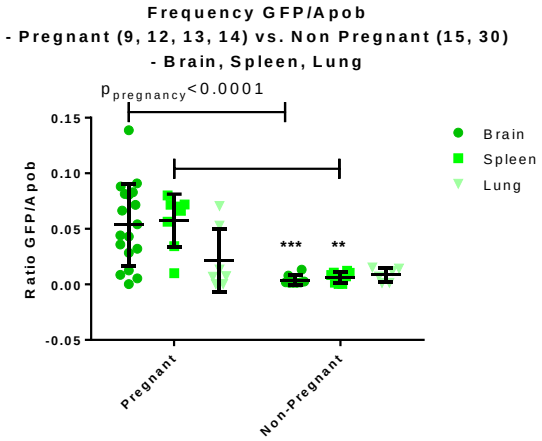
Frequency GFP/Apob
- Pregnant (9, 12, 13, 14) vs. Non Pregnant (15, 30)
- Brain, Spleen, Lung
p pregnancy<0.0001
Ratio GFP/Apob
0.15
0.10
0.05
0.00
-0.05
***
**
Brain
Spleen
Lung
Pregnant
Non-Pregnant

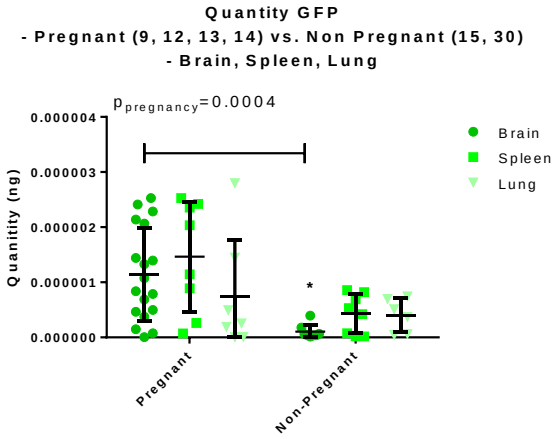
Quantity GFP
- Pregnant (9, 12, 13, 14) vs. Non Pregnant (15, 30)
- Brain, Spleen, Lung
p pregnancy=0.0004
Quanitity (ng)
0.000004
0.000003
0.000002
0.000001
0.000000
*
Brain
Spleen
Lung
Pregnant
Non-Pregnant

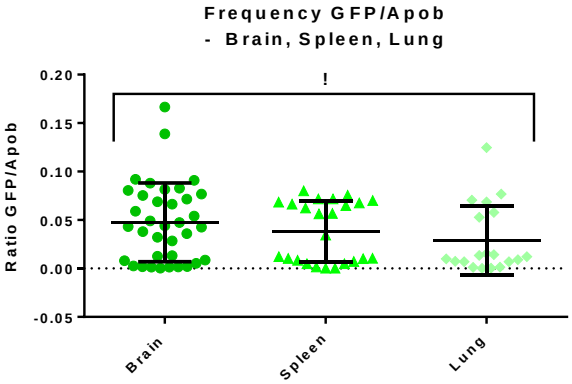
Frequency GFP/Apob
- Brain, Spleen, Lung
!
Ratio GFP/Apob
0.20
0.15
0.10
0.05
0.00
-0.05
Brain
Spleen
Lung

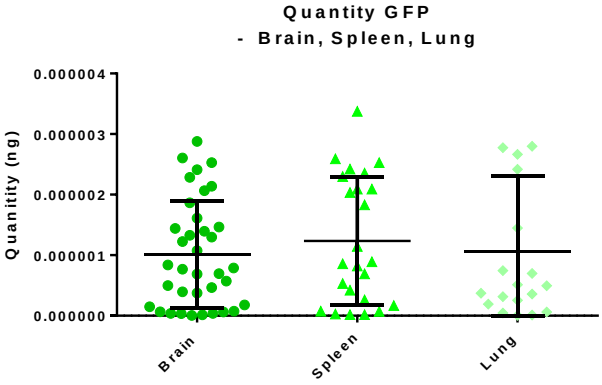
Quantity GFP
- Brain, Spleen, Lung
Quanitity (ng)
0.000004
0.000003
0.000002
0.000001
0.000000
Brain
Spleen
Lung

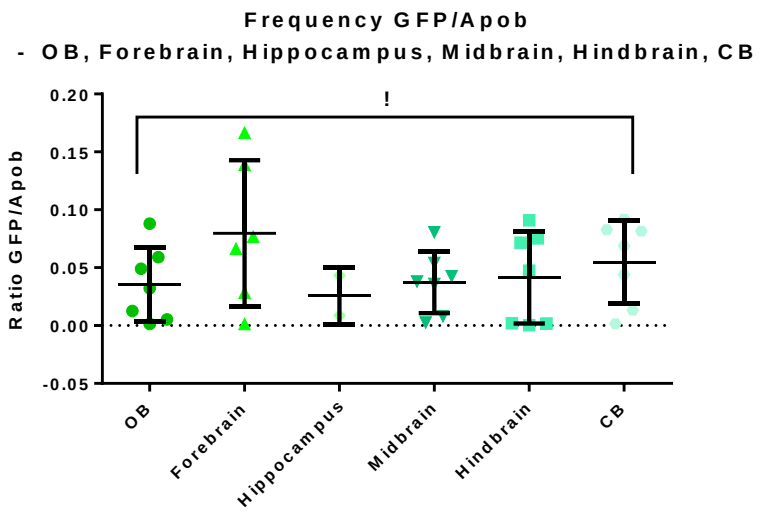
Frequency GFP/Apob
- OB, Forebrain, Hippocampus, Midbrain, Hindbrain, CB
!
Ratio GFP/Apob
0.20
0.15
0.10
0.05
0.00
-0.05
OB
Forebrain
Hippocampus
Midbrain
Hindbrain
CB

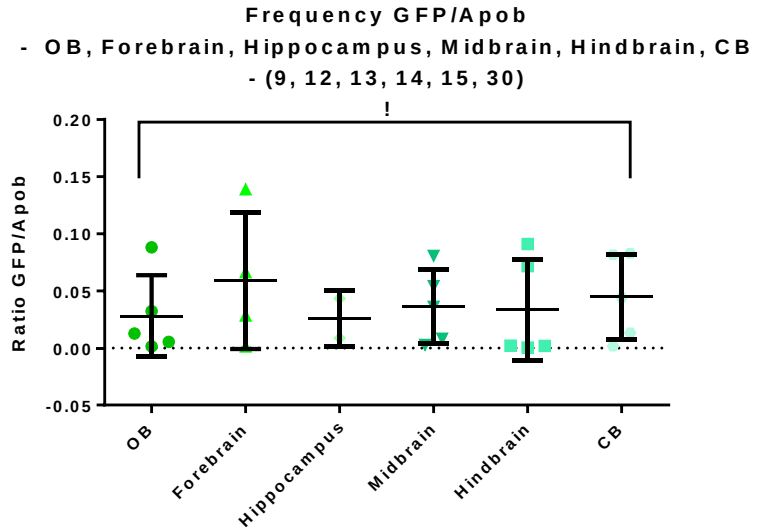
Frequency GFP/Apob
- OB, Forebrain, Hippocampus, Midbrain, Hindbrain, CB
- (9, 12, 13, 14, 15, 30)
!
Ratio GFP/Apob
0.20
0.15
0.10
0.05
0.00
-0.05
OB
Forebrain
Hippocampus
Midbrain
Hindbrain
CB

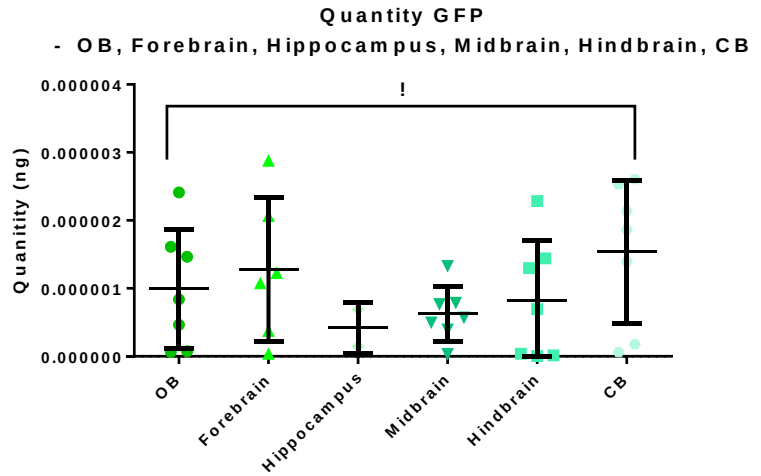
Quantity GFP
- OB, Forebrain, Hippocampus, Midbrain, Hindbrain, CB
!
Quanitity (ng)
0.000004
0.000003
0.000002
0.000001
0.000000
OB
Forebrain
Hippocampus
Midbrain
Hindbrain
CB

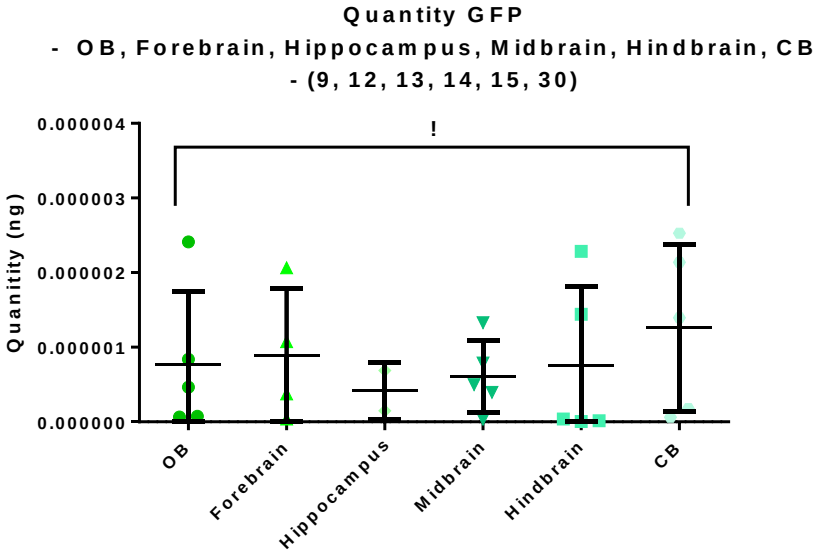
Quantity GFP
- OB, Forebrain, Hippocampus, Midbrain, Hindbrain, CB
- (9, 12, 13, 14, 15, 30)
Quanitity (ng)
0.000004
0.000003
0.000002
0.000001
0.000000
!
OB
Forebrain
Hippocampus
Midbrain
Hindbrain
CB

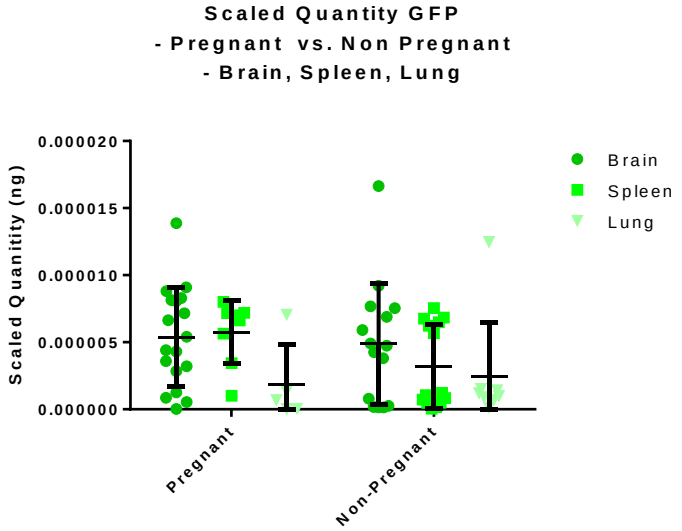
Scaled Quantity GFP
- Pregnant vs. Non Pregnant
- Brain, Spleen, Lung
Scaled Quanitity (ng)
0.000020
0.000015
0.000010
0.000005
0.000000
Pregnant
Non-Pregnant
Brain
Spleen
Lung

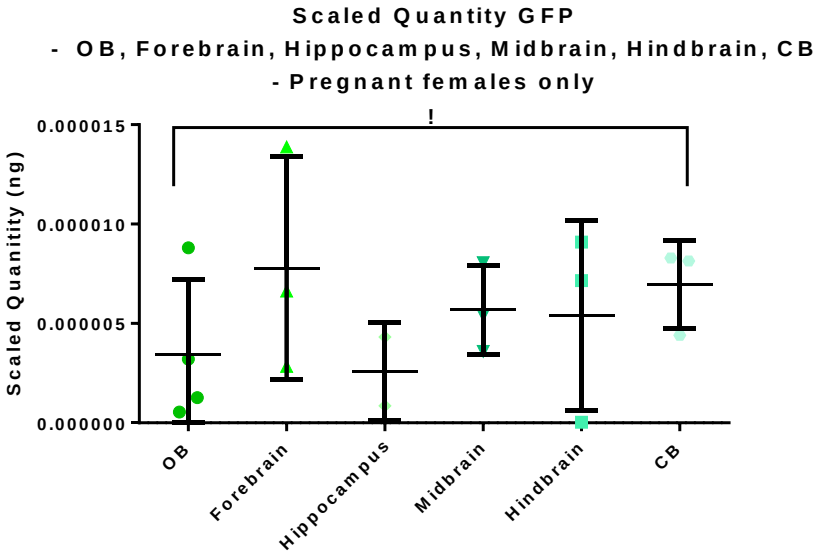
Scaled Quantity GFP
- OB, Forebrain, Hippocampus, Midbrain, Hindbrain, CB
- Pregnant females only
Scaled Quanitity (ng)
0.000015
0.000010
0.000005
0.000000
!
OB
Forebrain
Hippocampus
Midbrain
Hindbrain
CB